SEISMOTECTONIC EVALUATION OF FAULT STRUCTURES IN EAST OTAGO

EQC funded project 91/53

Report compiled by
R. J. NORRIS, P. O. KOONS, C. A. LANDIS

Dept of Geology, University of Otago, PO Box 56, Dunedin.

SEISMOTECTONIC EVALUATION OF FAULT STRUCTURES IN EAST OTAGO

EQC funded project 91/53

Report compiled by

R. J. NORRIS, P. O. KOONS, C. A. LANDIS

With major contributions from: Dr C. Pearson (strain calculation) and G. Salton (Hyde fault);

Field and other assistance from R. Cotton, D Smith and T. Johnstone (Akatore fault)

Dept of Geology, University of Otago, PO Box 56, Dunedin.

OBJECTIVES

The objectives for this project are:

1) To determine the current rate of strain accumulation south of Dunedin City from an examination of the existing triangulation data, in particular (i) the Akatore Fault monitoring network, (ii) the Dunedin West network, and (iii) the Dunedin East network.

2) To examine the Akatore and Hyde faults in order to establish, where possible, (a) geometry and surface expression of these structures by detailed field studies (b) magnitude and timing of displacements of observed features.

3) To assess as far as possible the potential contributions of these two structures to earthquake hazard in the Dunedin district.

4) to make available to Soils and Foundations Ltd outcomes of this research to assist in their assessment of seismic risk in Dunedin.

The Report is divided into three major parts:

PART 1: Calculation of strain rates in the Dunedin area from retriangulation of geodetic networks (Work completed by C. Pearson, Research fellow).

PART 2: Neotectonics of the Hyde Fault and the Rock and Pillar Range (Work mainly carried out by G. Salton, MSc student, with assistance from R. J. Norris and P. O. Koons).

PART 3: Neotectonics of the Akatore Fault (Work carried out by R. J. Norris, C. A. Landis and P. O. Koons, with assistance from R. Cotton and D. Smith).

GENERAL SUMMARY

The work undertaken for this project falls into three parts:

1) Determination of the present rate of strain in the Dunedin area from geodetic data.
2) Investigation of the structure and mechanics of the Hyde Fault and the Rock and Pillar Range, with an assessment of the earthquake potential of this structure.
3) Investigation into the structure and paleoseismicity of the Akatore Fault and and assessment of its earthquake potential.

Part One was undertaken by Dr C. Pearson and involved locating and extracting survey records for three triagulation networks around Dunedin and then calculating strain rates from repeated measurements. The purpose was to determine whether strain rates in the Dunedin area are high enough to be detectable geodetically with existing data, and if not, what are the maximum rates possible.

Part Two used a combination of field observation and computer modelling to investigate the structure and mechanics of the Hyde fault and Rock and Pillar Range, located about 50km west of Dunedin. The purpose was to increase our understanding of this structure as a potential source of large earthquakes in the region.

Part Three concentrated on collecting field data on the Akatore Fault, a young fault situated 20 km south of Dunedin. The purpose was to produce an accurrate map of the fault trace, determine its structure, and investigate its seismic history. This is the closest demonstrably active fault to Dunedin City. Offshore data has also been incorporated into the report.

The main conclusions are as follows:

Part 1: Geodetic strain determination

1.1 Three survey networks were investigated. One, a fault monitoring pattern across the Akatore Fault, was set up in 1979 for the purpose of detecting strain in the vicinity of the fault. The other two, Dunedin East and Dunedin West, are part of the national triangulation network.

1.2 No significant strain rates, greater than the margin of error, were determined for any of the networks. With regard to the Akatore network, this is not surprising as it is of small aperture and has only been in existence since 1979. In the absence of any ground displacement on the fault, and the estimated rate of displacement determined geologically, the result would be expected.

1.3 Large survey errors on the Dunedin networks preclude significant strain rates being calculated. Strain may be accumulating within the region, but it is below the level of detection with the quality of data available. This seems particularly the case with measurements last century. The Dunedin East network gives high strains if this data is included, but the high rates disappear if other combinations of survey data are used. Errors in the data appear the only explanantion.

1.4 While it is disappointing in one sense that strain rates cannot be determined from the data available, a maximum strain rate of about 0.1 microradians/year can be placed across the Dunedin area. This maximum value indicates that no unusually high strain rates exist and the data is compatible with the geological evidence for deformation.

Part 2: Hyde Fault and Rock and Pillar Range

2.1 The structure of the Rock and Pillar range is better viewed as a large asymmetric fold in schistosity and in the peneplain surface, rather than as a rigid block uplift along a range front master fault.

2.2 Modelling of the fold mechanics suggests that the fold may be forming above a major thrust fault at depth. The tip of the master fault is best modelled at a depth of 3-5 km below the present ground surface.

2.3 There is little surface expression of a continuous major fault along the range front. A recent fault trace crosses and displaces an alluvial fan surface at one locality and a similar fault trace may occur at a second locality.

2.4 The presence of local fault traces together with rejuvenation and deep incision of the heads of alluvial fans towards the range front suggest continued uplift of the Rock and Pillar range.

2.5 Without any firm dates of the surfaces, the best estimate of seismic hazard is based on longterm average uplift rates and a maximum displacement per event similar to those determined on parallel faults in the region. A return period for a magnitude 7 event would be of the order of 5000 yr.

Part 3: The Akatore Fault

3.1 The Akatore Fault is a single structure striking generally NE-SW and dipping 60° E. The slip is right-lateral reverse over most of its length except in two more northerly striking sections where it is nearly pure reverse.

3.2 The total vertical offset of the Late Cretaceous peneplain reaches a maximum of 120-130 m between Big and Akatore Creeks and reduces to the NE and SW. This together with the drainage pattern suggests that the fault has propogated NE and SW with time.

3.3 The fault is relatively young and postdates drainage development on the Titri block to the west.

3.4 Evidence of postglacial displacements is strong. The last event has an offset of approximately 2m and occurred about 1200 years ago. This would correspond to an earthquake of magnitude 6.8-7.3.

3.5 At least two such events have occurred since 14000 years ago.

3.6 Parallel faults offshore also show Holocene displacements.

3.7 The Akatore Fault System represents a significant potential hazard for the City of Dunedin.

ACKNOWLEDGEMENTS

The compilers are grateful to many people for help during the course of this work.

R. Cotton and D. Smith assisted in the Akatore study; members of the Stage 3 mapping class at Otago University also contributed data from Big Creek.

Professor R. H. Sibson gave advice to G. Salton during the course of her MSc study.

John Williams administered the grant.

Various landowners gave permission for entry onto their properties.

Caroline Read and Craig Jones assisted in collating the final copies of the report.

DOSLI provided access to survey records.

Mark Yetton of Soils & Foundations Ltd kept us informed of their parallel study of Earthquake Risk in Dunedin and sent us a copy of their report.

The director of EQC agreed to an extension of time for the submission of this report due to unforseen circumstances.

Part of the work reported was funded from University of Otago Research Grants.

PART 1

CALCULATION OF STRAIN RATES IN THE DUNEDIN AREA FROM RETRIANGULATION OF GEODETIC NETWORKS

by Dr C. Pearson, Research Fellow

Report edited by R. J. Norris & P. O. Koons

PART 1

CALCULATION OF STRAIN RATES IN THE DUNEDIN AREA FROM RETRIANGULATION OF GEODETIC NETWORKS

Work completed by Dr C. Pearson, Research Fellow

CONTENTS

SECTION 1: INTRODUCTION

Dr Chris Pearson was employed as a Research Fellow for 12 weeks to undertake a study of contemporary strain rates in the Dunedin region by examining survey data for triangulation networks that had been resurveyed on several occasions since their inception.

The three networks available were Dunedin West and Dunedin East, emplaced last century and resurveyed by Lands and Survey Department (now DOSLI), and the Akatore Fault monitoring network set up by the Earth Deformation Section of the NZ Geological Survey (now Institute of Geology and Nuclear Sciences Ltd.). The latter network is of small aperture and straddles the trace of the Akatore Fault.

In the absence of any ground displacement on the Akatore Fault since the network was set up, and the probable low rate of displacement on the fault (probably no more than 0.4 mm/yr; see Part 3 of this report), we would not expect to see any significant strain on the monitoring network. Indeed this is the case and is consistent with the geologically determined displacement rate.

The other two networks have over 100 years of data and are regional in extent, so some measurable strain is possible. The survey errors in these networks are such, however, that the minimum detectable strain is still above what we might expect for this area. The results do indicate, however, that while not excessively high, accumulation of elastic strain in the Dunedin area may be commensurate with expectations from the regional geology.

SECTION 2: STRAIN DETERMINATION FOR THE AKATORE NETWORK

2.1 Introduction

The Akatore Fault Monitoring pattern is located on a rolling paddock immediately south of the town of Taieri Mouth. The network, which consists of 9 stations, was established by the Earth Deformation Section of the New Zealand Geological Survey (Now DSIR Geology and Geophysics) in May 1979 (Brill 1981). The location of the trigs is shown in figure 2.1. Since then the network has been surveyed a total of 5 times at rather irregular intervals, most recently in 1989. The networks established in these surveys are shown in figures 2.2-2.6 and the measured directions are listed in Appendix 2.1. For this strain determination, I have used only triangulation data, even though a limited amount of EDM and GPS data are available. I have excluded the the EDM data because it is available for only one epoch and thus cannot be used to calculate the dilatation. I have excluded the GPS data because I have no way to analyze mixed data sets including both GPS and triangulation data. The strains were determined using a uniform strain code (NOSTRN) described by Bibby (1981). The strains determined from this data are listed in Table 2.1.

2.2 Results of strain determinations

TABLE 2.1

NETWORK	$\gamma 1$ µrad/yr	±1 SE µrad/yr	$\gamma 2$ µrad/yr	±1 S.E. µrad/yr	covariance
Akatore	-0.178	0.406	0.277	0.485	-0.243E-13

The strains are not significant at the 1 S.E. level of confidence and all we can say is that the strains are likely to be less than about 1 µrad/yr. at the 95% level of confidence.

In this readjustment, there is no reason to suspect any trig or group of trigs. All of the trigs are located in a gently rolling paddock and there is no evidence that any of the trigs have been disturbed by cultural activity so I just present an analysis of residuals. The trigs included in the readjustment are shown in Fig. 2.1.

The residuals from the NOSTRN readjustment are shown in Figs. 2.7 and 2.8. All of the residuals are listed in Appendix 2.2. In figure 2.2 I have plotted the residuals vs. the trigs that are involved in the observation. Since each measured angle involves 3 trigs (i.e the two trigs that are observed and the trig from which the observations are made), each residual is plotted three times. In figure 2.3 I have plotted the trigs vs. the year on which the observations were made. The major point from figures 2.2 and 2.3 is that the residuals are comparable. The fact that all of the trigs have similar errors is important because it suggests that all of the trigs have been stable since 1979 since any observations involving unstable trigs would be expected to give larger residuals than those which involve only stable trigs which will fit the uniform strain model more closely. The fact that the residuals are relatively constant with time is to be expected because all of the surveys were conducted using similar techniques. It does suggest that there have been no dramatic changes in strain rate or displacements on the Akatore Fault during the time since the network was established.

2.3 Conclusions

Currently there is no significant strain within the limits of detection on the Akatore Fault Monitoring Pattern. The errors are fairly large. These will decrease with time so it is important to continue monitoring the network every few years. With regard to displacement on the Akatore Fault, this result is not surprising as there has been no ground displacement on the fault during the life of the network. A slip rate on the fault of 2m per 5000 yr would give an annual displacement of 0.4mm. If this were stored as elastic strain within a zone say 5km either side of the fault, the annual strain increment would be 0.04 μrad. Thus even over the 10 year time span of the network, an accumulated elastic strain of 0.4 μrad. would be undetectable.

Fig. 2.1: Map showing location of Akatore monitoring network and distribution of survey stations.

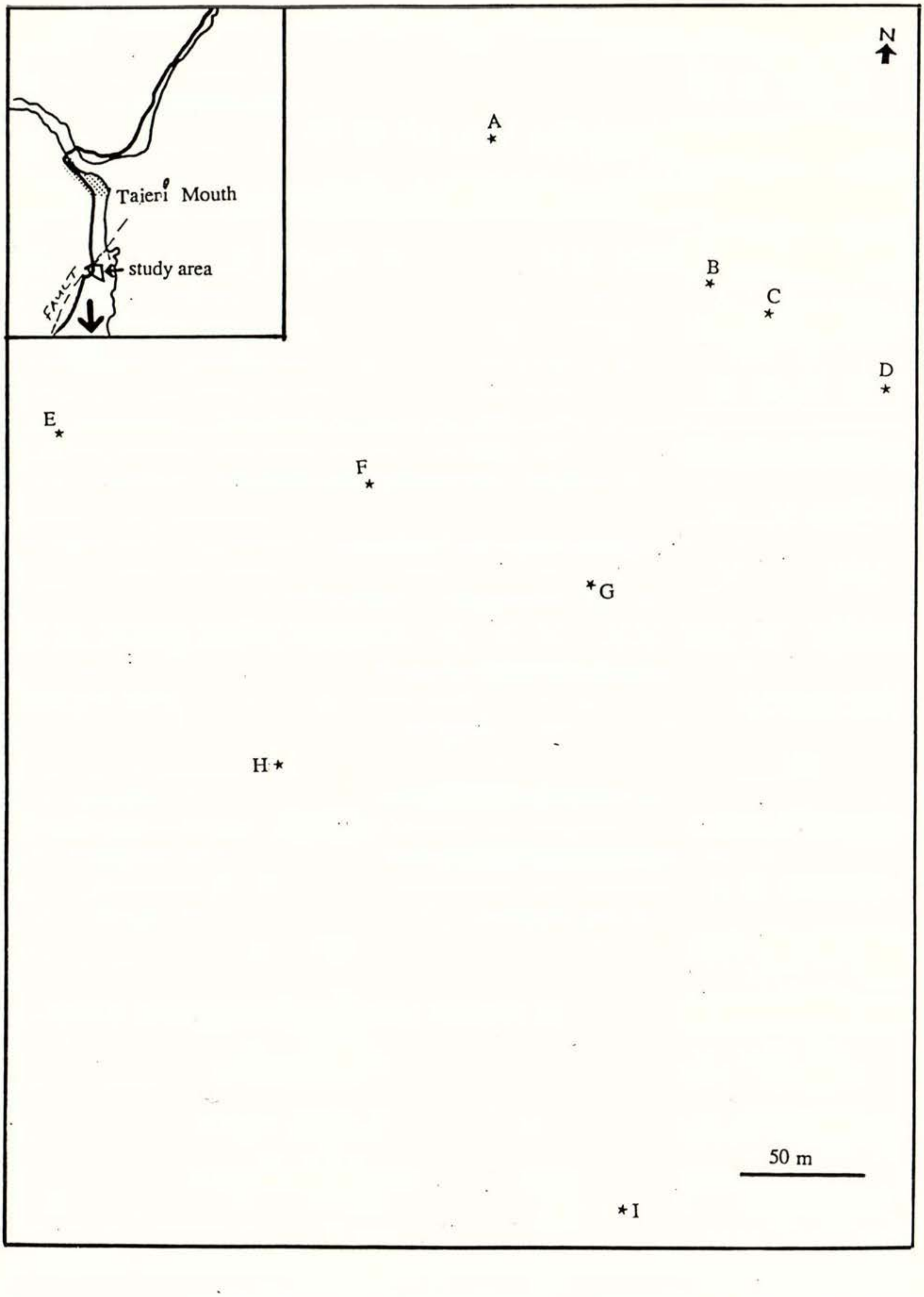

Fig. 2.2: Map showing observations of Akatore network made in 1979.

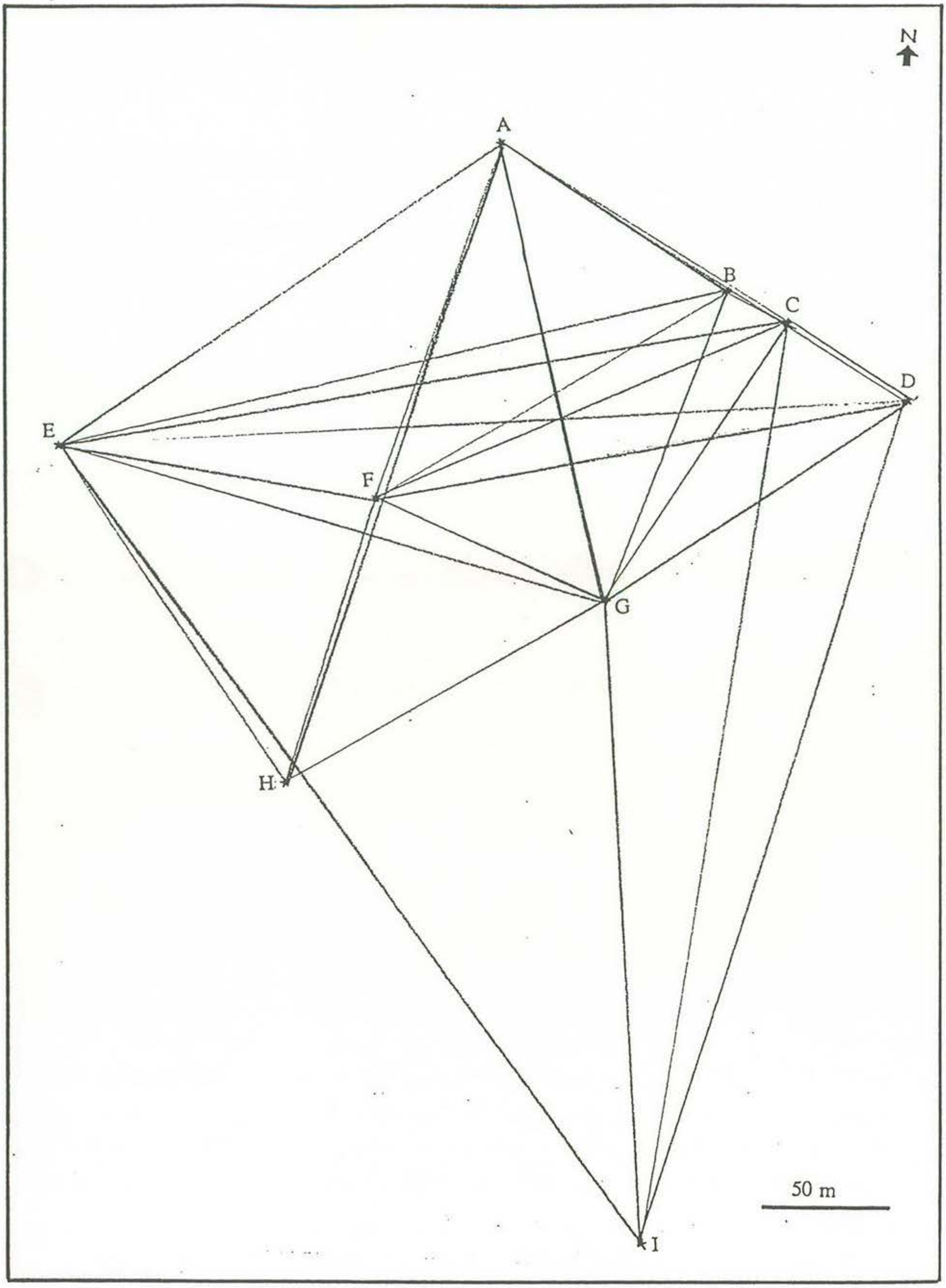

Fig. 2.3: Map showing observations of Akatore network made in 1980.

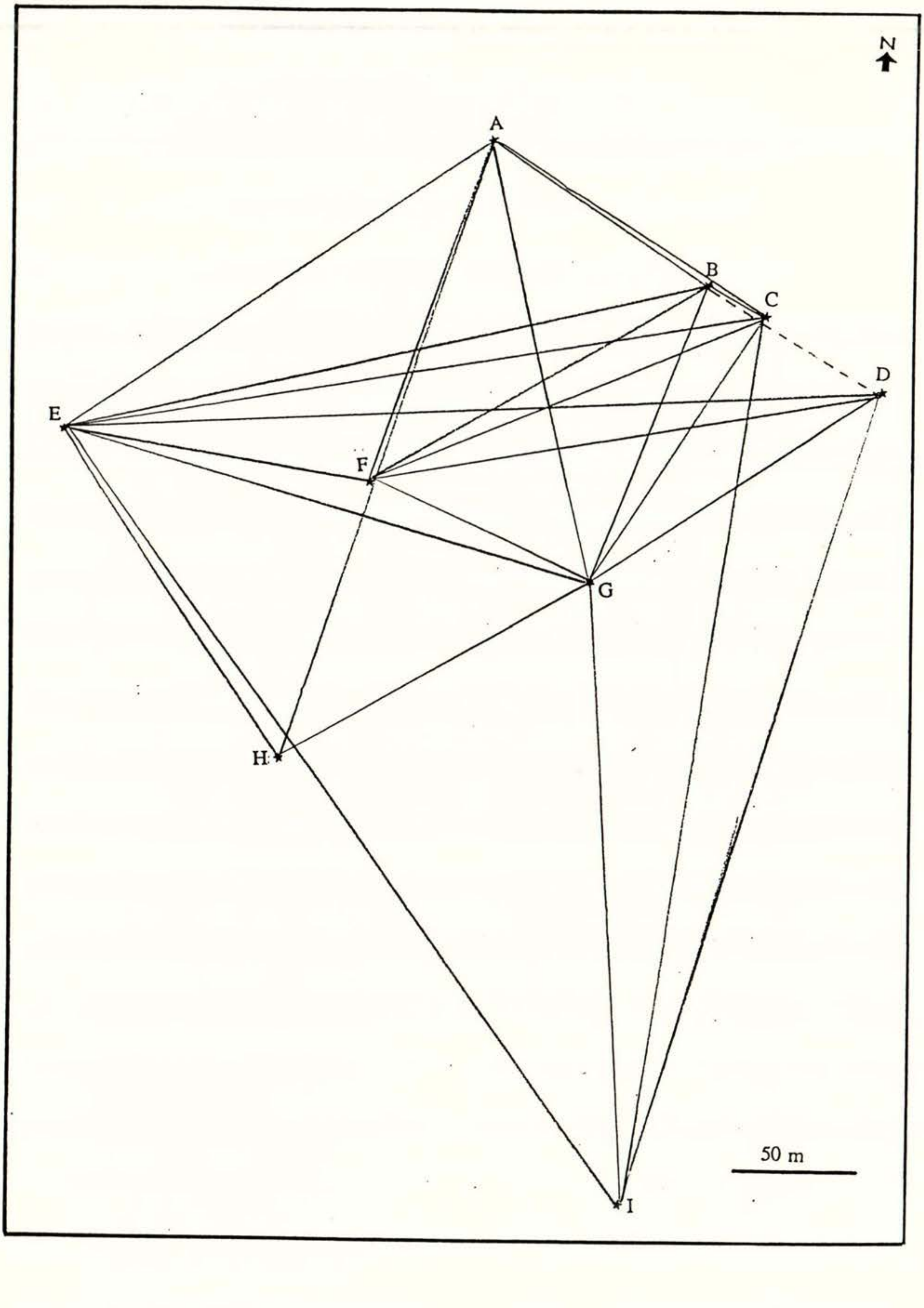

Fig. 2.4: Map showing observations of Akatore network made in 1985.

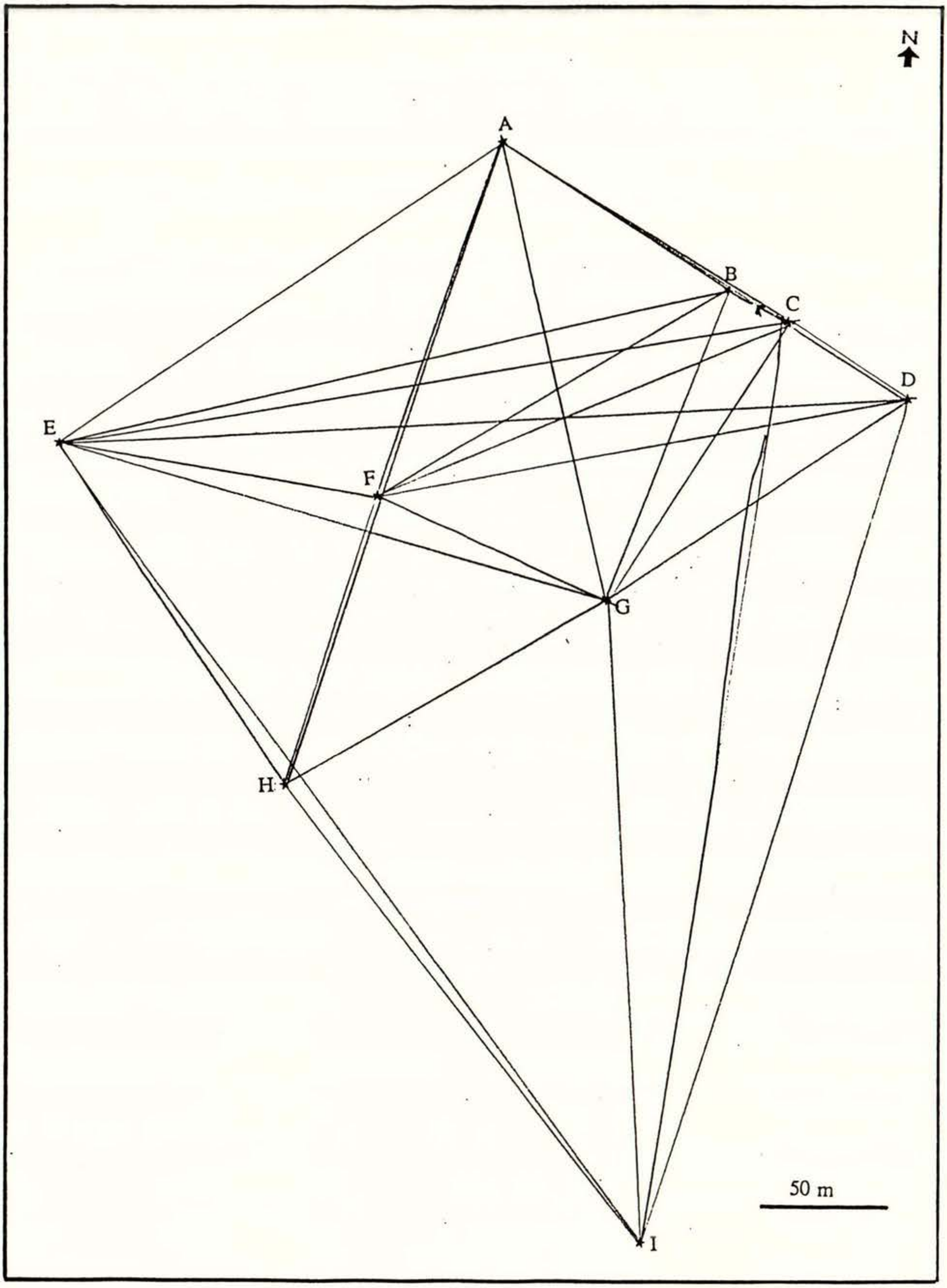

Fig. 2.5: Map showing observations of Akatore network made in 1986.

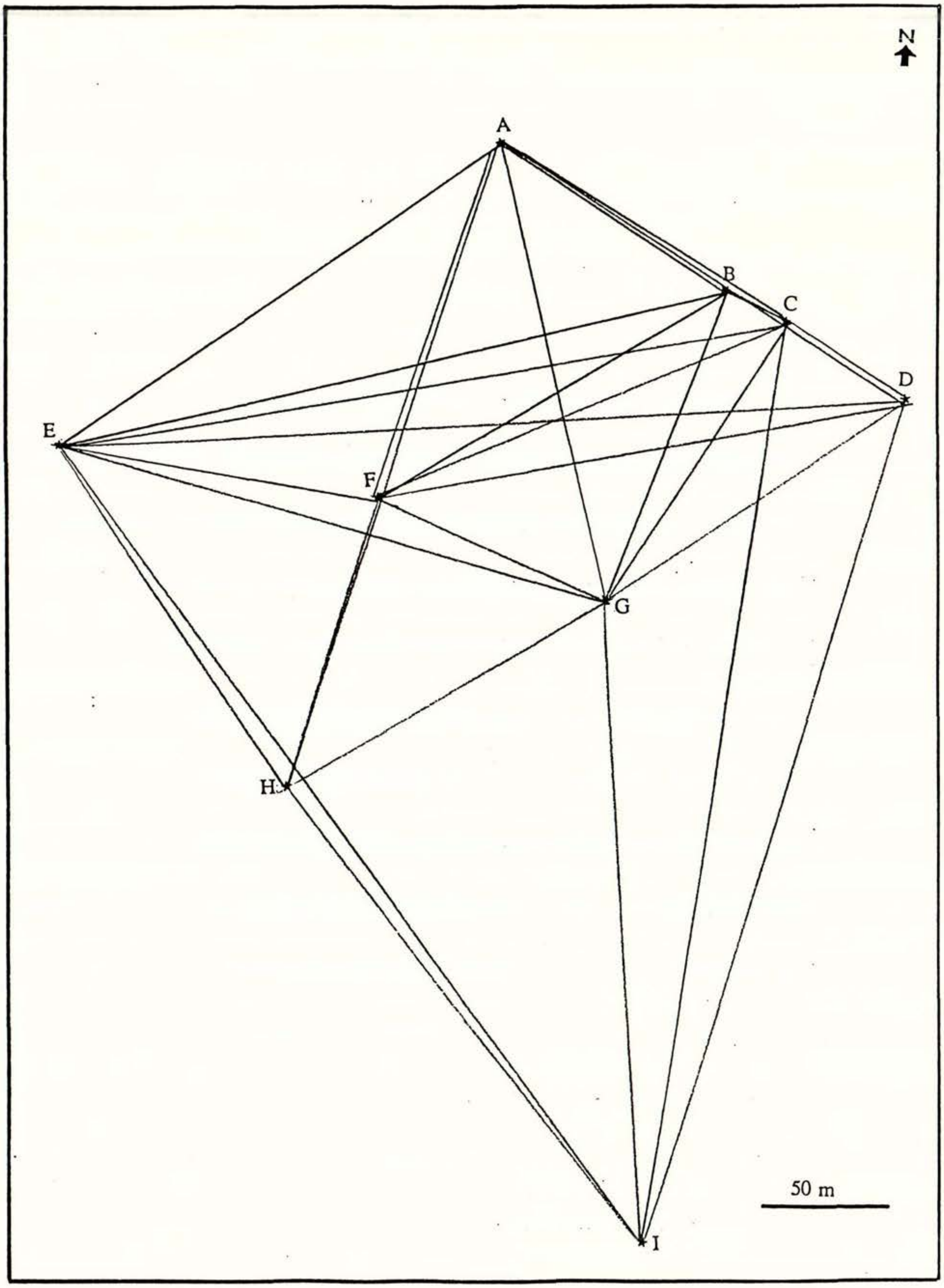

Fig. 2.6: Map showing observations of Akatore network made in 1989.

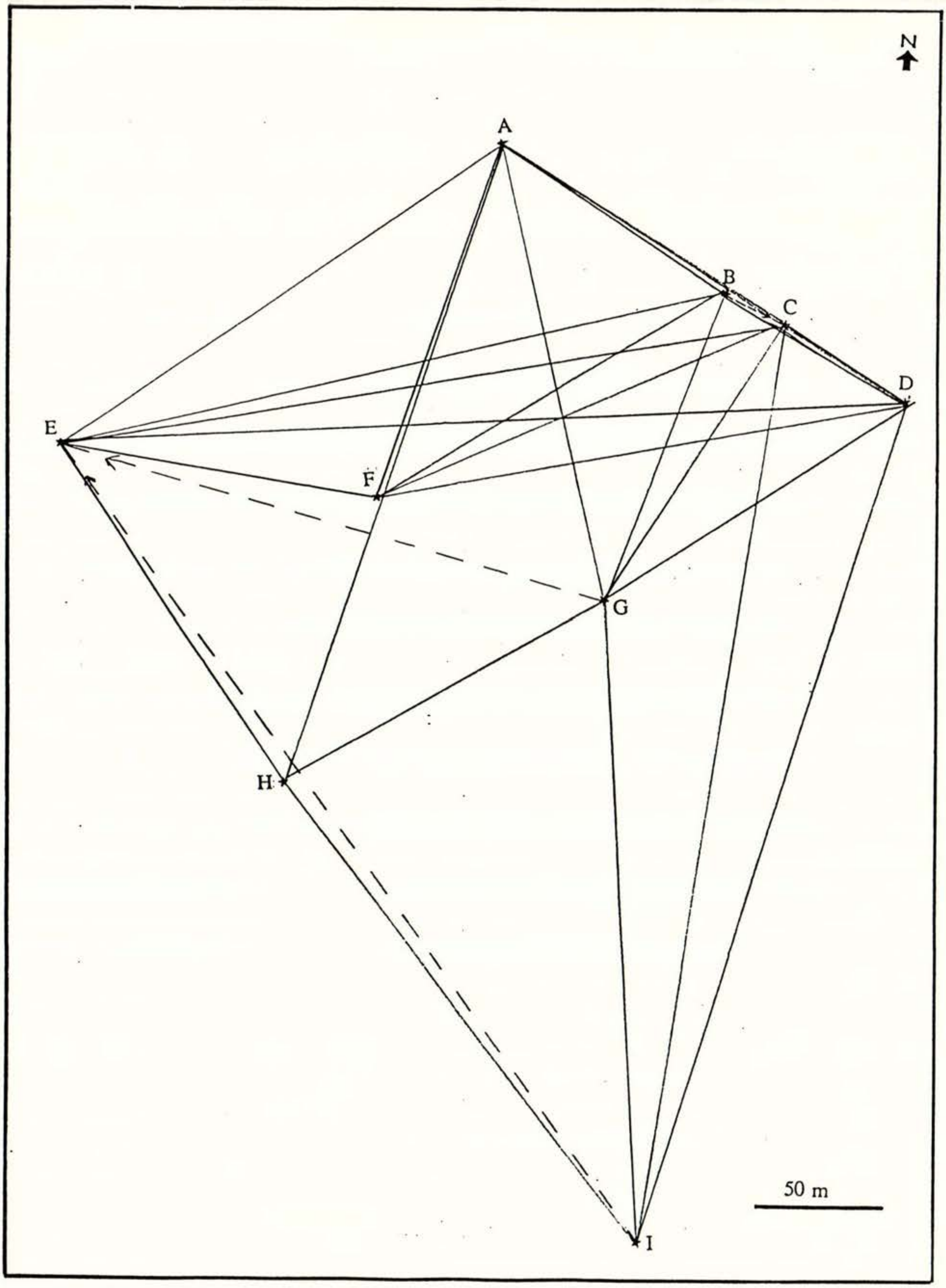

Appendix 2·1

APPENDIX 1 TRIANGULATION DATA FOR THE AKATORE FAULT MONITORING PATTERN
DATA RECORDED IN 1979.62

From	To	Dist	Deg	Min	Sec
A	G	0.00	0	0	0.00
	H	0.00	30	59	57.44
	F	0.00	31	41	37.49
	E	0.00	67	22	56.63
	D	0.00	315	24	45.86
	C	0.00	315	26	53.34
	B	0.00	315	26	19.40
B	G	0.00	0	0	0.00
	F	0.00	37	20	45.05
	E	0.00	55	16	49.25
	A	0.00	102	1	25.88
	C	0.00	282	3	53.48
C	I	0.00	0	0	0.00
	G	0.00	23	6	56.83
	F	0.00	56	59	5.55
	E	0.00	70	57	39.65
	A	0.00	113	54	34.15
	B	0.00	113	56	31.00
	D	0.00	293	47	46.86
D	I	0.00	0	0	0.00
	G	0.00	38	33	13.65
	F	0.00	61	34	55.90
	E	0.00	69	7	33.63
	A	0.00	105	10	7.44
	C	0.00	105	5	25.750
E	A	0.00	0	0	0.00
	B	0.00	21	18	52.29
	C	0.00	25	7	7.50
	D	0.00	31	59	21.72
	F	0.00	44	55	56.99
	G	0.00	51	8	55.20
	I	0.00	89	59	17.09
	H	0.00	91	16	55.37
F	A	0.00	0	0	0.00
	B	0.00	39	4	2.78
	C	0.00	46	49	46.36
	D	0.00	60	7	54.64
	G	0.00	94	42	31.03
	H	0.00	178	23	39.19

	E	0.00	260	37	11.18
G	I	0.00	0	0	0.00
	H	0.00	63	12	23.48
	E	0.00	108	31	8.64
	F	0.00	116	23	33.55
	A	0.00	169	59	24.36
	B	0.00	203	24	23.21
	C	0.00	214	38	40.17
	D	0.00	238	47	19.20
H	E	0.00	0	0	0.00
	F	0.00	51	25	33.29
	A	0.00	52	20	11.00
	G	0.00	94	33	15.34
	I	0.00	177	49	21.68
I	H	0.00	0	0	0.00
	E	0.00	0	52	58.55
	G	0.00	33	31	27.40
	C	0.00	45	3	11.42
	D	0.00	53	45	32.96

DATA RECORDED IN 1980.42

From	To	Dist	Deg	Min	Sec
A	G	0.	0	0	0.00
	H	0.	30	59	54.52
	F	0.	31	41	38.13
	E	0.	67	22	55.07
	D	0.	315	24	46.23
	C	0.	315	26	53.98
	B	0.	315	26	22.95
B	G	0.	0	0	0.00
	F	0.	37	20	42.98
	E	0.	55	16	47.15
	A	0.	102	1	24.15
	D	0.	281	57	47.16
	C	0.	282	3	48.36
C	I	0.	0	0	0.00
	G	0.	23	6	54.27
	F	0.	56	59	4.97
	E	0.	70	57	40.22
	A	0.	113	54	32.68
	B	0.	113	56	26.77
D	I	0.	0	0	0.00
	G	0.	38	33	12.45
	F	0.	61	34	50.93
	E	0.	69	7	30.76
	A	0.	105	10	3.89
E	D	0.	0	0	0.00
	F	0.	12	56	34.78
	G	0.	19	9	29.55
	I	0.	57	59	51.21
	H	0.	59	17	32.22
	A	0.	328	0	41.22
	B	0.	349	19	32.47
	C	0.	353	7	47.57
F	D	0.	0	0	0.00
	G	0.	34	34	31.83
	H	0.	118	15	43.69
	E	0.	200	29	15.32
	A	0.	299	52	9.55
	B	0.	338	56	9.89
	C	0.	346	41	52.47

G	D	0.	0	0	0.00
	I	0.	121	12	39.78
	H	0.	184	25	2.79
	E	0.	229	43	48.76
	F	0.	237	36	14.63
	A	0.	291	12	4.98
	B	0.	324	37	2.92
	C	0.	335	51	20.14
H	E	0.	0	0	0.00
	F	0.	51	25	32.68
	A	0.	52	20	8.91
	G	0.	94	33	14.79
	I	0.	177	49	19.46
I	D	0.	0	0	0.00
	H	0.	306	14	25.63
	E	0.	307	7	25.41
	G	0.	339	45	55.81
	C	0.	351	17	40.84

DATA RECORDED IN 1985.94

From	To	Dist	Deg	Min	Sec
A	B	0.0	315	26	23.35
	C	0.0	315	26	51.72
	D	0.0	315	24	47.21
	E	0.0	67	22	54.6
	F	0.0	31	41	41.58
	G	0.0	0	0	0.0
	H	0.0	30	59	55.83
B	A	0.0	102	1	21.16
	E	0.0	55	16	46.64
	F	0.0	37	20	40.67
	G	0.0	0	0	0.0
C	A	0.0	113	54	31.0
	B	0.0	113	56	31.82
	D	0.0	293	47	43.31
	E	0.0	70	57	40.96
	F	0.0	56	59	4.48
	G	0.0	23	6	56.24
	I	0.0	0	0	0.0
D	A	0.0	105	10	3.7
	C	0.0	105	5	20.14
	E	0.0	69	7	31.07
	F	0.0	61	34	48.95
	G	0.0	38	33	13.3
	I	0.0	0	0	0.0
E	A	0.0	0	0	0.0
	B	0.0	21	18	48.68
	C	0.0	25	7	3.34
	D	0.0	31	59	14.94
	F	0.0	44	55	50.6
	G	0.0	51	8	44.9
	H	0.0	91	16	47.69
	I	0.0	89	59	7.39
F	A	0.0	299	52	6.42
	B	0.0	338	56	7.08
	C	0.0	346	41	49.24
	D	0.0	0	0	0.0
	E	0.0	200	29	15.52
	G	0.0	34	34	32.21
	H	0.0	118	15	45.45

G	A	0.0	0	0	0.0
	B	0.0	33	24	59.11
	C	0.0	44	39	15.6
	D	0.0	68	47	58.78
	E	0.0	298	31	43.61
	F	0.0	306	24	8.26
	H	0.0	253	12	56.18
	I	0.0	190	0	37.22
H	A	0.0	52	20	14.62
	E	0.0	0	0	0.0
	F	0.0	51	25	36.8
	G	0.0	94	33	18.29
	I	0.0	177	49	24.37
I	C	0.0	351	17	39.25
	D	0.0	0	0	0.0
	E	0.0	307	7	23.63
	G	0.0	339	45	54.32
	H	0.0	306	14	26.25

DATA RECORDED IN 1986.75

From	To	Dist	Deg	Min	Sec
A	B	0.0	315	26	24.06
	C	0.0	315	26	52.2
	D	0.0	315	24	48.81
	E	0.0	67	22	55.19
	F	0.0	31	41	40.81
	G	0.0	0	0	0.0
	H	0.0	30	59	52.28
B	A	0.0	102	1	24.44
	C	0.0	282	3	49.2
	E	0.0	55	16	47.83
	F	0.0	37	20	40.56
	G	0.0	0	0	0.0
C	A	0.0	113	54	29.06
	B	0.0	113	56	29.75
	D	0.0	293	47	40.00
	E	0.0	70	57	41.25
	F	0.0	56	59	6.69
	G	0.0	23	6	52.56
	I	0.0	0	0	0.0
D	A	0.0	105	10	5.63
	C	0.0	105	5	23.31
	E	0.0	69	7	33.69
	F	0.0	61	34	52.69
	G	0.0	38	33	15.5
	I	0.0	0	0	0.0
E	A	0.0	0	0	0.0
	B	0.0	21	18	52.17
	C	0.0	25	7	7.72
	D	0.0	31	59	18.88
	F	0.0	44	55	54.22
	G	0.0	51	8	49.56
	H	0.0	91	16	46.13
	I	0.0	89	59	12.75
F	A	0.0	299	52	5.61
	B	0.0	338	56	8.39
	C	0.0	346	41	52.33
	D	0.0	0	0	0.0
	E	0.0	200	29	9.19
	G	0.0	34	34	34.25
	H	0.0	118	15	38.78

G	A	0.0	0	0	0.0
	B	0.0	33	24	56.92
	C	0.0	44	39	13.3
	D	0.0	68	47	52.93
	E	0.0	298	31	44.67
	F	0.0	306	24	11.17
	H	0.0	253	12	59.1
	I	0.0	190	0	42.44
H	A	0.0	52	20	12.56
	E	0.0	0	0	0.0
	F	0.0	51	25	28.44
	G	0.0	94	33	15.9
	I	0.0	177	49	22.25
I	C	0.0	351	17	37.00
	D	0.0	0	0	0.0
	E	0.0	307	7	29.63
	G	0.0	339	45	55.31
	H	0.0	306	14	25.81

Appendix 2·2

APPENDIX 2 RESIDUALS FROM JOINT ADJUSTMENT PROCEEDURE

ANGLE	OBSERVED deg min sec	CALCULATED deg min sec	DIFFERENCE seconds
SURVEY NUMBER A DATE	1979.62		
STATION A TO G AND B	44 33 40.60	44 33 37.34	3.264
STATION A TO H AND G	30 59 57.44	30 59 55.58	1.863
STATION A TO F AND H	0 41 40.05	0 41 44.95	-4.902
STATION A TO E AND F	35 41 19.14	35 41 14.58	4.558
STATION A TO D AND E	248 1 49.23	248 1 51.27	-2.041
STATION A TO C AND D	0 2 7.48	0 2 5.74	1.744
STATION A TO B AND C	359 59 26.06	359 59 30.54	-4.485
STATION B TO G AND C	77 56 6.52	77 56 7.92	-1.395
STATION B TO F AND G	37 20 45.05	37 20 43.58	1.466
STATION B TO E AND F	17 56 4.20	17 56 5.03	-0.829
STATION B TO A AND E	46 44 36.63	46 44 35.41	1.223
STATION B TO C AND A	180 2 27.60	180 2 28.06	-0.465
STATION C TO I AND D	66 12 13.14	66 12 16.05	-2.909
STATION C TO G AND I	23 6 56.83	23 6 55.74	1.089
STATION C TO F AND G	33 52 8.72	33 52 9.72	-0.997
STATION C TO E AND F	13 58 34.10	13 58 36.09	-1.986
STATION C TO A AND E	42 56 54.50	42 56 50.63	3.873
STATION C TO B AND A	0 1 56.85	0 1 58.61	-1.760
STATION C TO D AND B	179 51 15.86	179 51 13.17	2.690
STATION D TO I AND C	254 54 34.25	254 54 37.76	-3.514
STATION D TO G AND I	38 33 13.65	38 33 14.14	-0.491
STATION D TO F AND G	23 1 42.25	23 1 37.71	4.541
STATION D TO E AND F	7 32 37.73	7 32 40.74	-3.011
STATION D TO A AND E	36 2 33.81	36 2 32.13	1.681
STATION D TO C AND A	359 55 18.31	359 55 17.52	0.794
STATION E TO A AND H	268 43 4.63	268 43 9.71	-5.080
STATION E TO B AND A	21 18 52.29	21 18 52.14	0.146
STATION E TO C AND B	3 48 15.21	3 48 14.23	0.976
STATION E TO D AND C	6 52 14.22	6 52 12.76	1.457
STATION E TO F AND D	12 56 35.27	12 56 35.06	0.210
STATION E TO G AND F	6 12 58.21	6 12 54.56	3.650
STATION E TO I AND G	38 50 21.89	38 50 22.24	-0.346
STATION E TO H AND I	1 17 38.28	1 17 39.29	-1.014
STATION F TO A AND E	99 22 48.82	99 22 51.22	-2.399
STATION F TO B AND A	39 4 2.78	39 4 1.70	1.081
STATION F TO C AND B	7 45 43.58	7 45 43.18	0.404
STATION F TO D AND C	13 18 8.28	13 18 8.11	0.174
STATION F TO G AND D	34 34 36.39	34 34 35.79	0.599
STATION F TO H AND G	83 41 8.16	83 41 9.40	-1.238
STATION F TO E AND H	82 13 31.99	82 13 30.61	1.379
STATION G TO I AND D	121 12 40.80	121 12 40.17	0.631
STATION G TO H AND I	63 12 23.48	63 12 23.02	0.459
STATION G TO E AND H	45 18 45.16	45 18 44.88	0.282
STATION G TO F AND E	7 52 24.91	7 52 25.43	-0.521
STATION G TO A AND F	53 35 50.81	53 35 50.70	0.114

STATION G TO B AND A	33 24 58.85	33 24 58.65	0.204
STATION G TO C AND B	11 14 16.96	11 14 17.04	-0.083
STATION G TO D AND C	24 8 39.03	24 8 40.11	-1.085
STATION H TO E AND I	182 10 38.32	182 10 38.86	-0.535
STATION H TO F AND E	51 25 33.29	51 25 33.30	-0.011
STATION H TO A AND F	0 54 37.71	0 54 36.88	0.832
STATION H TO G AND A	42 13 4.34	42 13 3.41	0.925
STATION H TO I AND G	83 16 6.34	83 16 7.55	-1.212
STATION I TO H AND D	306 14 27.04	306 14 24.88	2.157
STATION I TO E AND H	0 52 58.55	0 52 59.56	-1.011
STATION I TO G AND E	32 38 28.85	32 38 29.87	-1.016
STATION I TO C AND G	11 31 44.02	11 31 43.97	0.045
STATION I TO D AND C	8 42 21.54	8 42 21.72	-0.175
SURVEY NUMBER 2 DATE	1980.42		
STATION A TO G AND B	44 33 37.05	44 33 37.39	-0.337
STATION A TO H AND G	30 59 54.52	30 59 55.57	-1.052
STATION A TO F AND H	0 41 43.61	0 41 44.95	-1.342
STATION A TO E AND F	35 41 16.94	35 41 14.54	2.402
STATION A TO D AND E	248 1 51.16	248 1 51.27	-0.109
STATION A TO C AND D	0 2 7.75	0 2 5.74	2.014
STATION A TO B AND C	359 59 28.97	359 59 30.54	-1.575
STATION B TO G AND C	77 56 11.64	77 56 7.96	3.682
STATION B TO F AND G	37 20 42.98	37 20 43.54	-0.558
STATION B TO E AND F	17 56 4.17	17 56 5.01	-0.842
STATION B TO A AND E	46 44 37.00	46 44 35.43	1.573
STATION B TO D AND A	179 56 23.01	179 56 23.96	-0.950
STATION B TO C AND D	0 6 1.20	0 6 4.11	-2.905
STATION C TO I AND B	246 3 33.23	246 3 29.27	3.959
STATION C TO G AND I	23 6 54.27	23 6 55.72	-1.451
STATION C TO F AND G	33 52 10.70	33 52 9.67	1.026
STATION C TO E AND F	13 58 35.25	13 58 36.08	-0.826
STATION C TO A AND E	42 56 52.46	42 56 50.65	1.811
STATION C TO B AND A	0 1 54.09	0 1 58.61	-4.520
STATION D TO I AND A	254 49 56.11	254 49 55.33	0.784
STATION D TO G AND I	38 33 12.45	38 33 14.09	-1.644
STATION D TO F AND G	23 1 38.48	23 1 37.69	0.792
STATION D TO E AND F	7 32 39.83	7 32 40.74	-0.909
STATION D TO A AND E	36 2 33.13	36 2 32.15	0.978
STATION E TO D AND C	6 52 12.43	6 52 12.76	-0.331
STATION E TO F AND D	12 56 34.78	12 56 35.06	-0.282
STATION E TO G AND F	6 12 54.77	6 12 54.56	0.206
STATION E TO I AND G	38 50 21.66	38 50 22.28	-0.622
STATION E TO H AND I	1 17 41.01	1 17 39.30	1.714
STATION E TO A AND H	268 43 9.00	268 43 9.68	-0.681
STATION E TO B AND A	21 18 51.25	21 18 52.12	-0.873
STATION E TO C AND B	3 48 15.10	3 48 14.23	0.868
STATION F TO D AND C	13 18 7.53	13 18 8.10	-0.567
STATION F TO G AND D	34 34 31.83	34 34 35.80	-3.972
STATION F TO H AND G	83 41 11.86	83 41 9.45	2.405
STATION F TO E AND H	82 13 31.63	82 13 30.54	1.087
STATION F TO A AND E	99 22 54.23	99 22 51.29	2.945
STATION F TO B AND A	39 4 0.34	39 4 1.65	-1.311

STATION F TO C AND B	7 45 42.58	7 45 43.17	-0.587
STATION G TO D AND C	24 8 39.86	24 8 40.08	-0.223
STATION G TO I AND D	121 12 39.78	121 12 40.22	-0.443
STATION G TO H AND I	63 12 23.01	63 12 22.96	0.048
STATION G TO E AND H	45 18 45.97	45 18 44.87	1.103
STATION G TO F AND E	7 52 25.87	7 52 25.44	0.432
STATION G TO A AND F	53 35 50.35	53 35 50.76	-0.407
STATION G TO B AND A	33 24 57.94	33 24 58.64	-0.699
STATION G TO C AND B	11 14 17.22	11 14 17.03	0.189
STATION H TO E AND I	182 10 40.54	182 10 38.86	1.682
STATION H TO F AND E	51 25 32.68	51 25 33.32	-0.636
STATION H TO A AND F	0 54 36.23	0 54 36.88	-0.647
STATION H TO G AND A	42 13 5.88	42 13 3.36	2.517
STATION H TO I AND G	83 16 4.67	83 16 7.59	-2.916
STATION I TO D AND C	8 42 19.16	8 42 21.71	-2.550
STATION I TO H AND D	306 14 25.63	306 14 24.86	0.766
STATION I TO E AND H	0 52 59.78	0 52 59.56	0.217
STATION I TO G AND E	32 38 30.40	32 38 29.89	0.510
STATION I TO C AND G	11 31 45.03	11 31 43.97	1.057
SURVEY NUMBER 3 DATE	1985..94		
STATION A TO B AND H	284 26 27.52	284 26 26.73	0.793
STATION A TO C AND B	0 0 28.37	0 0 29.46	-1.085
STATION A TO D AND C	359 57 55.49	359 57 54.26	1.227
STATION A TO E AND D	111 58 7.39	111 58 8.74	-1.348
STATION A TO F AND E	324 18 46.98	324 18 45.76	1.216
STATION A TO G AND F	328 18 18.42	328 18 19.52	-1.095
STATION A TO H AND G	30 59 55.83	30 59 55.54	0.293
STATION B TO A AND G	102 1 21.16	102 1 23.68	-2.518
STATION B TO E AND A	313 15 25.48	313 15 24.44	1.043
STATION B TO F AND E	342 3 54.03	342 3 55.10	-1.073
STATION B TO G AND F	322 39 19.33	322 39 16.78	2.547
STATION C TO A AND I	113 54 31.00	113 54 31.76	-0.764
STATION C TO B AND A	0 2 0.82	0 1 58.61	2.210
STATION C TO D AND B	179 51 11.49	179 51 13.17	-1.678
STATION C TO E AND D	137 9 57.65	137 9 57.42	0.227
STATION C TO F AND E	346 1 23.52	346 1 23.99	-0.474
STATION C TO G AND F	326 7 51.76	326 7 50.62	1.140
STATION C TO I AND G	336 53 3.76	336 53 4.42	-0.661
STATION D TO A AND I	105 10 3.70	105 10 4.36	-0.656
STATION D TO C AND A	359 55 16.44	359 55 17.52	-1.075
STATION D TO E AND C	324 2 10.93	324 2 10.17	0.760
STATION D TO F AND E	352 27 17.88	352 27 19.28	-1.396
STATION D TO G AND F	336 58 24.35	336 58 22.45	1.896
STATION D TO I AND G	321 26 46.70	321 26 46.23	0.471
STATION E TO A AND I	270 0 52.61	270 0 48.78	3.826
STATION E TO B AND A	21 18 48.68	21 18 51.98	-3.300
STATION E TO C AND B	3 48 14.66	3 48 14.22	0.442
STATION E TO D AND C	6 52 11.60	6 52 12.75	-1.148
STATION E TO F AND D	12 56 35.66	12 56 35.08	0.581
STATION E TO G AND F	6 12 54.30	6 12 54.59	-0.290
STATION E TO H AND G	40 8 2.79	40 8 1.91	0.882
STATION E TO I AND H	358 42 19.70	358 42 20.69	-0.993

STATION F TO A AND H	181 36 20.97	181 36 21.82	-0.849
STATION F TO B AND A	39 4 0.66	39 4 1.32	-0.660
STATION F TO C AND B	7 45 42.16	7 45 43.11	-0.948
STATION F TO D AND C	13 18 10.76	13 18 8.03	2.731
STATION F TO E AND D	200 29 15.52	200 29 15.80	-0.282
STATION F TO G AND E	194 5 16.69	194 5 20.08	-3.387
STATION F TO H AND G	83 41 13.24	83 41 9.84	3.395
STATION G TO A AND I	169 59 22.78	169 59 24.00	-1.222
STATION G TO B AND A	33 24 59.11	33 24 58.59	0.521
STATION G TO C AND B	11 14 16.49	11 14 16.95	-0.456
STATION G TO D AND C	24 8 43.18	24 8 39.86	3.316
STATION G TO E AND D	229 43 44.83	229 43 47.94	-3.107
STATION G TO F AND E	7 52 24.65	7 52 25.49	-0.837
STATION G TO H AND F	306 48 47.92	306 48 49.72	-1.805
STATION G TO I AND H	296 47 41.04	296 47 37.45	3.590
STATION H TO A AND I	234 30 50.25	234 30 49.17	1.078
STATION H TO E AND A	307 39 45.38	307 39 49.70	-4.324
STATION H TO F AND E	51 25 36.80	51 25 33.42	3.376
STATION H TO G AND F	43 7 41.49	43 7 39.88	1.610
STATION H TO I AND G	83 16 6.08	83 16 7.82	-1.739
STATION I TO C AND H	45 3 13.00	45 3 13.59	-0.590
STATION I TO D AND C	8 42 20.75	8 42 21.67	-0.922
STATION I TO E AND D	307 7 23.63	307 7 24.31	-0.679
STATION I TO G AND E	32 38 30.69	32 38 30.06	0.629
STATION I TO H AND G	326 28 31.93	326 28 30.37	1.562
SURVEY NUMBER 4 DATE	1986.75		
STATION A TO B AND H	284 26 31.78	284 26 26.68	5.099
STATION A TO C AND B	0 0 28.14	0 0 29.46	-1.315
STATION A TO D AND C	359 57 56.61	359 57 54.26	2.347
STATION A TO E AND D	111 58 6.38	111 58 8.74	-2.359
STATION A TO F AND E	324 18 45.62	324 18 45.81	-0.188
STATION A TO G AND F	328 18 19.19	328 18 19.52	-0.331
STATION A TO H AND G	30 59 52.28	30 59 55.53	-3.252
STATION B TO A AND G	102 1 24.44	102 1 23.63	0.806
STATION B TO C AND A	180 2 24.76	180 2 28.07	-3.305
STATION B TO E AND C	133 12 58.63	133 12 56.35	2.279
STATION B TO F AND E	342 3 52.73	342 3 55.12	-2.390
STATION B TO G AND F	322 39 19.44	322 39 16.83	2.610
STATION C TO A AND I	113 54 29.06	113 54 31.71	-2.651
STATION C TO B AND A	0 2 0.69	0 1 58.61	2.080
STATION C TO D AND B	179 51 10.25	179 51 13.17	-2.918
STATION C TO E AND D	137 10 1.25	137 9 57.40	3.849
STATION C TO F AND E	346 1 25.44	346 1 24.00	1.436
STATION C TO G AND F	326 7 45.87	326 7 50.66	-4.793
STATION C TO I AND G	336 53 7.44	336 53 4.44	2.998
STATION D TO A AND I	105 10 5.63	105 10 4.31	1.321
STATION D TO C AND A	359 55 17.68	359 55 17.51	0.165
STATION D TO E AND C	324 2 10.38	324 2 10.15	0.234
STATION D TO F AND E	352 27 19.00	352 27 19.28	-0.278
STATION D TO G AND F	336 58 22.81	336 58 22.48	0.335
STATION D TO I AND G	321 26 44.50	321 26 46.28	-1.776
STATION E TO A AND I	270 0 47.25	270 0 48.76	-1.505
STATION E TO B AND A	21 18 52.17	21 18 51.96	0.211

STATION E TO C AND B	3 48 15.55	3 48 14.22	1.334
STATION E TO D AND C	6 52 11.16	6 52 12.75	-1.586
STATION E TO F AND D OB	12 56 35.34	12 56 35.08	0.259
STATION E TO G AND F	6 12 55.34	6 12 54.59	0.746
STATION E TO H AND G	40 7 56.57	40 8 1.96	-5.387
STATION E TO I AND H	358 42 26.62	358 42 20.69	5.928
STATION F TO A AND H	181 36 26.83	181 36 21.82	5.012
STATION F TO B AND A	39 4 2.78	39 4 1.27	1.509
STATION F TO C AND B	7 45 43.94	7 45 43.10	0.840
STATION F TO D AND C	13 18 7.67	13 18 8.02	-0.349
STATION F TO E AND D	200 29 9.19	200 29 15.80	-6.612
STATION F TO G AND E	194 5 25.06	194 5 20.09	4.972
STATION F TO H AND G	83 41 4.53	83 41 9.90	-5.372
STATION G TO A AND I	169 59 17.56	169 59 24.00	-6.439
STATION G TO B AND A	33 24 56.92	33 24 58.58	-1.662
STATION G TO C AND B	11 14 16.38	11 14 16.93	-0.554
STATION G TO D AND C	24 8 39.63	24 8 39.83	-0.202
STATION G TO E AND D	229 43 51.74	229 43 47.92	3.820
STATION G TO F AND E	7 52 26.50	7 52 25.49	1.006
STATION G TO H AND F	306 48 47.93	306 48 49.73	-1.799
STATION G TO I AND H	296 47 43.34	296 47 37.51	5.829
STATION H TO A AND I	234 30 50.31	234 30 49.19	1.120
STATION H TO E AND A	307 39 47.44	307 39 49.69	-2.249
STATION H TO F AND E	51 25 28.44	51 25 33.44	-5.000
STATION H TO G AND F	43 7 47.46	43 7 39.83	7.633
STATION H TO I AND G	83 16 6.35	83 16 7.85	-1.503
STATION I TO C AND H	45 3 11.19	45 3 13.61	-2.424
STATION I TO D AND C	8 42 23.00	8 42 21.67	1.334
STATION I TO E AND D	307 7 29.63	307 7 24.29	5.338
STATION I TO G AND E	32 38 25.68	32 38 30.09	-4.406
STATION I TO H AND G	326 28 30.50	326 28 30.34	0.158
SURVEY NUMBER 5 DATE	1989.79		
STATION A TO B AND H	284 26 23.89	284 26 26.51	-2.619
STATION A TO C AND B	0 0 32.69	0 0 29.46	3.235
STATION A TO D AND C	359 57 55.19	359 57 54.26	0.927
STATION A TO E AND D	111 58 6.81	111 58 8.74	-1.933
STATION A TO F AND E	324 18 47.19	324 18 45.97	1.216
STATION A TO G AND F	328 18 20.37	328 18 19.54	0.827
STATION A TO H AND G	30 59 53.86	30 59 55.51	-1.653
STATION B TO A AND E	46 44 34.25	46 44 35.66	-1.408
STATION B TO C AND A	180 2 39.74	180 2 28.07	11.674
STATION B TO D AND C	359 53 50.17	359 53 55.89	-5.720
STATION B TO G AND D	78 2 9.31	78 2 12.57	-3.259
STATION B TO F AND G	37 20 40.92	37 20 42.99	-2.070
STATION B TO E AND F	17 56 5.60	17 56 4.82	0.783
STATION C TO A AND I	113 54 32.19	113 54 31.52	0.674
STATION C TO D AND A	179 53 9.97	179 53 11.78	-1.808
STATION C TO E AND D	137 10 0.65	137 9 57.32	3.331
STATION C TO F AND E	346 1 21.99	346 1 24.04	-2.053
STATION C TO G AND F	326 7 52.41	326 7 50.82	1.586
STATION C TO I AND G	336 53 2.79	336 53 4.52	-1.730
STATION D TO A AND I	105 10 5.24	105 10 4.13	1.105

STATION D TO B AND A	359 58 1.08	359 58 0.24	0.845
STATION D TO C AND B	359 57 12.81	359 57 17.27	-4.462
STATION D TO E AND C	324 2 13.31	324 2 10.06	3.256
STATION D TO F AND E	352 27 19.80	352 27 19.29	0.513
STATION D TO G AND F	336 58 23.57	336 58 22.55	1.021
STATION D TO I AND G	321 26 44.17	321 26 46.45	-2.278
STATION E TO I AND H	358 42 20.07	358 42 20.69	-0.616
STATION E TO A AND I	270 0 47.68	270 0 48.65	-0.970
STATION E TO B AND A	21 18 50.16	21 18 51.88	-1.720
STATION E TO C AND B	3 48 16.58	3 48 14.21	2.376
STATION E TO D AND C	6 52 12.69	6 52 12.74	-0.051
STATION E TO F AND D	12 56 33.58	12 56 35.09	-1.513
STATION E TO H AND F	46 20 59.24	46 20 56.75	2.493
STATION F TO A AND E	99 22 49.30	99 22 52.06	-2.758
STATION F TO B AND A	39 4 0.13	39 4 1.09	-0.965
STATION F TO C AND B	7 45 46.88	7 45 43.07	3.817
STATION F TO D AND C	13 18 7.23	13 18 7.98	-0.752
STATION F TO E AND D	200 29 16.46	200 29 15.80	0.657
STATION G TO A AND I	169 59 26.02	169 59 23.99	2.033
STATION G TO B AND A	33 24 58.70	33 24 58.55	0.146
STATION G TO C AND B	11 14 13.80	11 14 16.89	-3.083
STATION G TO D AND C	24 8 38.88	24 8 39.71	-0.836
STATION G TO E AND D	229 43 49.95	229 43 47.86	2.093
STATION G TO H AND E	314 41 13.36	314 41 15.27	-1.906
STATION G TO I AND H	296 47 39.29	296 47 37.74	1.553
STATION H TO A AND I	234 30 48.61	234 30 49.26	-0.647
STATION H TO E AND A	307 39 49.19	307 39 49.63	-0.443
STATION H TO G AND E	94 33 12.86	94 33 13.13	-0.268
STATION H TO I AND G	83 16 9.34	83 16 7.98	1.359
STATION I TO C AND H	45 3 14.42	45 3 13.70	0.721
STATION I TO D AND C	8 42 20.23	8 42 21.65	-1.420
STATION I TO E AND D	307 7 24.42	307 7 24.23	0.198
STATION I TO G AND E	32 38 30.02	32 38 30.18	-0.155
STATION I TO H AND G	326 28 30.90	326 28 30.24	0.656

SECTION 3: STRAIN DETERMINATION FOR THE DUNEDIN WEST NETWORK

3.1 Introduction

The Dunedin West strain determination covers the eastern end of the Taieri Depression and most of the developed part of the City of Dunedin. Figure 3.1 shows the extent of the study area and the trigs which were included in the analysis. The trigs are also listed, with approximate coordinates in table 3.3. There are numerous sources of data for this project with the oldest being original 1857 and 1859 surveys of the Province of Otago and the most recent being surveys conducted by DOSLI in the mid 1980s. The specific sources of data for this strain determination are listed in table 3.1 and the actual data used in the calculation are listed in appendix 3.1. The strains were determined using a uniform strain code (NOSTRN) described by Bibby (1981). The strains determined from this data are listed in Table 3.2.

TABLE 3.1

SOURCES OF DATA FOR STRAIN DETERMINATIONS

YEAR	S.O. Plan ref	Brief description	Surveyor
1857	425	4th Order Province of Otago	Alex Garvie
1859	1262A	4th Order Dunedin & E Taieri S.D.	Alex Garvie
1859	1259	4th Order Dunedin & Otago Harbour	N. Mull
1887	4098	4th Order W Dunedin - Lookout Point	E. Farnie
1891	426	4th Order Forbury - Jefferys Hill	N.L. Falkiner
1918	1262	4th Order Flagstaff - A North Taieri	N Mull
1936-39	2299	2nd Order Upper Harbour	J. Meale
1938-39	2298	2nd Order E Taieri S.D	J. Meale
1955		2nd Order E Taieri	N.Z. Gov. Surv.
1983		2nd Order E Taieri	N.Z. Gov. Surv.

3.2 Results of Strain Determinations

TABLE 3.2

RESULTS OF STRAIN DETERMINATIONS

NETWORK	$\gamma1$ (μrad/yr)	±1 S.E.	$\gamma2$ (μrad/yr)	±1 S.E.	covariance
Dunedin	0.083	0.233	0.150	0.218	-0.593E-14

The strains are not significant at the 1 S.E. level of confidence and all we can say is that the strains are likely to be less than about 0.2 μrad/yr. at the 1 S.E. level of confidence.

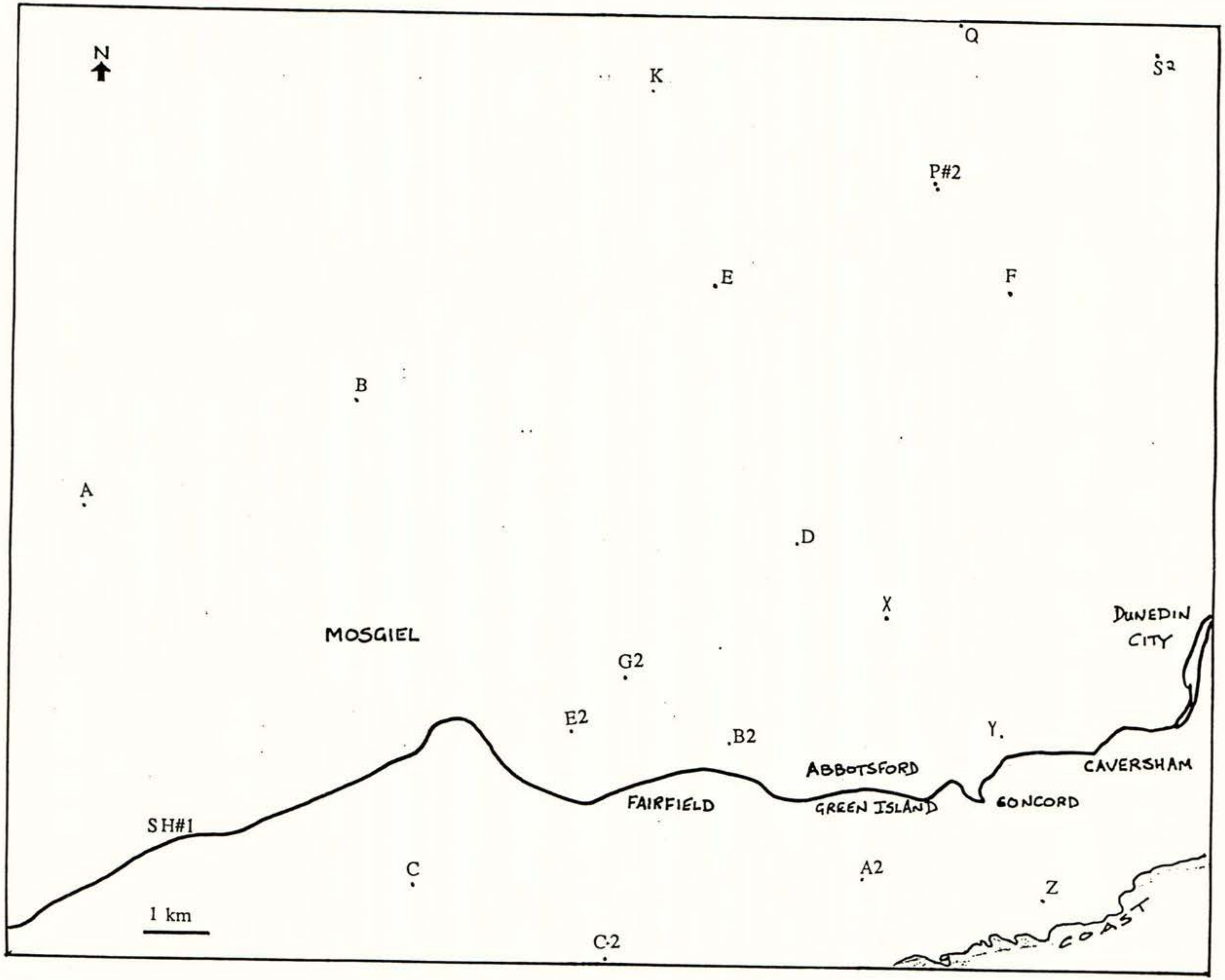

Fig. 3.1: Map showing locations of trigs in the Dunedin West network

3.3 Trig Stability

Table 3.3 lists the approximate coordinates of the trigs and the type of bedrock on which the trigs are constructed. The type of bedrock was identified from the Benson (1968) and McKellar (1990) geological maps of the Dunedin area. The type of bedrock is important because the Dunedin area has a history of large landslides (McKellar 1990). Most of the landslides have occurred in sedimentary rocks, particularly the Abbotsford Mudstone. Most of the Trigs included in this readjustment are located on volcanic bedrock (as for F Flagstaff and Z Forbury Hill for example). A few are on Quaternary Alluvium but these are generally located on flat or gently rolling terrain (as for trigs A and B for example). Some of the trigs (such as Q, K and B2) are located on Abbotsford Mudstone, in which case, trig instability is a potential problem. In addition, in the 130 years since the first surveys, it is always possible that some unreported cultural disturbance of the trigs may have occurred. For this reason, the residuals from NOSTRN have been carefully examined to see if some evidence of trig instability can be found. It would be expected that any trig that has been disturbed either by site instability or relocation by later surveyors would have significantly higher residuals because this trig probably would not fit the uniform strain model as well as the other trigs.

TABLE 3.3

TRIGS USED IN THE DUNEDIN WEST STRAIN DETERMINATION

Trig#	Trig Name	Latitude			Longitude			Height	Rock*
		Deg	Min	Sec	Deg	Min	Sec	m amsl	Type
1	F Flagstaff	-45	50	3.9375	170	27	58.8384	668.0	V
14	Z Forbury Hill	-45	55	4.3280	170	28	15.9859	159.0	V
15	C J.H	-45	54	51.3870	170	20	47.2101	410.	V
18	A N-T	-45	51	41.4684	170	16	54.6748	7	Q
17	B E-T	-45	50	51.8217	170	20	13.1194	28	Q
3	Q	-45	47	43.9246	170	27	26.4539	505.0	A
2	K	-45	48	22.2966	170	23	47.0363	483.0	A
5	S2 Swampy Spur	-45	47	46.7092	170	28	36.7402	739.0	V
25	E Dn&Et	-45	49	57.4724	170	24	27.7572	259.	V
10	D Abbots.Hill	-45	52	6.6178	170	25	21.3945	361.0	V
27	E2	-45	53	37.0605	170	22	39.1727	170.	S
28	G2	-45	53	9.0413	170	23	16.6201	172.	S
30	C2	-45	55	28.2826	170	22	57.8534	80.	V
29	B2	-45	53	44.3476	170	24	30.6792	52.	A
11	X Kaikorai Hill	-45	52	44.2444	170	26	23.7521	334.0	V
21	A2 GI B	-45	54	52.7615	170	26	3.2662	189.	V
36	Y Farne	-45	53	42.3633	170	27	45.6577	162.	C
4	P#2	-45	49	10.9832	170	27	6.4504	376.0	V

KEY*
V Volcanic Rocks
Q Quaternary Alluvium
S Schist
A Abbotsford Mudstone
C Caversham Sandstone

The residuals from the NOSTRN readjustment are shown in figure 3.2 and 3.3. All of the residuals are listed in appendix 3.2. In figure 3.2, the residuals have been plotted against the trigs involved in the observation. Since each measured angle involves 3 trigs (i.e the two trigs that are observed and the trig from which the observations are made), each residual is plotted three times.

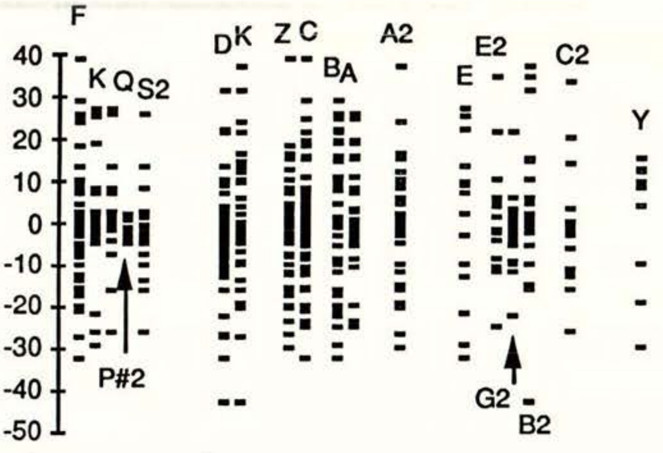

FIGURE 3.2: Residuals for all of the stations included in the Dunedin West strain determinations

FIGURE 3.3: Residuals for the surveys used in the Dunedin West strain determination

In figure 3.3, the trigs are plotted against the year in which the observations were made. This figure provides a measure of the relative accuracy of the surveys. The major point from figure 3.2 is that the residuals for most of the trigs are comparable. One trig (P#2) has residuals an order of magnitude lower than the other trigs but this trig was only included in the 1948 survey which, as shown in figure 3.3, has much lower residuals than the pre 1900's surveys that include all of the other trigs. With this exception, there is no evidence that any one trig has vastly greater errors than the others. The fact that all of the trigs have similar errors is important because it suggests that all of the trigs have been stable since they were established. Any observations involving unstable trigs would be expected to give larger residuals than those involving only stable trigs which fit the uniform strain model more closely. Figure 3.3 shows the residuals plotted as a function of time. As expected, the residuals of the original surveys are much greater (by more than an order of magnitude) than the residuals of the later surveys. The very large residuals (of more than 40") for some of the original surveys are reflected by similarly large triangle closure errors for these surveys. In the Dunedin area, it is the large errors in the early (pre 1900) surveys that cause the large errors in the strain determination listed in table 3.2.

3.4 Conclusions

Significant strain for the Dunedin West Network was not detected within the limits of error. All that can be concluded from the results is that the strains are less than 0.2μrad/yr at the 1 S.E. level of confidence. The errors associated with the strain determination are rather disappointing. They appear to be controlled by the relatively poor quality of the pre-1900's data for the Dunedin area. It might be possible to determine the strains more precisely by repeating the 1937-8 and 1948 surveys using GPS techniques. Since 55 years have elapsed since the earliest of these surveys, a strain determination involving the 1937-1948 data and a sufficient amount of 1992 or later data could potentially improve our ability to resolve strains in the Dunedin Area.

Appendix 3·1

APPENDIX 1 DATA USED IN DUNEDIN WEST STRAIN DETERMINATION

Dunedin Area West all rays

	1857.5			
1 (F)	14 (Z)	178	20	17.0
	15 (C)	226	21	17.0
	17 (B)	261	38	4.0
14 (Z)	1 (F)	358	20	17.0
	15 (C)	272	9	17.0
15 (C)	14 (Z)	92	9	17.0
	1 (F)	46	21	17.0
	17 (B)	354	29	45.0
	18 (A)	319	59	24.0
18 (A)	17 (B)	69	56	14.0
	15 (C)	139	59	24.0
17 (B)	1 (F)	81	38	4.0
	15 (C)	174	29	45.0
	18 (A)	249	56	20.0
	1859.3			
1 (F)	11 (X)	202	23	18.0
	10 (D)	221	45	48.0
	25 (E)	272	26	38.0
	5 (S2)	11	4	58.0
3 (Q)	5 (S2)	92	2	7.0
	2 (K)	256	13	13.0
2 (K)	3 (Q)	76	12	53.0
	25 (E)	163	19	10.0
	17 (B)	225	2	7.0
5 (S2)	1 (F)	191	4	58.0
	25 (E)	232	59	11.0
	3 (Q)	272	2	15.0
25 (E)	1 (F)	92	26	43.0
	10 (D)	163	34	17.0
	17 (B)	253	6	47.0
	2 (K)	343	19	10.0
17 (B)	2 (K)	45	3	0.0
	25 (E)	73	6	47.0
	10 (D)	108	59	54.0
	11 (X)	113	28	57.0
	28 (G2)	136	58	47.0
	15 (C)	174	29	27.0
	18 (A)	249	56	20.0
10 (D)	1 (F)	41	45	57.0
	11 (X)	131	32	27.0

	29 (B2)	200	3	17.0
	15 (C)	229	18	50.0
	27 (E2)	231	6	50.0
	28 (G2)	233	1	14.0
	17 (B)	288	59	54.0
	25 (E)	343	34	17.0
18 (A)	17 (B)	69	56	20.0
	15 (C)	139	58	46.0
15 (C)	28 (G2)	46	35	57.0
	27 (E2)	46	54	17.0
	30 (C2)	111	59	11.0
	10 (D)	49	19	1.0
	18 (A)	319	59	24.0
	17 (B)	354	30	11.0
27 (E2)	15 (C)	226	54	17.0
	30 (C2)	173	31	24.0
	10 (D)	51	7	30.0
28 (G2)	10 (D)	53	0	54.0
	27 (E2)	225	43	7.0
	17 (B)	0	58	47.0
30 (C2)	27 (E2)	353	30	27.0
	29 (B2)	31	44	56.0
	21 (A2)	74	0	37.0
	15 (C)	291	59	11.0
29 (B2)	10 (D)	20	4	0.0
	11 (X)	52	50	13.0
	21 (A2)	136	53	0.0
	30 (C2)	211	45	10.0
	27 (E2)	274	42	57.0
11 (X)	1 (F)	22	23	23.0
	21 (A2)	186	39	20.0
	17 (B)	293	28	56.0
	29 (B2)	232	50	13.0
	10 (D)	311	32	43.0
21 (A2)	14 (Z)	97	16	0.0
	11 (X)	6	39	20.0
	29 (B2)	316	52	30.0
	30 (C2)	254	1	0.0
14 (Z)	1 (F)	358	20	40.0
	10 (D)	326	25	30.0
	21 (A2)	277	15	37.0
	15 (C)	272	9	17.0
	1887			
21 (A2)	11 (X)	6	39	20.0
	36 (Y)	45	42	12.0
	14 (Z)	97	16	10.0

11 (X)	21 (A2)	186	39	20.0
	36 (Y)	133	28	1.0
36 (Y)	11 (X)	313	28	1.0
	14 (Z)	169	14	23.0
	21 (A2)	225	42	9.0
14 (Z)	36 (Y)	349	14	21.0
	11 (X)	331	46	49.0
	21 (A2)	277	16	11.0
	1891.2			
15 (C)	30 (C2)	111	59	11.0
	14 (Z)	92	9	17.0
30 (C2)	15 (C)	291	59	11.0
	21 (A2)	74	0	44.0
21 (A2)	30 (C2)	254	0	44.0
	14 (Z)	97	16	0.0
14 (Z)	21 (A2)	277	15	37.0
	15 (C)	272	9	17.0
	1918.6			
18 (A)	17 (B)	69	58	9.0
	15 (C)	140	0	51.0
17 (B)	18 (A)	249	58	22.0
	15 (C)	174	31	40.0
	1 (F)	81	39	32.0
15 (C)	18 (A)	320	0	51.0
	17 (B)	354	31	40.0
	1 (F)	46	22	40.0
	14 (Z)	92	10	58.0
14 (Z)	1 (F)	358	21	37.0
	15 (C)	272	10	38.0
1 (F)	14 (Z)	178	21	37.0
	15 (C)	226	22	40.0
	17 (B)	261	39	50.0
	1937.5			
1 (F)	14 (Z)	178	21	43.4
	10 (D)	221	47	24.3
	28 (G2)	226	15	12.1
	15 (C)	226	22	58.6
14 (Z)	1 (F)	358	21	42.7
	10 (D)	326	26	38.5
	15 (C)	272	10	27.2

	1939.5			
18 (A)	28 (G2)	108	33	18.8
	15 (C)	140	0	51.0
1 (F)	15 (C)	226	22	58.6
	28 (G2)	226	15	12.1
	10 (D)	221	47	24.3
	14 (Z)	178	21	43.4
10 (D)	1 (F)	41	47	22.5
	14 (Z)	146	26	36.8
	15 (C)	229	20	13.5
	28 (G2)	233	2	45.4
28 (G2)	10 (D)	53	2	46.6
	15 (C)	226	37	12.0
	18 (A)	288	33	18.8
15 (C)	18 (A)	320	0	51.0
	1 (F)	46	22	54.2
	28 (G2)	46	37	11.2
	10 (D)	49	20	13.5
	14 (Z)	92	10	27.2
14 (Z)	1 (F)	358	21	42.7
	10 (D)	326	26	38.5
	15 (C)	272	10	27.2
	1948.5			
2 (K)	3 (Q)	76	15	14.2
	5 (S2)	79	58	54.2
	4 (P2)	109	15	37.2
	1 (F)	120	4	7.2
3 (Q)	2 (K)	256	15	0.2
	4 (P2)	189	31	39.2
	5 (S2)	92	3	25.2
5 (S2)	3 (Q)	272	3	25.2
	2 (K)	259	58	46.2
	4 (P2)	216	58	28.2
	1 (F)	191	6	34.2
4 (P2)	2 (K)	289	15	29.2
	3 (Q)	9	31	38.2
	5 (S2)	36	58	28.2
1 (F)	2 (K)	300	4	7.2
	5 (S2)	11	6	34.2
	1955.1			
21 (A2)	29 (B2)	44	34	41.7

	10 (D)	78	5	29.3
	11 (X)	94	21	41.3
29 (B2)	10 (D)	134	17	44.0
	11 (X)	167	4	38.5
	21 (A2)	251	6	47.5
	1983.5			
27 (E2)	10 (D)	191	1	47.6
	11 (X)	211	5	51.8
27 (E2)	28 (G2)	186	22	11.8
	10 (D)	191	45	22.8
1 (F)	10 (D)	278	28	20.7
	18 (A)	314	45	40.8
10 (D)	1 (F)	174	46	24.6
	11 (X)	264	33	14.0
	21 (A2)	303	23	22.3
	29 (B2)	333	3	35.6
	28 (G2)	6	1	44.1
	18 (A)	46	59	3.3
11 (X)	27 (E2)	10	37	21.9
	28 (G2)	17	46	15.4
	10 (D)	70	59	9.3
	21 (A2)	306	5	28.2
21 (A2)	29 (B2)	44	34	40.2
	11 (X)	94	21	37.3

Appendix 3.2

APPENDIX 2 DATA RESIDUALS FROM DUNEDIN WEST STRAIN DETERMINATION
Trigs are identified by number from table 3.

ANGLE Station #	OBSERVED deg min sec	CALCULATED deg min sec	DIFFERENCE seconds
SURVEY NUMBER 1 DATE 1857.50			
STATION 1 TO 14 AND 17	276 42 13.00	276 42 2.60	10.403
STATION 1 TO 15 AND 14	48 1 0.00	48 1 15.33	-15.326
STATION 1 TO 17 AND 15	35 16 47.00	35 16 42.08	4.922
STATION 14 TO 1 AND 15	86 11 0.00	86 11 4.70	-4.695
STATION 14 TO 15 AND 1	273 48 60.00	273 48 55.30	4.695
STATION 15 TO 14 AND 18	132 9 53.00	132 9 44.32	8.676
STATION 15 TO 1 AND 14	314 11 60.00	314 12 19.78	-19.782
STATION 15 TO 17 AND 1	308 8 28.00	308 8 27.84	0.156
STATION 15 TO 18 AND 17	325 29 39.00	325 29 28.05	10.95
STATION 18 TO 17 AND 15	289 56 50.00	289 57 9.50	-19.505
STATION 18 TO 15 AND 17	70 3 10.00	70 2 50.50	19.505
STATION 17 TO 1 AND 18	191 41 44.00	191 41 36.39	7.612
STATION 17 TO 15 AND 1	92 51 41.00	92 51 45.96	-4.957
STATION 17 TO 18 AND 15	75 26 35.00	75 26 37.65	-2.655
SURVEY NUMBER 2 DATE 1859.30			
STATION 1 TO 11 AND 5	191 18 20.00	191 18 33.36	-13.36
STATION 1 TO 10 AND 11	19 22 30.00	19 22 16.60	13.398
STATION 1 TO 25 AND 10	50 40 50.00	50 40 40.26	9.739
STATION 1 TO 5 AND 25	98 38 20.00	98 38 29.78	-9.776
STATION 3 TO 5 AND 2	195 48 54.00	195 48 28.40	25.603
STATION 3 TO 2 AND 5	164 11 6.00	164 11 31.60	-25.603
STATION 2 TO 3 AND 17	211 10 46.00	211 10 44.55	1.449
STATION 2 TO 25 AND 3	87 6 17.00	87 5 49.61	27.39
STATION 2 TO 17 AND 25	61 42 57.00	61 43 25.84	-28.839
STATION 5 TO 1 AND 3	279 2 43.00	279 2 58.63	-15.63
STATION 5 TO 25 AND 1	41 54 13.00	41 54 11.03	1.969
STATION 5 TO 3 AND 25	39 3 4.00	39 2 50.34	13.662
STATION 25 TO 1 AND 2	109 7 33.00	109 7 7.74	25.262
STATION 25 TO 10 AND 1	71 7 34.00	71 7 47.02	-13.023
STATION 25 TO 17 AND 10	89 32 30.00	89 32 20.74	9.26
STATION 25 TO 2 AND 17	90 12 23.00	90 12 44.50	-21.499
STATION 17 TO 2 AND 18	155 6 40.00	155 6 21.31	18.69
STATION 17 TO 25 AND 2	28 3 47.00	28 3 49.73	-2.73
STATION 17 TO 10 AND 25	35 53 7.00	35 53 38.73	-31.734
STATION 17 TO 11 AND 10	4 29 3.00	4 28 41.65	21.345
STATION 17 TO 28 AND 11	23 29 50.00	23 29 59.20	-9.201
STATION 17 TO 15 AND 28	37 30 40.00	37 30 51.75	-11.755
STATION 17 TO 18 AND 15	75 26 53.00	75 26 37.62	15.384
STATION 10 TO 1 AND 25	58 11 40.00	58 11 32.75	7.254
STATION 10 TO 11 AND 1	89 46 30.00	89 46 56.76	-26.763
STATION 10 TO 29 AND 11	68 30 50.00	68 30 18.64	31.357
STATION 10 TO 15 AND 29	29 15 33.00	29 15 38.25	-5.252
STATION 10 TO 27 AND 15	1 48 0.00	1 48 8.28	-8.279
STATION 10 TO 28 AND 27	1 54 24.00	1 54 22.42	1.582
STATION 10 TO 17 AND 28	55 58 40.00	55 59 2.30	-22.299
STATION 10 TO 25 AND 17	54 34 23.00	54 34 0.60	22.399
STATION 18 TO 17 AND 15	289 57 34.00	289 57 9.50	24.497
STATION 18 TO 15 AND 17	70 2 26.00	70 2 50.50	-24.497

STATION 15 TO 28 AND 17	52 5 46.00	52 5 46.85	-0.849
STATION 15 TO 27 AND 28	0 18 20.00	0 18 14.23	5.767
STATION 15 TO 30 AND 27	65 4 54.00	65 5 4.73	-10.733
STATION 15 TO 10 AND 30	297 19 50.00	297 19 48.69	1.305
STATION 15 TO 18 AND 10	270 40 23.00	270 40 33.50	-10.502
STATION 15 TO 17 AND 18	34 30 47.00	34 30 31.99	15.013
STATION 27 TO 15 AND 10	175 46 47.00	175 46 58.30	-11.295
STATION 27 TO 30 AND 15	306 37 7.00	306 36 45.56	21.443
STATION 27 TO 10 AND 30	237 36 6.00	237 36 16.15	-10.148
STATION 28 TO 10 AND 17	96 2 7.00	96 2 16.88	-9.882
STATION 28 TO 27 AND 10	172 42 13.00	172 42 24.42	-11.421
STATION 28 TO 17 AND 27	91 15 40.00	91 15 18.70	21.304
STATION 30 TO 27 AND 15	61 31 16.00	61 31 40.82	-24.823
STATION 30 TO 29 AND 27	38 14 29.00	38 13 54.67	34.332
STATION 30 TO 21 AND 29	42 15 41.00	42 15 55.39	-14.391
STATION 30 TO 15 AND 21	217 58 34.00	217 58 29.12	4.882
STATION 29 TO 10 AND 27	105 21 3.00	105 20 52.84	10.161
STATION 29 TO 11 AND 10	32 46 13.00	32 46 55.44	-42.44
STATION 29 TO 21 AND 11	84 2 47.00	84 2 10.06	36.945
STATION 29 TO 30 AND 21	74 52 10.00	74 52 19.52	-9.516
STATION 29 TO 27 AND 30	62 57 47.00	62 57 42.15	4.851
STATION 11 TO 1 AND 10	70 50 40.00	70 50 46.66	-6.66
STATION 11 TO 21 AND 1	164 15 57.00	164 15 33.18	23.82
STATION 11 TO 17 AND 21	106 49 36.00	106 49 51.69	-15.69
STATION 11 TO 29 AND 17	299 21 17.00	299 21 2.54	14.458
STATION 11 TO 10 AND 29	78 42 30.00	78 42 45.93	-15.928
STATION 21 TO 14 AND 30	203 14 60.00	203 15 11.50	-11.502
STATION 21 TO 11 AND 14	269 23 20.00	269 23 29.36	-9.362
STATION 21 TO 29 AND 11	310 13 10.00	310 13 4.24	5.755
STATION 21 TO 30 AND 29	297 8 30.00	297 8 14.89	15.109
STATION 14 TO 1 AND 15	86 11 23.00	86 11 4.76	18.245
STATION 14 TO 10 AND 1	328 4 50.00	328 4 57.93	-7.931
STATION 14 TO 21 AND 10	310 50 7.00	310 50 33.20	-26.197
STATION 14 TO 15 AND 21	354 53 40.00	354 53 24.12	15.883

SURVEY NUMBER 3 DATE 1887.00

STATION 21 TO 11 AND 14	269 23 10.00	269 23 30.37	-20.372
STATION 21 TO 36 AND 11	39 2 52.00	39 2 39.93	12.072
STATION 21 TO 14 AND 36	51 33 58.00	51 33 49.70	8.3
STATION 11 TO 21 AND 36	53 11 19.00	53 11 9.24	9.764
STATION 11 TO 36 AND 21	306 48 41.00	306 48 50.76	-9.764
STATION 36 TO 11 AND 21	87 45 52.00	87 46 10.87	-18.869
STATION 36 TO 14 AND 11	215 46 22.00	215 46 18.15	3.852
STATION 36 TO 21 AND 14	56 27 46.00	56 27 30.98	15.017
STATION 14 TO 36 AND 21	71 58 10.00	71 58 39.33	-29.332
STATION 14 TO 11 AND 36	342 32 28.00	342 32 15.47	12.529
STATION 14 TO 21 AND 11	305 29 22.00	305 29 5.20	16.803

SURVEY NUMBER 4 DATE 1891.20

STATION 15 TO 30 AND 14	19 49 54.00	19 49 53.47	0.535
STATION 15 TO 14 AND 30	340 10 6.00	340 10 6.53	-0.535
STATION 30 TO 15 AND 21	217 58 27.00	217 58 28.83	-1.83
STATION 30 TO 21 AND 15	142 1 33.00	142 1 31.17	1.83
STATION 21 TO 30 AND 14	156 44 44.00	156 44 48.79	-4.788
STATION 21 TO 14 AND 30	203 15 16.00	203 15 11.21	4.788
STATION 14 TO 21 AND 15	5 6 20.00	5 6 35.85	-15.848
STATION 14 TO 15 AND 21	354 53 40.00	354 53 24.15	15.848

SURVEY NUMBER 5 DATE 1918.60

STATION 18 TO 17 AND 15	289 57 18.00	289 57 9.47	8.532
STATION 18 TO 15 AND 17	70 2 42.00	70 2 50.53	-8.532
STATION 17 TO 18 AND 1	168 18 50.00	168 18 23.94	26.056
STATION 17 TO 15 AND 18	284 33 18.00	284 33 23.45	-5.454
STATION 17 TO 1 AND 15	267 7 52.00	267 8 12.60	-20.601
STATION 15 TO 18 AND 14	227 49 53.00	227 50 16.25	-23.253
STATION 15 TO 17 AND 18	34 30 49.00	34 30 33.02	15.978
STATION 15 TO 1 AND 17	51 50 60.00	51 51 31.84	-31.836
STATION 15 TO 14 AND 1	45 48 18.00	45 47 38.89	39.111
STATION 14 TO 1 AND 15	86 10 59.00	86 11 6.42	-7.421
STATION 14 TO 15 AND 1	273 49 1.00	273 48 53.58	7.421
STATION 1 TO 14 AND 17	276 41 47.00	276 42 4.11	-17.115
STATION 1 TO 15 AND 14	48 1 3.00	48 1 14.93	-11.929
STATION 1 TO 17 AND 15	35 17 10.00	35 16 40.96	29.043

SURVEY NUMBER 6 DATE 1937.50

STATION 1 TO 14 AND 15	311 58 44.80	311 58 45.28	-0.484
STATION 1 TO 10 AND 14	43 25 40.90	43 25 43.62	-2.716
STATION 1 TO 28 AND 10	4 27 47.80	4 27 46.55	1.255
STATION 1 TO 15 AND 28	0 7 46.50	0 7 44.56	1.945
STATION 14 TO 1 AND 15	86 11 15.50	86 11 7.35	8.155
STATION 14 TO 10 AND 1	328 4 55.80	328 4 56.53	-0.726
STATION 14 TO 15 AND 10	305 43 48.70	305 43 56.13	-7.429

SURVEY NUMBER 7 DATE 1939.50

STATION 18 TO 28 AND 15	328 32 27.80	328 32 30.41	-2.609
STATION 18 TO 15 AND 28	31 27 32.20	31 27 29.59	2.609
STATION 1 TO 15 AND 14	48 1 15.20	48 1 14.70	0.499
STATION 1 TO 28 AND 15	359 52 13.50	359 52 15.44	-1.945
STATION 1 TO 10 AND 28	355 32 12.20	355 32 13.46	-1.26
STATION 1 TO 14 AND 10	316 34 19.10	316 34 16.39	2.706
STATION 10 TO 1 AND 28	168 44 37.10	168 44 36.19	0.913
STATION 10 TO 14 AND 1	104 39 14.30	104 39 12.97	1.327
STATION 10 TO 15 AND 14	82 53 36.70	82 53 40.33	-3.63
STATION 10 TO 28 AND 15	3 42 31.90	3 42 30.51	1.39
STATION 28 TO 10 AND 18	124 29 27.80	124 29 27.49	0.308
STATION 28 TO 15 AND 10	173 34 25.40	173 34 21.96	3.437
STATION 28 TO 18 AND 15	61 56 6.80	61 56 10.54	-3.744
STATION 15 TO 18 AND 14	227 50 23.80	227 50 16.58	7.216
STATION 15 TO 1 AND 18	86 22 3.20	86 22 5.29	-2.09
STATION 15 TO 28 AND 1	0 14 17.00	0 14 14.69	2.309
STATION 15 TO 10 AND 28	2 43 2.30	2 43 7.53	-5.23
STATION 15 TO 14 AND 10	42 50 13.70	42 50 15.90	-2.205
STATION 14 TO 1 AND 15	86 11 15.50	86 11 7.41	8.089
STATION 14 TO 10 AND 1	328 4 55.80	328 4 56.49	-0.69
STATION 14 TO 15 AND 10	305 43 48.70	305 43 56.10	-7.399

SURVEY NUMBER 8 DATE 1948.50

STATION 2 TO 3 AND 1	316 11 7.00	316 10 59.65	7.347
STATION 2 TO 5 AND 3	3 43 40.00	3 43 40.18	-0.179
STATION 2 TO 4 AND 5	29 16 43.00	29 16 47.35	-4.349
STATION 2 TO 1 AND 4	10 48 30.00	10 48 32.82	-2.819
STATION 3 TO 2 AND 5	164 11 35.00	164 11 32.20	2.801
STATION 3 TO 4 AND 2	293 16 39.00	293 16 37.83	1.172
STATION 3 TO 5 AND 4	262 31 46.00	262 31 49.97	-3.972

STATION 5 TO 3 AND 1	80 56 51.00	80 56 58.17	-7.174
STATION 5 TO 2 AND 3	347 55 21.00	347 55 12.38	8.621
STATION 5 TO 4 AND 2	316 59 42.00	316 59 45.32	-3.323
STATION 5 TO 1 AND 4	334 8 6.00	334 8 4.12	1.875
STATION 4 TO 2 AND 5	252 17 1.00	252 17 2.01	-1.008
STATION 4 TO 3 AND 2	80 16 9.00	80 16 10.33	-1.326
STATION 4 TO 5 AND 3	27 26 50.00	27 26 47.67	2.333
STATION 1 TO 2 AND 5	288 57 33.00	288 57 30.64	2.356
STATION 1 TO 5 AND 2	71 2 27.00	71 2 29.36	-2.356

SURVEY NUMBER 9 DATE 1955.10

STATION 21 TO 29 AND 11	310 13 0.40	310 13 1.73	-1.333
STATION 21 TO 10 AND 29	33 30 47.60	33 30 46.12	1.478
STATION 21 TO 11 AND 10	16 16 12.00	16 16 12.15	-0.145
STATION 29 TO 10 AND 21	243 10 56.50	243 10 57.05	-0.549
STATION 29 TO 11 AND 10	32 46 54.50	32 46 54.08	0.418
STATION 29 TO 21 AND 11	84 2 9.00	84 2 8.87	0.131

SURVEY NUMBER 10 DATE 1983.50

STATION 27 TO 10 AND 11	339 55 55.80	339 56 0.08	-4.28
STATION 27 TO 11 AND 10	20 4 4.20	20 3 59.92	4.28
STATION 27 TO 28 AND 10	354 36 49.00	354 36 47.25	1.755
STATION 27 TO 10 AND 28	5 23 11.00	5 23 12.75	-1.755
STATION 1 TO 10 AND 18	323 42 39.90	323 42 40.67	-0.766
STATION 1 TO 18 AND 10	36 17 20.10	36 17 19.33	0.766
STATION 10 TO 1 AND 18	127 47 21.30	127 47 21.01	0.292
STATION 10 TO 11 AND 1	89 46 49.37	89 46 54.03	-4.659
STATION 10 TO 21 AND 11	38 50 8.33	38 50 11.18	-2.848
STATION 10 TO 29 AND 21	29 40 13.27	29 40 11.14	2.132
STATION 10 TO 28 AND 29	32 58 8.53	32 58 7.17	1.359
STATION 10 TO 18 AND 28	40 57 19.20	40 57 15.48	3.725
STATION 11 TO 27 AND 21	64 31 53.70	64 31 43.64	10.058
STATION 11 TO 28 AND 27	7 8 53.50	7 8 55.42	-1.917
STATION 11 TO 10 AND 28	53 12 53.90	53 12 57.47	-3.57
STATION 11 TO 21 AND 10	235 6 18.90	235 6 23.47	-4.571
STATION 21 TO 29 AND 11	310 13 2.90	310 13 0.99	1.912
STATION 21 TO 11 AND 29	49 46 57.10	49 46 59.01	-1.912

SECTION 4: STRAIN DETERMINATION FOR THE DUNEDIN EAST NETWORK

4.1 Introduction

Triangulation data for the Dunedin East strain determination covers the City of Dunedin and the Otago Harbour west of Port Chalmers. Figure 4.1 shows the extent of the study area and the trigs which were included in the analysis. The trigs are also listed, with approximate coordinates, in table 4.3. There are numerous sources of data for this project with the oldest being original 1857 and 1859 surveys of the Province of Otago and the most recent being surveys conducted by DOSLI in the mid 1980s. The specific sources of data for this strain determination are listed in table 4.1 and the actual data used in the calculation are listed in appendix 4.1. The strains were determined using a uniform strain code (NOSTRN) described by Bibby (1981). The strains determined from this data are listed in Table 4.2.

TABLE 4.1

SOURCES OF DATA FOR STRAIN DETERMINATIONS

YEAR	S.O. Plan ref	Brief description	Surveyor
1857	425	4th Order Province of Otago	Alex Garvie
1859	1259	4th Order Dunedin & Otago Harbor	N. Mull
1936-39	2299	2nd Order Upper Harbour	J. Meale
1955		2 nd Order E Taieri	N.Z. Gov. Surv.
1983		2nd Order E Taieri	N.Z. Gov. Surv.

4.2 Results of Strain Determinations

TABLE 4.2

RESULTS OF STRAIN DETERMINATIONS

NETWORK	$\gamma 1$ µrad/yr	±1 S.E. µrad/yr	$\gamma 2$ µrad/yr	±1 S.E. µrad/yr	covariance
All data	0.157	0.234	1.560	0.221	0.104D-13
1937&1979 only	0.008	0.173	-0.119	0.155	-0.123D-14
1909, 1937 & 1979	-0.357	0.324	0.289	0.306	0.103D-13
1857, 1859 & 1909	0.569	0.758	3.61	0.715	-0.148D-13
Ex. 1909	0.086	0.225	1.23	0.221	0.131D-13
Ex. 1859	0.381	0.315	1.62	0.267	0.147D-13
Ex. 1857	-0.088	0.269	0.894	0.288	-0.131D-13

Fig. 4.1: Map of the Dunedin East network showing location of trigs.

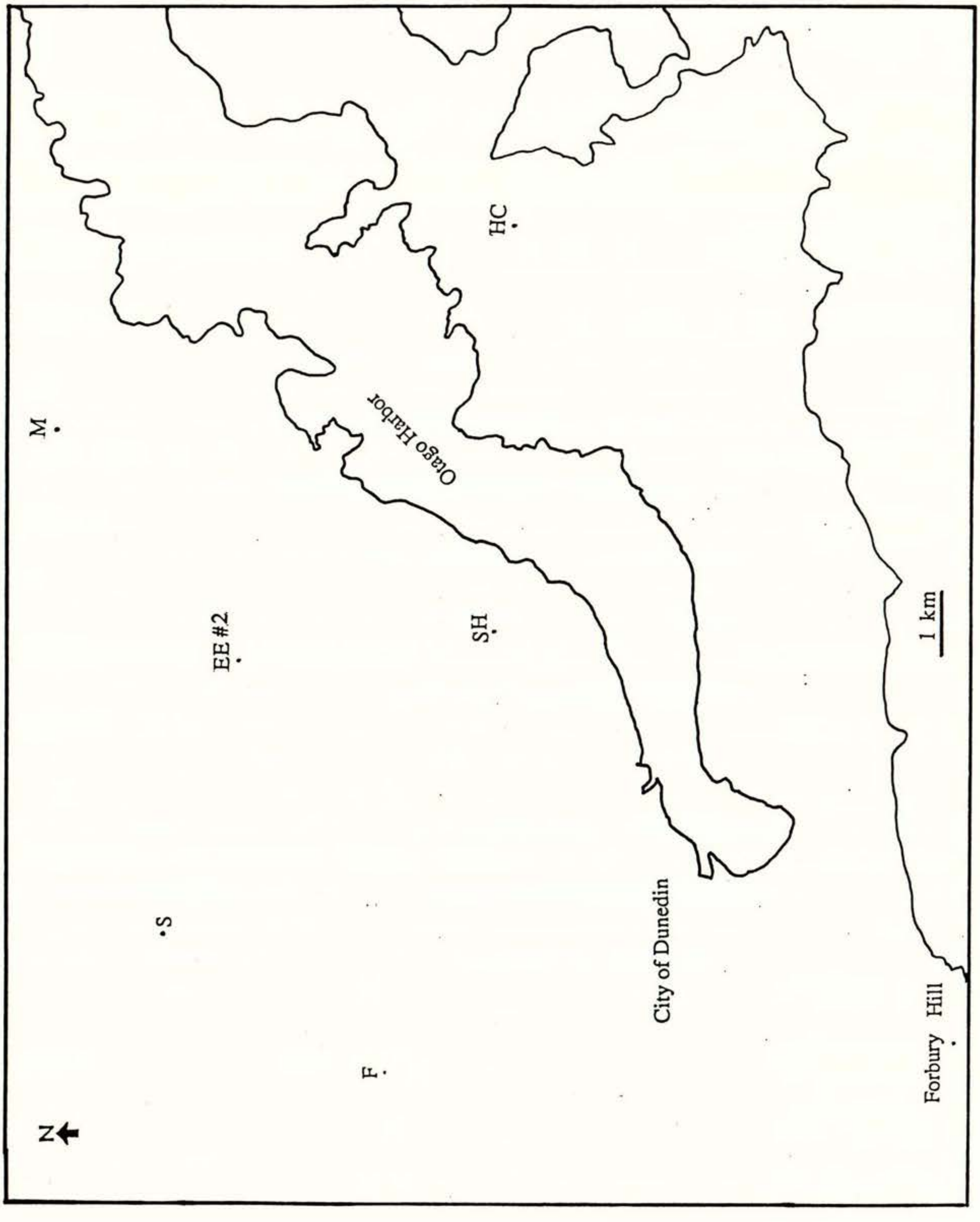

For the 1937 & 1979 data, the strains are not significant at the 1 S.E. level of confidence and all we can say is that the strains are likely to be less than about 0.2 μrad/yr. at the 1 S.E. level of confidence. The full data set did detect quite large strains which are significant at the 2 S.E. level of confidence.This corresponds to a maximum (engineering) shear strain (Γ) of 1.57 ± 0.24 μrad/yr with the orientation of the principal axis of contraction (Θ) = $186^\circ \pm 8^\circ$ (see Walcott 1984 for the mathematical definition of these quantities).

These high strains are rather unexpected in the Dunedin area. For this reason I suspected that they might be caused by a surveying error of some sort, such as a beacon which was not installed over its ground mark. If such an error exists it must be in the 1857, 1859 or 1909 survey as surveys after 1909 do not give these high strains. To test this possibility, I repeated the strain determination excluding each of these three surveys in turn. If the high strain rates are caused by a surveying error, then the high strains should disappear once this survey is removed from the strain determination. In all strain determinations, however, values of Γ remain near 1 μrad/yr, and the values of Θ are always 180°. Thus it does not appear that the high strains detected in the Dunedin East network are a function of poor surveying technique. It is still possible that the high strains might have been caused by local movement of an unstable trig, although in this case movement must have stopped in 1909.

4.3 Trig stability

Table 4.3 lists the approximate coordinates of the trigs and the type of bedrock on which the trigs are constructed. The type of bedrock was identified from the Benson (1968) and McKellar (1990) geological maps of the Dunedin area. The type of bedrock is important because the Dunedin area has a history of large landslides (McKellar 1990). Most of the landslides have occurred in sedimentary rocks, particularly the Abbotsford Mudstone. All of the Trigs included in this readjustment are located on volcanic bedrock. In addition, in the 130 years since the first surveys, it is always possible that some unreported cultural disturbance of the trigs may have occurred. In the case of Harbour Cone, the original monument was was not found by J. Meale in the 1936-1939 survey (Warburton 1991 pers. com.). He located a beacon close to the site of the original trig, and this beacon, without any benchmark, remained until the 1970's when a benchmark was placed under the beacon. For this reason, I have treated all observations to Harbour Cone made during and subsequent to J. Meale's survey as if they were to a separate trig (HC#2). There are no other suspect trigs in the Dunedin Area (Warburton 1991 pers. com.).

TABLE 3

TRIGS USED IN THE DUNEDIN EAST STRAIN DETERMINATION

Trig#	Trig Name	Latitude Deg	Min	Sec	Longitude Deg	Min	Sec	Height m amsl	Rock* Type
1	F Flagstaff	-45	50	3.9375	170	27	58.8384	668.0	V
6	EE#2	-45	48	52.3719	170	33	12.3784	740.07	V
8	S. Swampy Spur	-45	48	9.2580	170	29	47.5722	666.1	V
14	Z Forbury Hill	-45	55	4.3280	170	28	15.9859	159.0	V
16	SH Signal Hill	-45	51	6.3013	170	33	34.1369	393.0	V
33	M Mihiwaka	-45	47	21.1403	170	36	15.4147	315.0	V
34	HC Harbour Cone	-45	51	20.6216	170	38	45.5828	315.0	V
134	HC #2	-45	51	20.6216	170	38	45.5828	315.0	V

KEY*
V Volcanic Rocks

The residuals from the NOSTRN readjustment are shown in figure 4.2 and 4.3. All of the residuals are listed in appendix 4.2. In figure 4.2, the residuals are plotted against the trigs that are involved in the observation. Since each measured angle involves 3 trigs (i.e the two trigs that are observed and the trig from which the observations are made), each residual is plotted three times. In figure 4.3, the trigs are plotted against the year on which the observations were made. This figure provides a measure of the relative accuracy of the surveys. The major point from figure 4.2 is that the residuals for most of the trigs are comparable. One trig (EE#2) has residuals an order of magnitude lower than the other trigs but this trig was only included in the 1937 and 1979 surveys which, as shown in figure 4.3b, have much lower residuals than the pre 1900 surveys that include all of the other trigs. With this exception, there is no evidence that any one trig has significantly greater errors than the others. The fact that all of the trigs have similar errors is important because it suggests that all of the trigs have been stable since they were established. This is because any observations involving unstable trigs might be expected to give larger residuals than those involving only stable trigs which will fit the uniform strain model more closely.

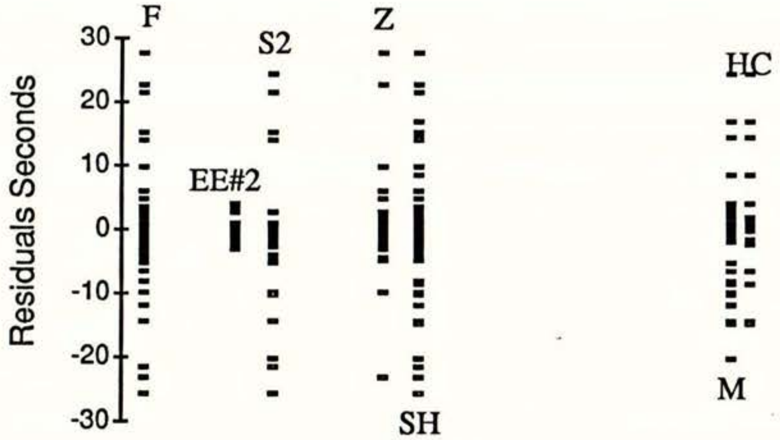

Fig. 4.2: Residuals plotted vs. trig for the full model

Figure 4.3b shows the residuals plotted as a function of time for the full data set. As expected, the residuals of the original surveys are much greater (by more than an order of magnitude) than the residuals of the later surveys. The very large residuals (of more than 40") for some of the original surveys are reflected by similarly large triangle closure errors for these surveys. In the Dunedin area, it is the large errors in the early (pre 1900) surveys that causes the large errors in the strain determination listed in table 4.2. There are two rather surprising conclusions from figure 4.3b. Firstly, the residuals for the 1909 survey are very large, nearly 40" and comparable to the 1859 survey. Secondly, the residuals for the 1857 survey are much smaller than the 1859 and 1909 surveys and actually comparable to those for the 1937 and 1979 surveys. This suggests that the data for the 1857 survey fits a model involving large strains better than the 1859 and 1909 data.

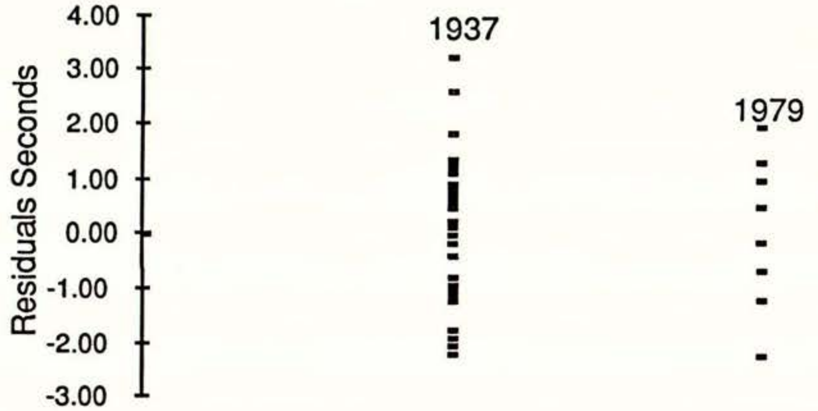

Figure 4.3a Residuals for the 1937 and 1979 strain determination

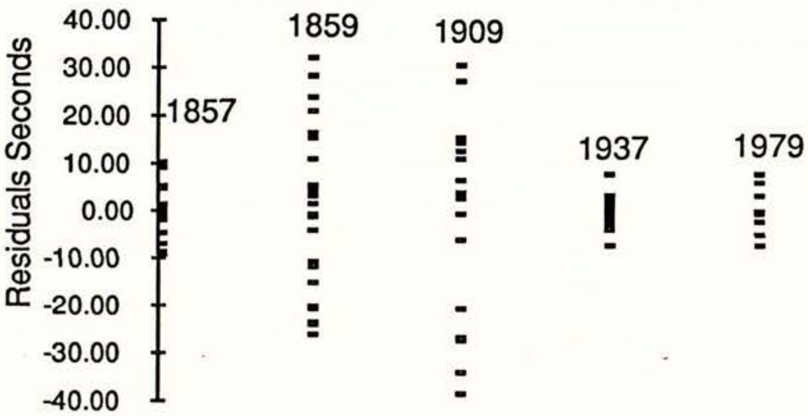

Figure 4.3b Residuals for the full data set

Fig. 4.3: Residuals plotted against year of survey

The mean residuals and the RMS residuals for each of the surveys calculated from the combined readjustment are listed in table 4.4, . All of the mean residuals are near zero, as would be expected, but the RMS residuals for the 1909 and 1859 data are quite large. The residuals for the 1909 survey are much larger than would be expected for a survey of this era. Even the residuals for the 1937 and 1979 data, while much smaller than for the earlier surveys, are still larger than would normally be expected for surveys of this era. Table 3.4 also shows residuals for the readjustment including only the 1937 and 1979 data. Note that the residuals are reduced by a factor greater than 2. This shows that 1937 and 1979 data fit a low strain rate model much better than the high strain rate model derived from the full data set. Residuals for the 1937 and 1939 data are shown graphically in figure 3.3a and are listed in appendix 3.3.

TABLE 3.4

RESULTS OF STRAIN DETERMINATIONS

Network	mean residual. (second)	RMS residual (second)
Full data set		
1857	-1.3E-16	5.8
1859	-3.7E-05	17.1
1909	-2.0E-16	20.7
1937	1.3E-04	2.8
1979	0.0E+00	4.9
1937 & 1979 data set		
1937	-2.7E-18	1.4
1979	-1.3E-04	1.3

4.4 CONCLUSIONS

Analysis of the full data set suggests that the Dunedin East area has undergone quite large strains which are significant at the 2 S.E. level of confidence.This corresponds to a maximum (engineering) shear strain (Γ) of 1.57 ± 0.24 µrad/yr with the orientation of the principal axis of contraction (Θ) $186^{\circ} \pm 8^{\circ}$. These strains were not detected by an analysis of the 1909, 1937 and 1979 data. The post 1900's data do not give significant strains, and the 1 S.E errors are only about 0.2 µrad/yr. There are two possible causes for the discrepancy between the strain determinations. Firstly, there may have been an episode of high tectonic strain between 1857 and 1909 in the Dunedin area. There are no records of earthquakes in Dunedin during this period, however, so the strain cannot have been associated with co-seismic movement on a fault. Secondly, the high strains may have been caused by some as yet unrecognised disturbance of the the trig points between 1859 and 1909. The second explanation is more likely because there is no evidence for fault creep in the Dunedin Area. In any event, it would be expected that the tectonic strain rates associated with the buildup of elastic strain energy on faults would be rather constant with time. As a result, the high strain rates detected between 1857 and 1909 should not be used to support a high seismic hazard for Dunedin because they are not constant with time.

Appendix 4.1

Appendix 1 Triangulation data for the Dunedin East area. Trigs are identified both by number and name (see table 2).

1857.50				
33 (M)	M Mikw			
-45	47	21.1403		
170	36	15.4147		
315.				
1 (F)	0.000	245	12	52.000
14 (SH)	0.000	206	50	33.000
34 (HC)	0.000	156	30	33.000
0				
34 (HC)	HC			
-45	51	20.6216		
170	38	45.5828		
315.				
33 (M)	0.000	336	30	33.000
14 (SH)	0.000	274	29	3.000
0				
14 (SH)	SHil			
-45	51	6.3013		
170	33	34.1369		
393.0				
14 (Z)	0.000	223	36	57.000
1 (F)	0.000	284	55	37.000
33 (M)	0.000	26	50	33.000
34 (HC)	0.000	94	29	6.000
0				
1 (F)	F			
-45	50	3.9375		
170	27	58.8384		
668.0				
-1	16	104	56	33.300
33 (M)	0.000	65	12	52.000
14 (SH)	7499.000	104	55	37.000
14 (Z)	0.000	178	20	17.000
0				
14 (Z)	ZFH			
-45	55	4.3280		
170	28	15.9859		
159.0				
14 (SH)	0.000	43	36	57.000
1 (F)	0.000	358	20	17.000
00				
1859.30				
14 (SH)				
8 (S)	0.000	318	7	30.000
1 (F)	0.000	284	55	37.000

14 (Z)	0.000	223	37	4.000
0				
8 (S)	S	swam		
-45	48	9.2580		
170	29	47.5722		
666.0				
14 (SH)	0.000	138	7	35.000
1 (F)	0.000	213	59	25.000
0				
1 (F)				
8 (S)	0.000	33	58	24.000
14 (SH)	0.000	104	55	14.000
0				
14 (Z)				
14 (SH)	0.000	43	36	57.000
1 (F)	0.000	358	20	40.000
0				
14 (SH)				
34 (HC)	0.000	94	29	14.000
33 (M)	0.000	26	51	7.000
8 (S)	0.000	318	7	34.000
1 (F)	0.000	284	55	37.000
14 (Z)	0.000	223	37	7.000
0				
1 (F)				
8 (S)	0.000	33	59	34.000
14 (SH)	0.000	104	55	37.000
14 (Z)	0.000	178	20	50.000
0				
14 (Z)				
14 (SH)	0.000	43	37	7.000
1 (F)	0.000	358	20	37.000
0				
8 (S)				
33 (M)	0.000	80	12	27.000
14 (SH)	0.000	138	7	34.000
1 (F)	0.000	213	59	25.000
0				
33 (M)				
8 (S)	0.000	260	12	47.000
14 (SH)	0.000	206	51	7.000
34 (HC)	0.000	156	30	38.000
0				
34 (HC)				
33 (M)	0.000	336	30	22.000
14 (SH)	0.000	274	29	14.000
0				
0				

1909.60				
33 (M)				
34 (HC)	0.000	156	31	19.000
14 (SH)	0.000	206	51	35.000
8 (S)	0.000	260	12	30.000
0				
34 (HC)				
33 (M)	0.000	336	31	19.000
14 (SH)	0.000	274	29	10.000
0				
14 (SH)				
34 (HC)	0.000	94	29	38.000
33 (M)	0.000	26	51	42.000
8 (S)	0.000	318	8	38.000
1 (F)	0.000	284	56	34.000
14 (Z)	0.000	223	38	24.000
0				
8 (S)				
33 (M)	0.000	80	12	30.000
14 (SH)	0.000	138	8	30.000
1 (F)	0.000	214	0	12.000
0				
1 (F)				
8 (S)	0.000	34	0	12.000
14 (SH)	0.000	104	56	34.000
14 (Z)	0.000	178	21	37.000
0				
14 (Z)				
14 (SH)	0.000	43	38	38.000
1 (F)	0.000	358	21	37.000
0				
0				
1937.50				
134 (HC2)	HC#2			
-45	51	20.6216		
170	38	45.5828		
315.				
14 (SH)	0.000	274	29	54.800
6 (EE2)	0.000	303	8	31.500
33 (M)	0.000	336	32	3.800
0				
33 (M)				
134 (HC2)	0.000	156	31	56.500
14 (SH)	0.000	206	52	4.300
6 (EE2)	0.000	234	2	37.900
8 (S)	0.000	260	13	10.600
0				
6 (EE2)	EE#2			
-45	48	52.3719		

170	33	12.3784		
740.0				
33 (M)	0.000	54	2	38.000
134 (HC2)	0.000	123	8	29.100
14 (SH)	0.000	174	53	36.400
14 (Z)	0.000	210	6	3.400
1 (F)	0.000	252	35	38.700
8 (S)	0.000	286	42	9.600
0				
14 (SH)				
134 (HC2)	0.000	94	29	54.800
33 (M)	0.000	26	52	6.700
6 (EE2)	0.000	354	53	39.900
8 (S)	0.000	318	8	45.400
1 (F)	0.000	284	56	33.500
14 (Z)	0.000	223	38	15.500
0				
8 (S)				
33 (M)	0.000	80	13	10.600
6 (EE2)	0.000	106	42	11.400
14 (SH)	0.000	138	8	44.700
1 (F)	0.000	214	0	21.900
0				
1 (F)				
8 (S)	0.000	34	0	21.900
6 (EE2)	0.000	72	35	36.000
14 (SH)	0.000	104	56	33.300
14 (Z)	0.000	178	21	43.400
0				
14 (Z)				
14 (SH)	0.000	43	38	15.500
6 (EE2)	0.000	30	6	3.400
1 (F)	0.000	358	21	42.700
00				
1979.00				
134 (HC2)				
14 (SH)	0.000	120	43	48.970
33 (M)	0.000	182	45	53.600
0				
33 (M)				
134 (HC2)	0.000	309	38	35.100
14 (SH)	0.000	359	58	42.330
6 (EE2)	0.000	27	9	14.570
0				
14 (SH)				
134 (HC2)	0.000	312	5	11.830
33 (M)	0.000	244	27	26.900
1 (F)	0.000	142	31	56.530

Appendix 4·2

Appendix 2 Residuals for the full model. Trigs are identified using trig number from table 2

ANGLE Station #	OBSERVED deg min sec	CALCULATED deg min sec	DIFFERENCE seconds
SURVEY NUMBER 1 DATE 1857.50			
STATION 33 TO 1 AND 34	88 42 19.00	88 42 19.18	-0.18
STATION 33 TO 16 AND 1	321 37 41.00	321 37 49.81	-8.81
STATION 33 TO 34 AND 16	309 39 60.00	309 39 51.02	8.98
STATION 34 TO 33 AND 16	62 1 30.00	62 1 28.35	1.65
STATION 34 TO 16 AND 33	297 58 30.00	297 58 31.65	-1.65
STATION 16 TO 14 AND 34	129 7 51.00	129 7 57.91	-6.91
STATION 16 TO 1 AND 14	61 18 40.00	61 18 34.47	5.53
STATION 16 TO 33 AND 1	101 54 56.00	101 55 4.84	-8.84
STATION 16 TO 34 AND 33	67 38 33.00	67 38 22.78	10.22
STATION 1 TO 33 AND 14	246 52 35.00	246 52 30.26	4.74
STATION 1 TO 16 AND 33	39 42 45.00	39 42 45.09	-0.09
STATION 1 TO 14 AND 16	73 24 40.00	73 24 44.65	-4.65
STATION 14 TO 16 AND 1	45 16 40.00	45 16 41.05	-1.05
STATION 14 TO 1 AND 16	314 43 20.00	314 43 18.95	1.05
SURVEY NUMBER 2 DATE 1859.30			
STATION 16 TO 8 AND 14	94 30 26.00	94 30 30.06	-4.06
STATION 16 TO 1 AND 8	326 48 7.00	326 48 4.09	2.91
STATION 16 TO 14 AND 1	298 41 27.00	298 41 25.84	1.16
STATION 8 TO 16 AND 1	284 8 10.00	284 8 25.30	-15.30
STATION 8 TO 1 AND 16	75 51 50.00	75 51 34.70	15.30
STATION 1 TO 8 AND 16	289 3 10.00	289 3 30.52	-20.52
STATION 1 TO 16 AND 8	70 56 50.00	70 56 29.48	20.52
STATION 14 TO 16 AND 1	45 16 17.00	45 16 40.80	-23.80
STATION 14 TO 1 AND 16	314 43 43.00	314 43 19.20	23.80
STATION 16 TO 34 AND 14	230 52 7.00	230 52 1.75	5.25
STATION 16 TO 33 AND 34	292 21 53.00	292 21 37.70	15.30
STATION 16 TO 8 AND 33	291 16 27.00	291 16 50.61	-23.61
STATION 16 TO 1 AND 8	326 48 3.00	326 48 4.09	-1.09
STATION 16 TO 14 AND 1	298 41 30.00	298 41 25.84	4.16
STATION 1 TO 8 AND 14	215 38 44.00	215 38 45.32	-1.32
STATION 1 TO 16 AND 8	70 56 3.00	70 56 29.48	-26.48
STATION 1 TO 14 AND 16	73 25 13.00	73 24 45.20	27.80
STATION 14 TO 16 AND 1	45 16 30.00	45 16 40.80	-10.80
STATION 14 TO 1 AND 16	314 43 30.00	314 43 19.20	10.80
STATION 8 TO 33 AND 1	226 13 2.00	226 13 2.89	-0.89
STATION 8 TO 16 AND 33	57 55 7.00	57 55 22.41	-15.41
STATION 8 TO 1 AND 16	75 51 51.00	75 51 34.70	16.30
STATION 33 TO 8 AND 34	103 42 9.00	103 41 37.32	31.68
STATION 33 TO 16 AND 8	306 38 20.00	306 38 31.69	-11.69
STATION 33 TO 34 AND 16	309 39 31.00	309 39 51.00	-20.00
STATION 34 TO 33 AND 16	62 1 8.00	62 1 28.82	-20.82
STATION 34 TO 16 AND 33	297 58 52.00	297 58 31.18	20.82
SURVEY NUMBER 3 DATE 1909.60			
STATION 33 TO 34 AND 8	256 18 49.00	256 18 34.96	14.04
STATION 33 TO 16 AND 34	50 20 16.00	50 20 9.56	6.44
STATION 33 TO 8 AND 16	53 20 55.00	53 21 15.47	-20.47
STATION 34 TO 33 AND 16	62 2 9.00	62 1 41.88	27.12
STATION 34 TO 16 AND 33	297 57 51.00	297 58 18.12	-27.12
STATION 16 TO 34 AND 14	230 51 14.00	230 51 52.40	-38.40
STATION 16 TO 33 AND 34	292 22 4.00	292 21 51.33	12.67
STATION 16 TO 8 AND 33	291 16 56.00	291 16 45.19	10.81
STATION 16 TO 1 AND 8	326 47 56.00	326 47 56.58	-0.58

STATION 16 TO 14 AND 1	298 41 50.00	298 41 34.50	15.50
STATION 8 TO 33 AND 1	226 12 18.00	226 12 51.73	-33.73
STATION 8 TO 16 AND 33	57 56 0.00	57 55 29.83	30.17
STATION 8 TO 1 AND 16	75 51 42.00	75 51 38.44	3.56
STATION 1 TO 8 AND 14	215 38 35.00	215 38 41.07	-6.07
STATION 1 TO 16 AND 8	70 56 22.00	70 56 18.23	3.77
STATION 1 TO 14 AND 16	73 25 3.00	73 25 0.71	2.29
STATION 14 TO 16 AND 1	45 17 1.00	45 16 33.96	27.04
STATION 14 TO 1 AND 16	314 42 59.00	314 43 26.04	-27.04

SURVEY NUMBER 4 DATE 1937.50

STATION134 TO 16 AND 33	297 57 51.00	297 57 58.62	-7.62
STATION134 TO 6 AND 16	28 38 36.70	28 38 36.74	-0.04
STATION134 TO 33 AND 6	33 23 32.30	33 23 24.64	7.66
STATION 33 TO134 AND 8	256 18 45.90	256 18 43.87	2.03
STATION 33 TO 16 AND134	50 20 7.80	50 20 7.78	0.02
STATION 33 TO 6 AND 16	27 10 33.60	27 10 34.83	-1.23
STATION 33 TO 8 AND 6	26 10 32.70	26 10 33.52	-0.82
STATION 6 TO 33 AND 8	127 20 28.40	127 20 27.39	1.01
STATION 6 TO134 AND 33	69 5 51.10	69 5 52.80	-1.71
STATION 6 TO 16 AND134	51 45 7.30	51 45 5.41	1.90
STATION 6 TO 14 AND 16	35 12 27.00	35 12 29.39	-2.40
STATION 6 TO 1 AND 14	42 29 35.30	42 29 35.99	-0.69
STATION 6 TO 8 AND 1	34 6 30.90	34 6 29.01	1.89
STATION 16 TO134 AND 14	230 51 39.30	230 51 37.06	2.24
STATION 16 TO 33 AND134	292 22 11.90	292 22 9.04	2.86
STATION 16 TO 6 AND 33	328 1 33.20	328 1 33.02	0.18
STATION 16 TO 8 AND 6	323 15 5.50	323 15 9.17	-3.67
STATION 16 TO 1 AND 8	326 47 48.10	326 47 52.41	-4.31
STATION 16 TO 14 AND 1	298 41 42.00	298 41 39.31	2.69
STATION 8 TO 33 AND 1	226 12 48.70	226 12 45.54	3.16
STATION 8 TO 6 AND 33	26 29 0.80	26 28 59.15	1.65
STATION 8 TO 16 AND 6	31 26 33.30	31 26 34.80	-1.50
STATION 8 TO 1 AND 16	75 51 37.20	75 51 40.51	-3.31
STATION 1 TO 8 AND 14	215 38 38.50	215 38 38.71	-0.21
STATION 1 TO 6 AND 8	38 35 14.10	38 35 15.72	-1.63
STATION 1 TO 16 AND 6	32 20 57.30	32 20 56.26	1.04
STATION 1 TO 14 AND 16	73 25 10.10	73 25 9.31	0.79
STATION 14 TO 16 AND 1	45 16 32.80	45 16 30.16	2.64
STATION 14 TO 6 AND 16	346 27 47.90	346 27 48.41	-0.51
STATION 14 TO 1 AND 6	328 15 39.30	328 15 41.43	-2.13

SURVEY NUMBER 5 DATE 1979.00

STATION134 TO 16 AND 33	297 57 55.37	297 57 47.84	7.53
STATION134 TO 33 AND 16	62 2 4.63	62 2 12.16	-7.53
STATION 33 TO134 AND 6	282 29 20.53	282 29 22.86	-2.33
STATION 33 TO 16 AND134	50 20 7.23	50 20 8.24	-1.01
STATION 33 TO 6 AND 16	27 10 32.24	27 10 28.89	3.35
STATION 16 TO134 AND 1	169 33 15.30	169 33 15.79	-0.49
STATION 16 TO 33 AND134	292 22 15.07	292 22 20.28	-5.21
STATION 16 TO 1 AND 33	258 4 29.63	258 4 23.93	5.70

Appendix 4·3

Appendix 3 Residuals for the strain determination involving 1937 and 1979 data only..
Trigs are identified using trig number from table 2

ANGLE Station #	OBSERVED deg min sec	CALCULATED deg min sec	DIFFERENCE seconds
SURVEY NUMBER 1 DATE 1937.50			
STATION134 TO 16 AND 33	297 57 51.00	297 57 53.24	-2.24
STATION134 TO 6 AND 16	28 38 36.70	28 38 37.65	-0.95
STATION134 TO 33 AND 6	33 23 32.30	33 23 29.10	3.20
STATION 33 TO134 AND 8	256 18 45.90	256 18 47.69	-1.79
STATION 33 TO 16 AND134	50 20 7.80	50 20 7.33	0.47
STATION 33 TO 6 AND 16	27 10 33.60	27 10 32.48	1.12
STATION 33 TO 8 AND 6	26 10 32.70	26 10 32.50	0.20
STATION 6 TO 33 AND 8	127 20 28.40	127 20 27.64	0.76
STATION 6 TO134 AND 33	69 5 51.10	69 5 51.13	-0.04
STATION 6 TO 16 AND134	51 45 7.30	51 45 8.31	-1.01
STATION 6 TO 14 AND 16	35 12 27.00	35 12 26.57	0.43
STATION 6 TO 1 AND 14	42 29 35.30	42 29 34.62	0.68
STATION 6 TO 8 AND 1	34 6 30.90	34 6 31.74	-0.84
STATION 16 TO134 AND 14	230 51 39.30	230 51 36.72	2.58
STATION 16 TO 33 AND134	292 22 11.90	292 22 13.97	-2.07
STATION 16 TO 6 AND 33	328 1 33.20	328 1 31.90	1.30
STATION 16 TO 8 AND 6	323 15 5.50	323 15 7.44	-1.94
STATION 16 TO 1 AND 8	326 47 48.10	326 47 49.18	-1.08
STATION 16 TO 14 AND 1	298 41 42.00	298 41 40.79	1.21
STATION 8 TO 33 AND 1	226 12 48.70	226 12 48.11	0.59
STATION 8 TO 6 AND 33	26 29 0.80	26 28 59.93	0.87
STATION 8 TO 16 AND 6	31 26 33.30	31 26 34.55	-1.25
STATION 8 TO 1 AND 16	75 51 37.20	75 51 37.42	-0.22
STATION 1 TO 8 AND 14	215 38 38.50	215 38 38.94	-0.44
STATION 1 TO 6 AND 8	38 35 14.10	38 35 16.34	-2.24
STATION 1 TO 16 AND 6	32 20 57.30	32 20 55.51	1.79
STATION 1 TO 14 AND 16	73 25 10.10	73 25 9.22	0.88
STATION 14 TO 16 AND 1	45 16 32.80	45 16 31.73	1.07
STATION 14 TO 6 AND 16	346 27 47.90	346 27 49.06	-1.16
STATION 14 TO 1 AND 6	328 15 39.30	328 15 39.20	0.10
SURVEY NUMBER 2 DATE 1979.00			
STATION134 TO 16 AND 33	297 57 55.37	297 57 54.11	1.26
STATION134 TO 33 AND 16	62 2 4.63	62 2 5.89	-1.26
STATION 33 TO134 AND 6	282 29 20.53	282 29 19.63	0.91
STATION 33 TO 16 AND134	50 20 7.23	50 20 7.43	-0.20
STATION 33 TO 6 AND 16	27 10 32.24	27 10 32.95	-0.71
STATION 16 TO134 AND 1	169 33 15.30	169 33 17.58	-2.28
STATION 16 TO 33 AND134	292 22 15.07	292 22 13.20	1.87
STATION 16 TO 1 AND 33	258 4 29.63	258 4 29.22	0.41

PART 2

NEOTECTONICS OF THE HYDE FAULT AND THE ROCK AND PILLAR RANGE

Work mainly carried out by G. Salton, MSc student, with assistance and further material from R. J. Norris and P. O. Koons

Report compiled by R. J. Norris and P. O. Koons

PART 2

NEOTECTONICS OF THE HYDE FAULT AND THE ROCK AND PILLAR RANGE

Work mainly carried out by G. Salton, MSc student, with assistance and further material from R. J. Norris and P. O. Koons

Report compiled by R. J. Norris and P. O. Koons

CONTENTS

Contents continued:

SECTION 1: INTRODUCTION AND REGIONAL GEOLOGY

1.1 Introduction

The Rock and Pillar Range is one of a series of northeasterly trending ranges in central and eastern Otago. It is situated about 50 km northwest of Dunedin and rises at its centre to a height of around 1400 m (Fig. 1.1). It is a somewhat asymmetric range with a steeper southeastern range front forming the western margin of the Strath Taieri depression. The total relief at the range front reaches a maximum of around 1000m.

The range is underlain by chlorite-zone schist of textural grade IV. The rock has a well-developed schistosity with extensive veining and segregation, which confers a strong physical anisotropy. Over much of the area, the schistosity dips at low angles and is essentially subhorizontal.

1.2 Late Cenozoic Deformation

During the late Cretaceous, eastern Otago was eroded to an extensive peneplain, on which a series of fluvial, lacustrine and marine sediments were deposited. Basaltic lavas were erupted from a number of scattered small volcanic centres in the region during mid to late Miocene time Deformation during the late Cenozoic (mainly during the last 2-3 Myr) has deformed this peneplain, together with the overlying sediments and volcanics, into a series of uplifted ranges separated by elongate basins filled with Quaternary sediments. Since the basins are now well above sea-level, it is clear that the whole region has undergone uplift, superposed on which is the differential uplift of the ranges.

The uplift of the ranges has traditionally been thought to be due to rigid block displacement on reverse faults along their eastern fronts, a mechanism consistent with their asymmetry and linear character. Occasional reverse faults have been described near to the range fronts.

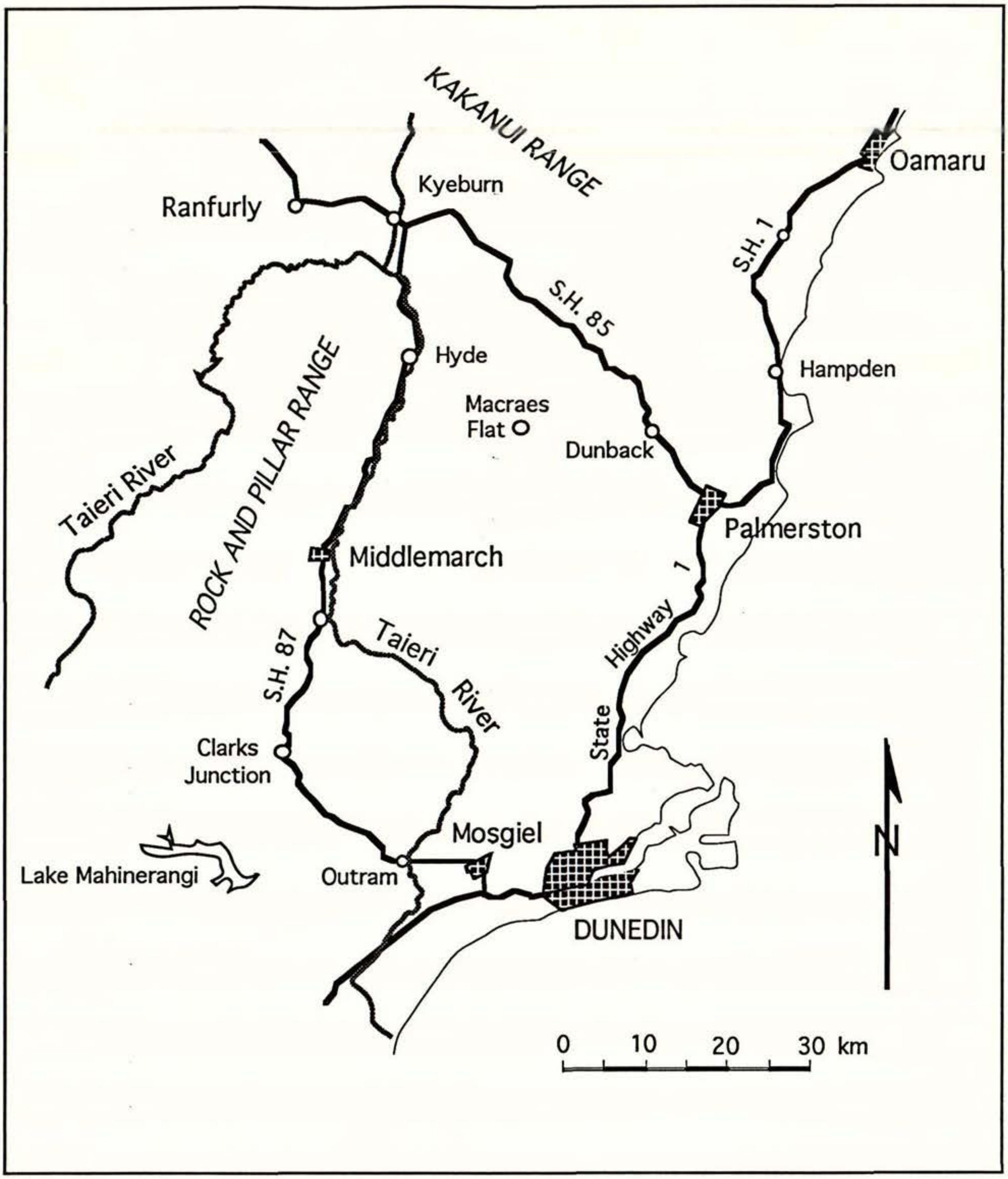

Fig. 1.1: Map of area west of Dunedin showing location of Rock and Pillar Range

SECTION 2: POST-METAMORPHIC DEFORMATION OF THE OTAGO SCHIST

2.1 Previous Work

The geological mapping of the Otago Schist, and the Rock and Pillar Range in particular, was first undertaken by Cotton (1917), who interpreted the Central Otago ranges as being tilted fault blocks between steeply dipping reverse faults. Williamson (1939) identified the peneplain surface as a datum, and also viewed the uplift of the range as due to displacement on steeply dipping faults. Benson (1940) on the other hand argued for a combined fold-fault mechanism for the Central Otago mountain ranges. The most recent geological maps covering the Rock and Pillar Range are sheets 23, Oamaru (A.R. Mutch, 1963) and 25, Dunedin (I.C. McKellar, 1966) of the 1:250,000 series published by the DSIR.

While much work has been carried out to elucidate the Mesozoic metamorphic history of the schist (Means, 1963, 1966; Wood, 1963; Bishop, 1971, 1972), relatively little has been published on the post-metamorphic history, particularly the Neogene deformation. Work in the region of the Rock and Pillar Range has been confined to the outskirts and focuses largely on economic and petrographic features of the Cenozoic strata overlying the schist. An MSc thesis by Brown (1962) documented the regional geology and structure of the area just east of Middlemarch on the Taieri Ridge (Brown, 1963, 1964). A BSc (Hons) thesis at Otago University by Hesson (1981) focuses on Tertiary stratigraphy and gold deposits at Hyde, while several third-year projects have examined areas at the northern end of the range. Waters (1990) and Whetter (1990) worked at Tiroiti and Hyde respectively to try to identify the Hyde Fault and characterise the relations between the schist and Tertiary strata while Simpson (1991) studied the old gold diggings at Hamiltons near Orangapai.

2.2 Rock and Pillar Range

For the purpose of this project, mapping of the schist in the Rock and Pillar Range was carried out at a scale of 1:25,000. The range was divided into five transects each extending from the northwest (or "back") side of the range to the southeast (or "front") side (Fig. 2.1). The transects follow bearings of 305°, perpendicular to the approximate trend of the range crest. They are about 8 km apart and as evenly spaced as outcrop and access allowed. The transects extend from the Patearoa-Styx road on the back of the range to the sediments covering the Strath Taieri plain on the range front. Where the latter are absent, the schist was mapped as far as the Taieri River. In addition, a further transect was taken along the crest of the range. The attitude of schistosity was of prime interest, and lineations and joint surface orientations were also measured. Maps showing the data measured in the field are presented as Figs. 2.2 and 2.3. Few geological contacts are mapped, with no Tertiary units preserved on the top of the range, at the front of the range south of Hyde, or south of Patearoa at the back of the range. Evidence of the peneplain surface, such as the distinctive weathered schist or rounded, silica-cemented sarsen stones that are weathered out of the basal Tertiary sediments (Stirling, 1988), was only observed where Tertiary units still cover the schist. Evidence of faulting and shear zones was sought, especially where these zones are indicated on the 1:250,000 geological map.

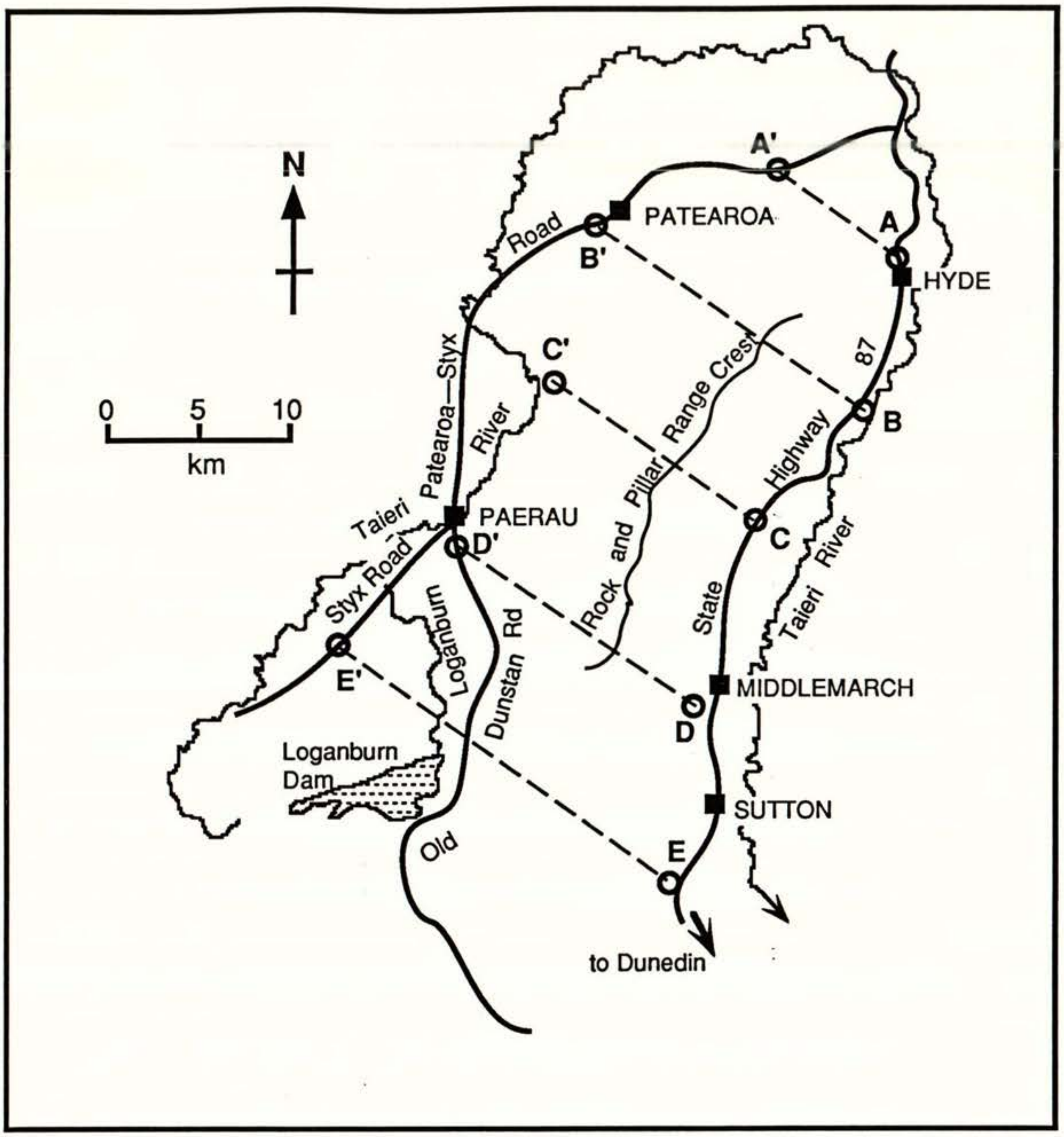

Fig 2.1: Map showing location of NW-SE transects across Rock and Pillar Range. Structural data is shown on maps in Figs. 2.2 & 2.3 and on stereonets in Fig. 2.4. Cross sections are drawn in Fig. 2.5.

FIG 2.2

SYMBOLS

- strike & dip of schistosity
- trend & plunge of lineations
- dip direction & dip of joints

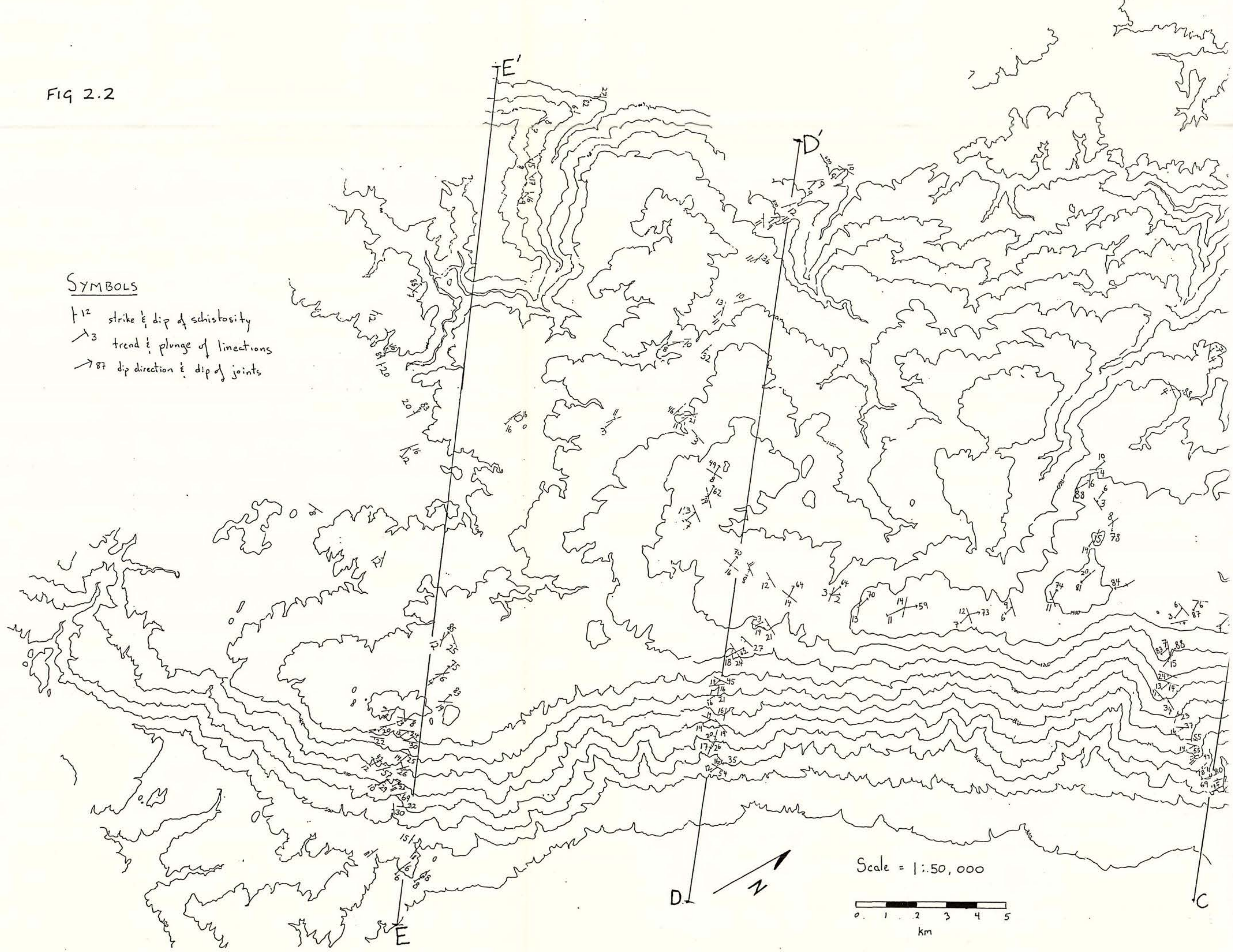

FIG 2.3

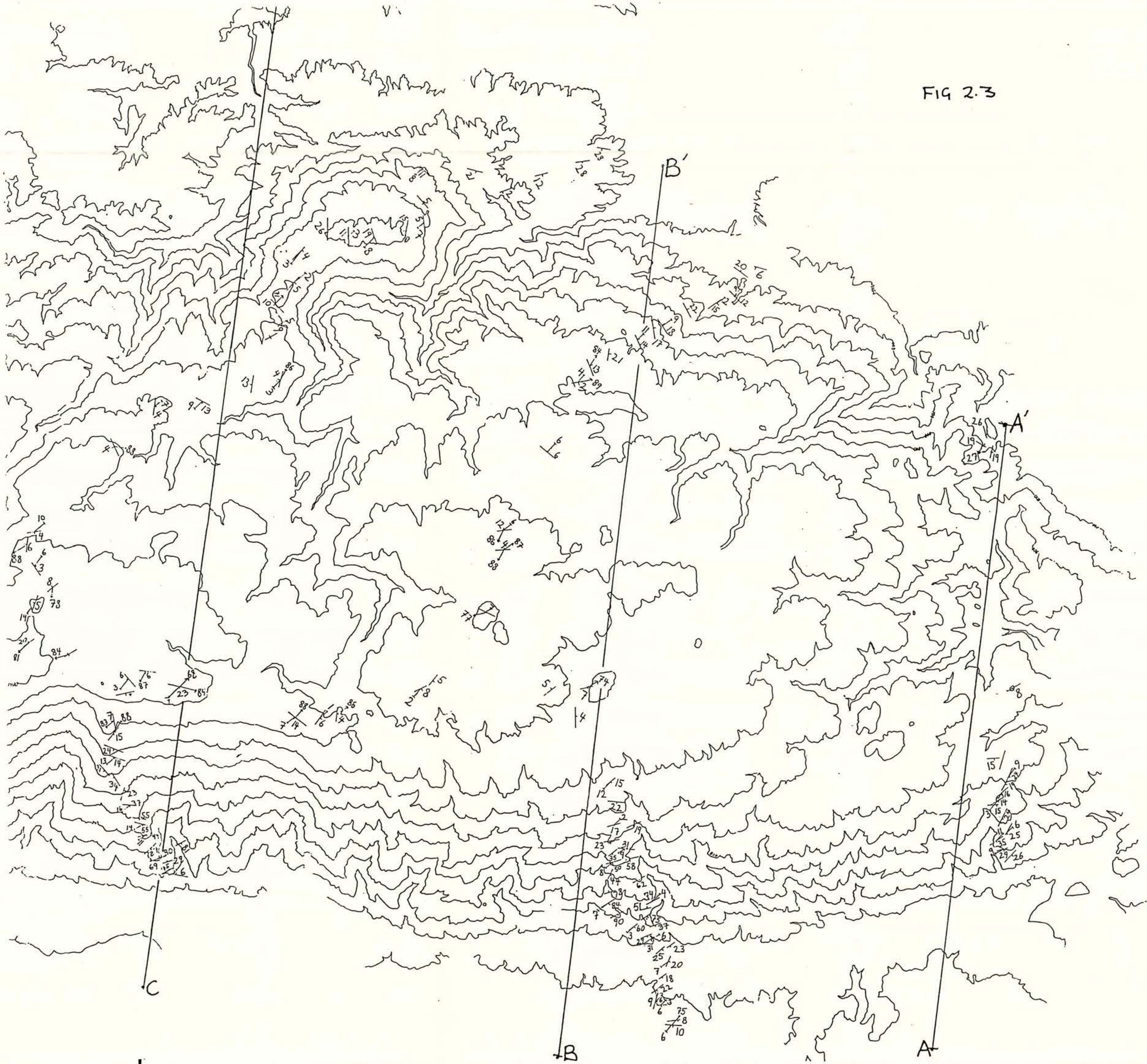

2.2.1 Nature of Outcrop

Outcrops in the Rock and Pillar Range often take the form of distinctive tors (the "Pillars" for which the range is named) tens of metres across and up to 10 metres high. These are widespread near the top of the range and occasionally present in the valleys. On both the northwest and southeast dipping flanks of the range outcrop is mainly available where streams have dissected the schist. Occasionally schistosity can be inferred from the general grain of the hillside, as sighted across drainages. Outcrop was also present in road-cuts on both major roads and 4WD tracks that extend onto the range. Unfortunately, this outcrop is usually not reliable, as the schist tends to collapse into road-cuts.

2.2.2 Schistosity

The poles to schistosity in all NW-SE transects are plotted on equal angle stereonets in Figure 2.4 a – e. The schistosity is crenulated, and at most of the outcrops three to five measurements were taken to provide an average, representative attitude over the outcrop. The schistosity clearly defines an asymmetric, SE-vergent upright fold. This fold is an open, gentle one, but the forelimb becomes steep and even overturned at a few localities along the centre of the range front. Outcrop dips inferred to be overturned are denoted in the stereonets by crosses.

To characterise all schistosity folds in this study, the π diagram method as outlined in Suppe (1985, p.54) is used. This method assumes a cylindrical fold model. The best-fit great circle through the poles to schistosity is drawn in manually. The pole to this plane is the derived schistosity fold axis.

Each transect was fitted separately, and the derived fold axes plotted in Figure 2.4. The plunge magnitude and direction of these fold axes, from north to south, are approximately 15°/025°; 10°/009°; 9°/189°; 7°/185°; 5°/190°. The fold axes are fairly consistent with each other, but not with the trend of the range crest, diverging from it by about 25° to the west. The range crest trends about 035°, while the plunge direction of the fold axes is usually closer to 010°. The fold thus appears to be propagating out into the Strath Taieri oblique to the range front.

On the transect along the range crest, the very shallow dips made strikes difficult to determine accurately (Fig. 2-6). The schistosity attitudes from this transect seem to delineate a slight warping about an axis perpendicular to the length of the range (6°/122°). This folding can be seen in the gentle "whaleback" shape of the range and in the variation of plunge of the main fold axes from north in the NE to slightly south in the SE. The schistosity thus seems to delineate a gentle, doubly plunging antiform which closely, but not exactly, matches the shape of the range.

The schistosity dips for all five transects are drawn out and connected into their fold shape in Figure 2-5, a-e. These are the schistosity folds projected into the plane of the transect, perpendicular to the trend of the range crest. Also shown is the topography profile across these transects. The topography is inferred to be also the shape of the peneplain (see section 3). In transect C, the overturned layers had to be sketched in, in order to connect the dips properly. In general, the shapes and sizes of each of pair of profiles is quite similar. They are similar to a sine curve ($\pi/10 \sin x$), although the range shapes are slightly asymmetric.

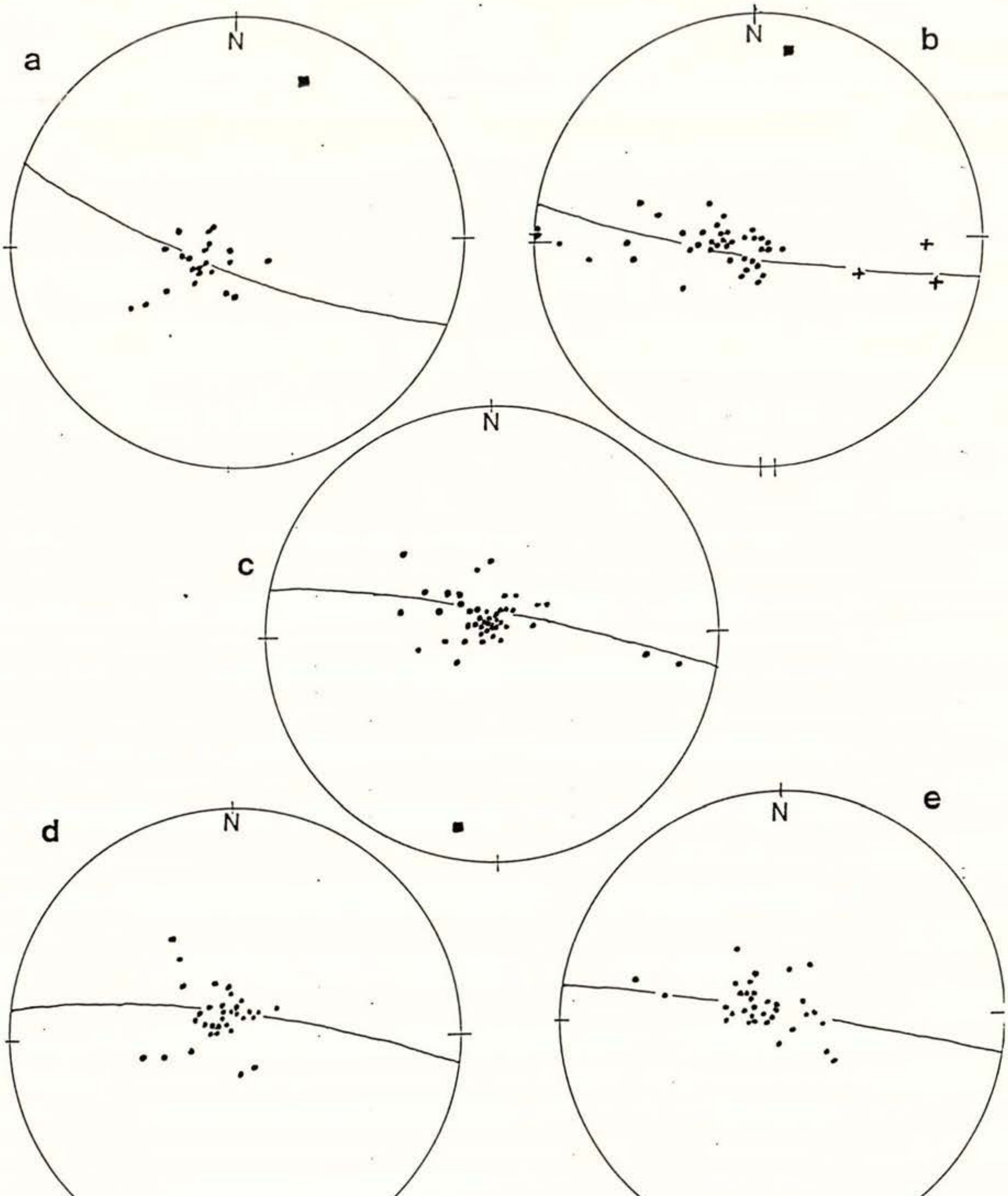

Fig. 2.4 a-e: Equal angle stereograms of poles to schistosity measured on NW-SE transects A-E respectively (locations of transects shown in Fig. 2.1). Crosses represent "overturned" schistosity attitudes. Best-fit great circle to poles and derived cylindrical fold axis are also shown for each transect.

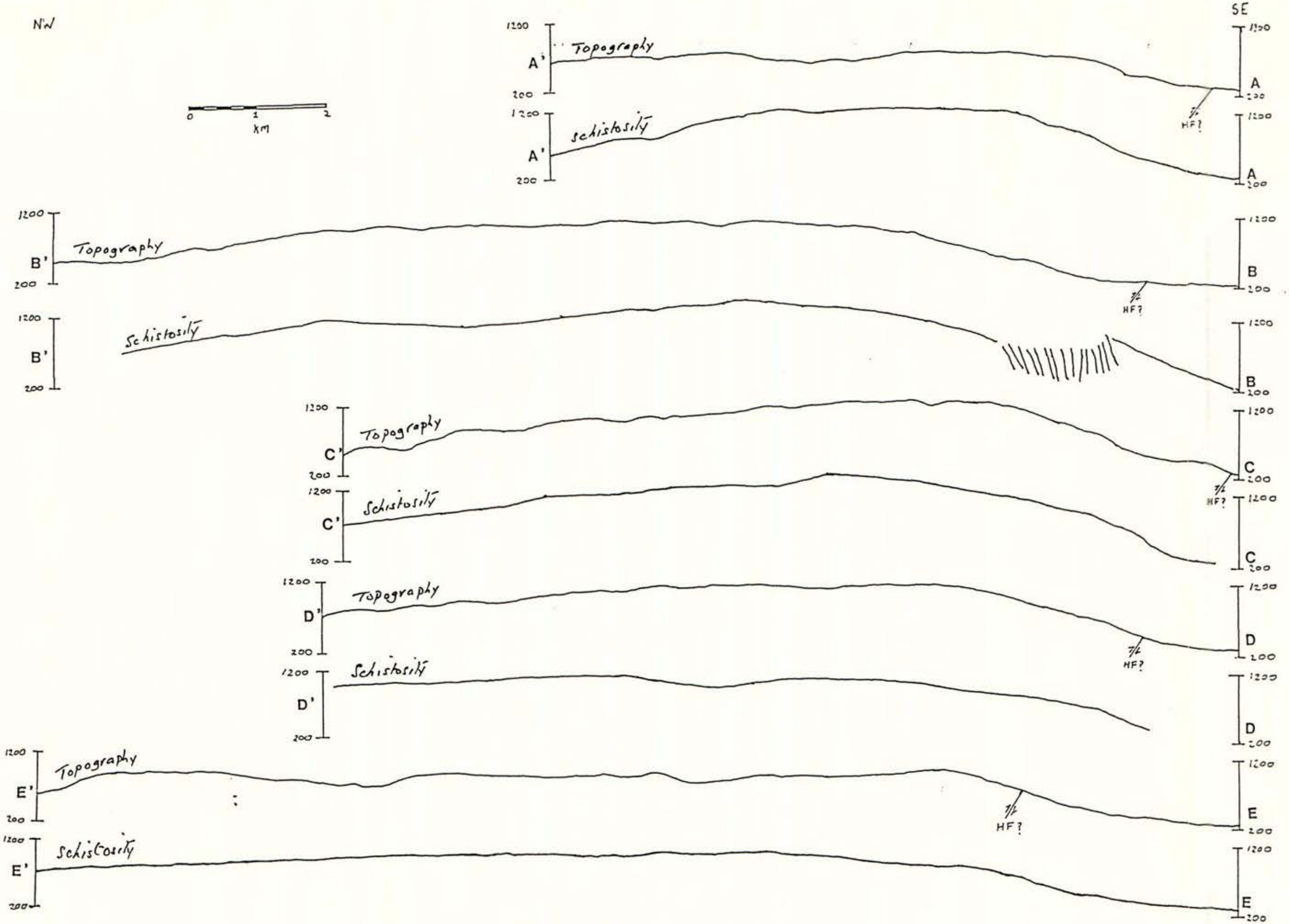

Figure 2-5 a-e : Profiles of topography (top profile of each pair) and schistosity projected into plane of transect for transects A-E. In profile B, the schistosity is sketched in where steep to overturned. No vertical exaggeration, scale is in meters. Putative location of the Hyde Fault from the 1:250,000 geological map is marked on topography profiles.

In the north, a palinspastic reconstruction of the topography to a flat-lying peneplain results in flat-lying schistosity, whereas further south, this reconstruction gives an initial southeast dip to the schistosity. This dip is 11°, 13°, and 15° in transects C, D, and E, respectively. In Figure 2-5 c-e, the schistosity profiles are back-rotated by these amounts in order to show the similarity of the fold shapes. The schistosity fold usually has a greater amplitude than the topography as would be expected due to erosion. Less than 100 m of erosion is needed to reduce the schistosity profiles to the height of the topography profiles for transects B-E and around 200 m for transect A.

This congruence of shapes was also documented in the Dunstan Range by Beanland et al. (1986) and Walcott (1988), and in the Old Man and Garvie Mountains by Stirling (1988). Two transects across the Raggedy Range, near Omakau and Oturehua, were also carried out for comparative purposes and showed very similar results (Fig. 2.8). These will be discussed in more detail below.

2.2.3 Lineation

The lineation in the schist is a metamorphic structure (Means, 1963) expressed by quartz rodding. It is pervasive and remarkably uniform throughout the range, regardless of schistosity attitude (Fig. 2-7a). Its plunge direction is approximately 345° to 350° (or 165° to 170°) with a plunge magnitude up to 15° either north or south. The plunge of the lineation roughly corresponds to that of the schistosity fold axis: north in the northeast and south in the southwest, suggesting it may have exerted some control on the schistosity fold axis (Cobbold & Watkinson, 1981).

2.2.4 Jointing

The tors on the range tops are formed by deep weathering controlled by jointing of the schists, and may indicate proximity to the peneplain surface (Stirling, 1988). Poles to joints in the Rock and Pillars are plotted in Fig. 2-7b: two distinct joint sets occur, a predominant one striking about 070°, and a secondary one at 295° to 300° both subvertical to vertical. This jointing is less apparent where tors are absent on the flanks of the range. On the few tors in the Strath and upper Taieri valleys, joints are also present, and quite similar in both attitude and character to those on the range top.

The joint surfaces are usually quite smooth and no striae were observed. This may indicate that the joints are purely tensional in origin — true joints (Mode I cracks), as opposed to shear fractures (Engelder, 1987; Pollard & Segall, 1987). No mineralised surfaces were observed, perhaps indicating that the joints formed near the peneplain surface, in a relatively dry environment away from hydrothermal fluids.

A possible mechanical origin of the joints is that they represent extensional features formed by bending stresses during flexure of the range. This explanation is favoured by the consistent orientation of the joint surfaces and their preferential distribution on the range tops where the flexure-induced stresses would be highest.

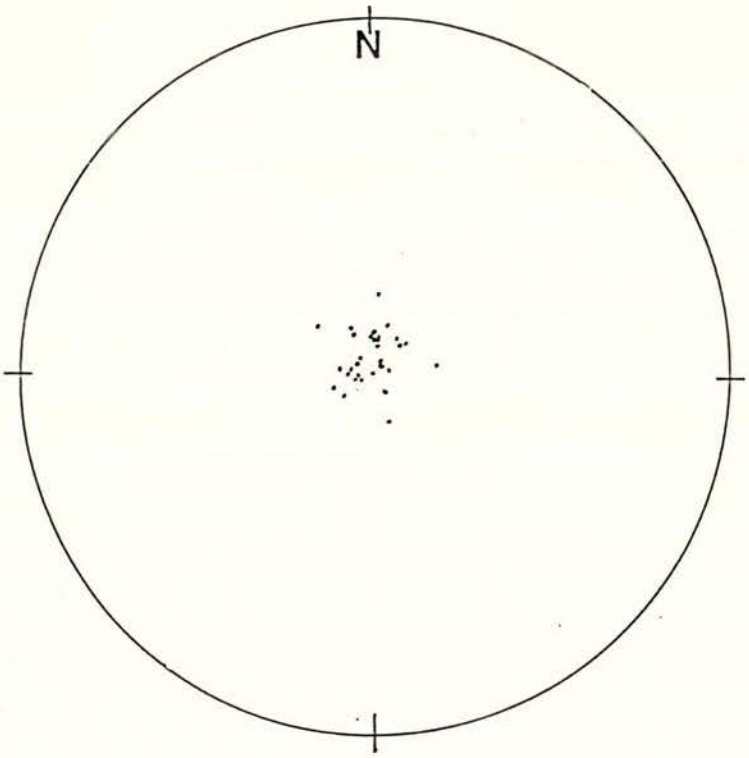

Fig. 2.6: Equal-angle sterogram of poles to schistosity measured on the transect along the range crest

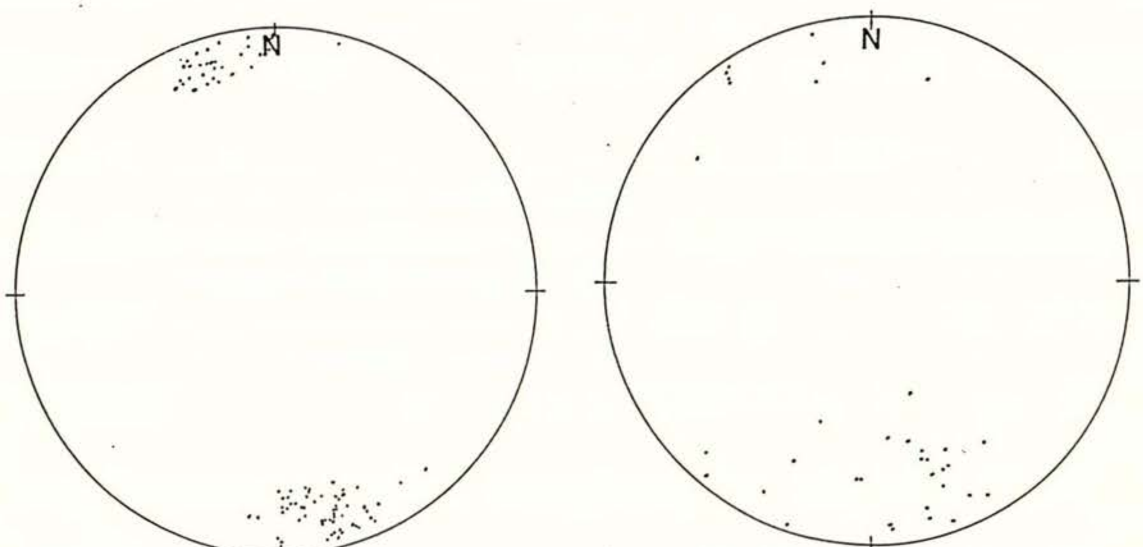

Fig. 2.7: Equal-angle sterograms of (a) lineations in the schist of the Rock and Pillar Range; (b) poles to joints measured across the range

2.2.5 Faulting

Evidence for major faulting in the area is rare. Two major faults are indicated on existing geological maps: the Hyde Fault bounding the range on the southeast, and an unnamed fault bounding the range on the northwest, which is referred to here as the Ewe Hill Fault. The Hyde Fault is considered in more detail in the next section. The Ewe Hill Fault is mapped from air photos as being responsible for uplift of the back of the range, inferred from the steep-sided back of the range in its southern part. Shear zones in the schist here are difficult to locate on the ground, because the foot of the range is usually paddock-covered. In a road-cut on Ewe Hill above Patearoa, two small shear zones are evident with a small, somewhat rotated block between them. We suspect that this is not a large displacement zone for several reasons: (1) its location a third of the way up the slope, rather than at the foot of the range, seems to preclude a large role in range uplift; (2) no gouge is present: (3) no systematic change in schistosity orientation across the shear zone is present: (4) efforts to trace this feature along strike failed to find further shear zones in either direction.

2.2.6 Tertiary and Quaternary Units

Other units in the region of the Rock and Pillars include a sequence of Tertiary sediments, capped by a Miocene basalt, which is restricted to the area north of Hyde in the Strath Taieri. (See Bishop (1974) for a thorough general description of these units, and Hesson(1981) for the stratigraphy at Hyde). The Upper Taieri and Strath Taieri basins are filled with alluvium (river and fan deposits) of no more than 20 metres thickness. The fans in the Strath Taieri are at their thickest in the middle of the range near Middlemarch, and thin to almost nothing at the ends of the range near Sutton and Hyde. These gravels are composed of reworked schist and Tertiary material.

2.3 Raggedy Range

Two transects were mapped across the Raggedy Range (Fig. 2.8) for comparison with the Rock and Pillar Range. The first follows Thurlow Road; the second, the Omakau-Poolburn Road (Fig. 2-8). Schistosity stereograms (Fig. 2-9a,b) and schistosity-topography profiles (Fig. 2-10) were constructed as for the Rock and Pillars. In the north, the schistosity fold is more exaggerated than the topography (Fig. 2-10a), with the SE limb of the fold dipping more steeply than in the southern transect. The schistosity fold axis plunges approximately 10°/022° (Fig. 2-9a). As in the Rock and Pillars, this is 20° to 25° more westerly than the trend of the range crest, which for the Raggedy Range is about 045°.

The schistosity profile across the southern transect closely mimics the topography (Fig. 2-10b). A gentle, upright, open fold is described with an approximate axis of 20°/198° (Fig. 2-9b). The plunge direction of the schistosity fold axis is again about 25° more westerly than the trend of the range crest. These data indicate that the Raggedy Range schistosity also describes a doubly plunging antiform, as in the Rock and Pillar Range.

Lineations in both transects are quite consistent with each other, regardless of schistosity (Fig. 2-9a,b). They roughly parallel the schistosity fold axis in both transects, as in the Rock and Pillars. Jointing was less apparent than in the Rock and Pillars, with the outcrops being smaller and not as distinctive.

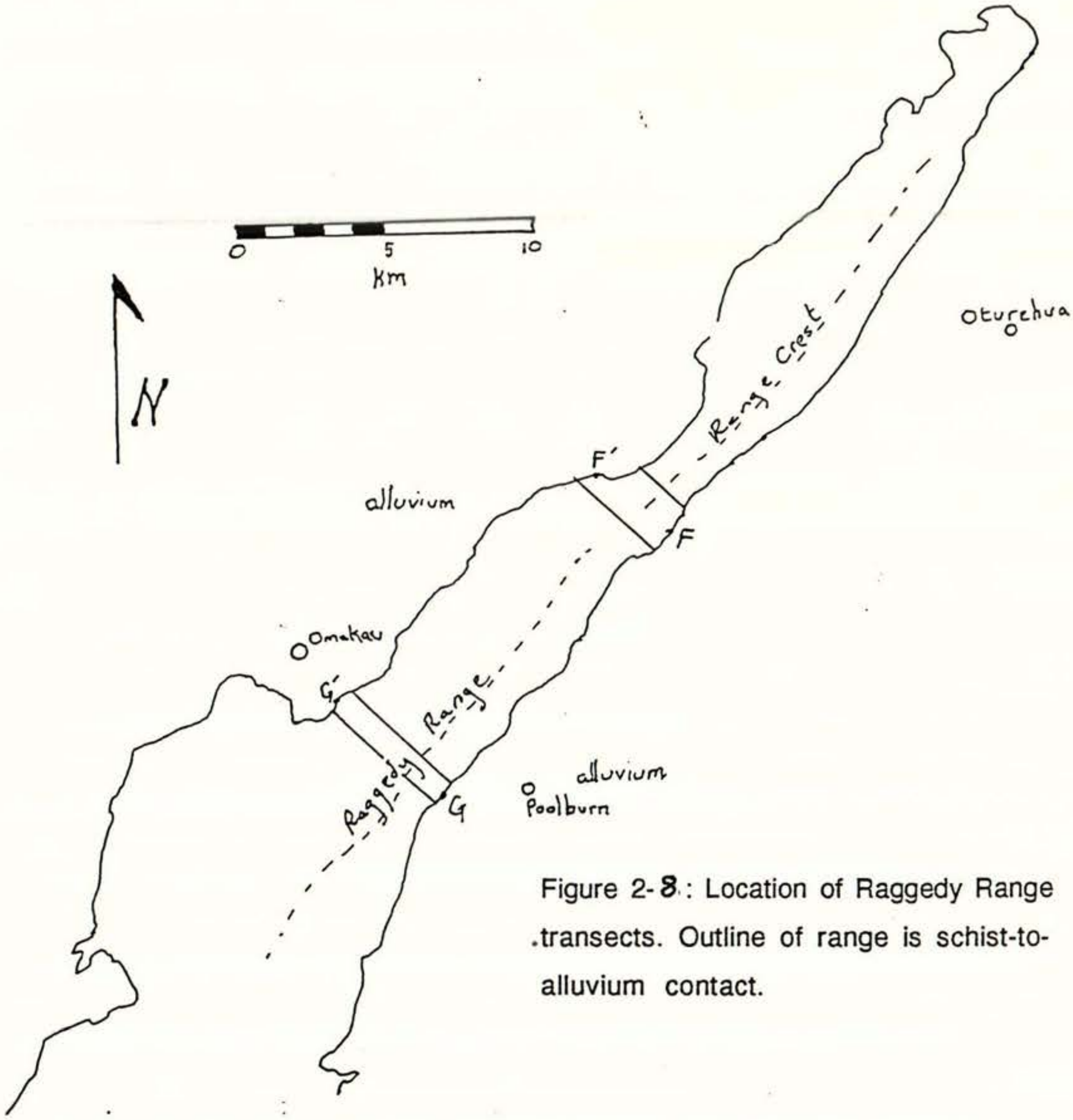

Figure 2-8 : Location of Raggedy Range transects. Outline of range is schist-to-alluvium contact.

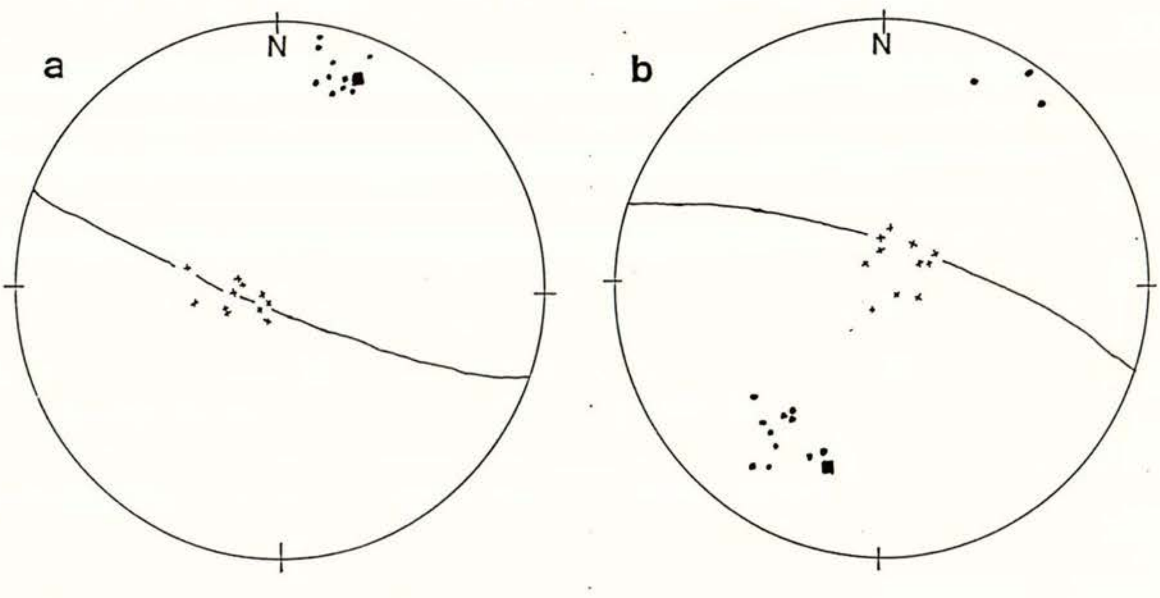

Figure 2-9 Equal-angle stereonets of poles to schistosity (crosses) and lineations (dots) for Raggedy Range. a) Northern transect. b) Southern transect.

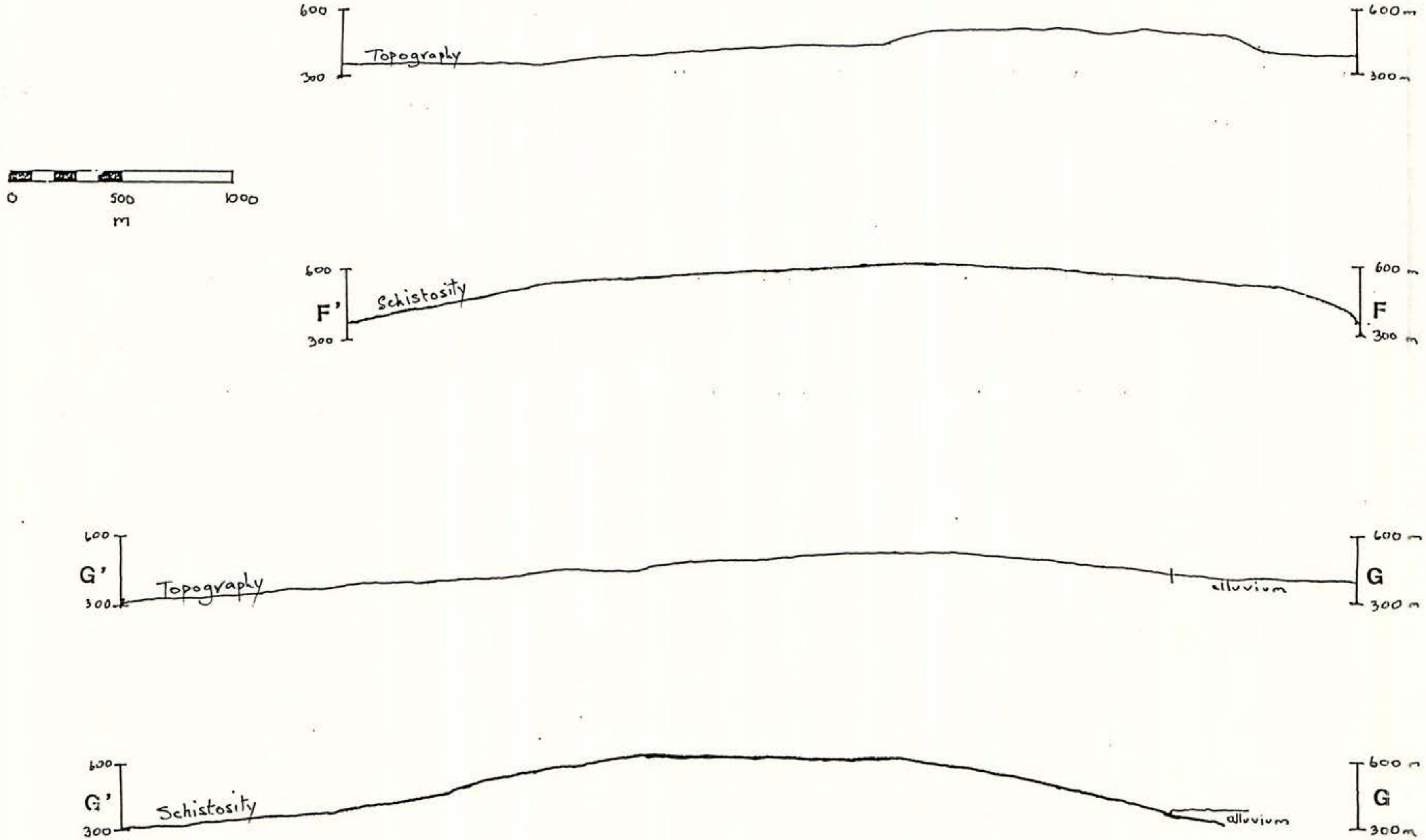

Figure 2-10 Profiles of topography (upper of each pair) and schistosity (lower of each pair) across Raggedy Range. a) F-F' is northern transect. b) G-G' is southern transect. Scale is in metres, with no vertical exaggeration.

SECTION 3: THE HYDE FAULT

3.1 Previous Work

The Hyde Fault is the structure originally mapped as controlling the uplift of the Rock and Pillar Range (Williamson, 1939). Figure 3-1 shows its location on existing geological maps. It is inferred from the offset of the peneplain to be a steep reverse fault with approximately 1000 m of throw. It is also inferred to be a reactivated Cretaceous normal fault (Mutch, 1963). This reversal of motion has been convincingly documented on other faults in east Otago, for example the Dansey Pass Fault to the north (Bishop, 1974), and the Titri Fault south of Dunedin (Mutch & Wilson, 1952).

The Hyde Fault has been the subject of several unpublished studies. Both Whetter (1990) and Waters (1990) were unable to identify the fault near Hyde as a large, through-going structure. Whetter studied the type locality of the Hyde Fault in gold diggings at Hyde. He identified the main fault and several subsidiary ones basin-ward of it, but was unable to demonstrate regional continuity or magnitude of slip on any of them. Waters (1990) studied the geology of Tiroiti, just north of Hyde, and concluded that the Hyde Fault does not run through the area as shown on the DSIR map, and is not a "main structural control on the Rock and Pillar" Range.

A study for the DSIR by Hull et al. (1982), identified a series of lineaments along the range front on aerial photographs (Fig. 3-2). These were inferred to be the surface expression of the Hyde Fault, by analogy with the similar subtle topographic expression of the Dunstan Fault (Hull, 1986). Several of these "scarps" were field checked just north of Middlemarch by Hull and coworkers, but it was unclear to them whether they represent a fault or the toe of a debris flow.

3.2 Evidence of Uplift

That uplift at the front of the range has occurred in the past is evident from the presence of the ranges and offset of the peneplain. That uplift processes are still active is suggested by the patterns of stream incision of alluvial fans visible on air photos (Fig. 3-6). Here small drainages coming into the Strath Taieri can be seen cutting down into fans they have earlier deposited. The incision is deepest near the range front, implying uplift of the range. However, incision due to climatic factors cannot be eliminated and further work is required.

Evidence presented in the last section is more consistent with the range being a large-scale fold structure rather than a simple upthrust fault block. An important question to be addressed during investigation of the neotectonics of the range front is the relative importance of folding and faulting in the uplift of the range.

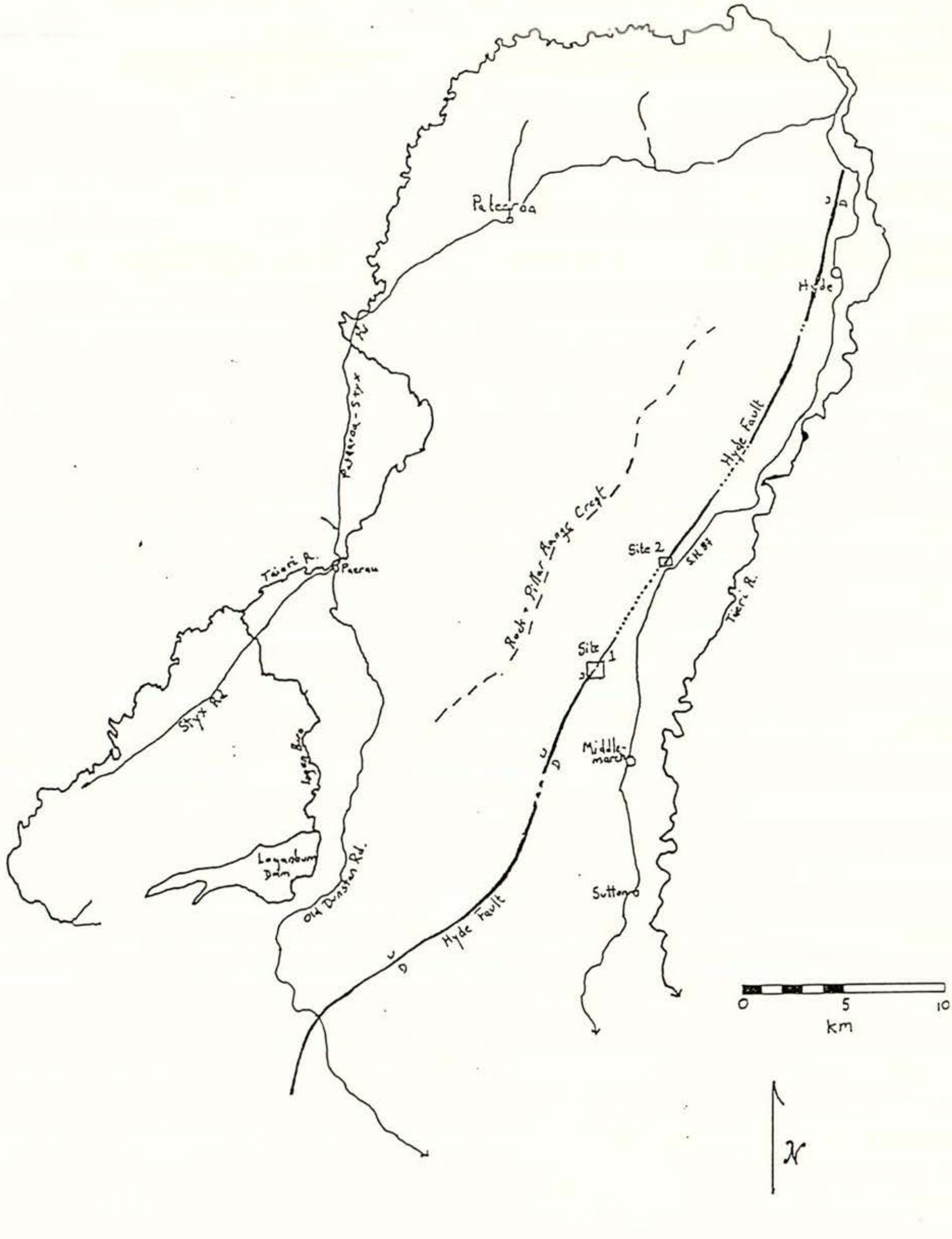

Fig. 3.1: Location of Hyde Fault on 1:250,000 geological maps (Mutch, 1963; McKellar, 1966). Sites 1 and 2, and area at Hyde were investigated in detail.

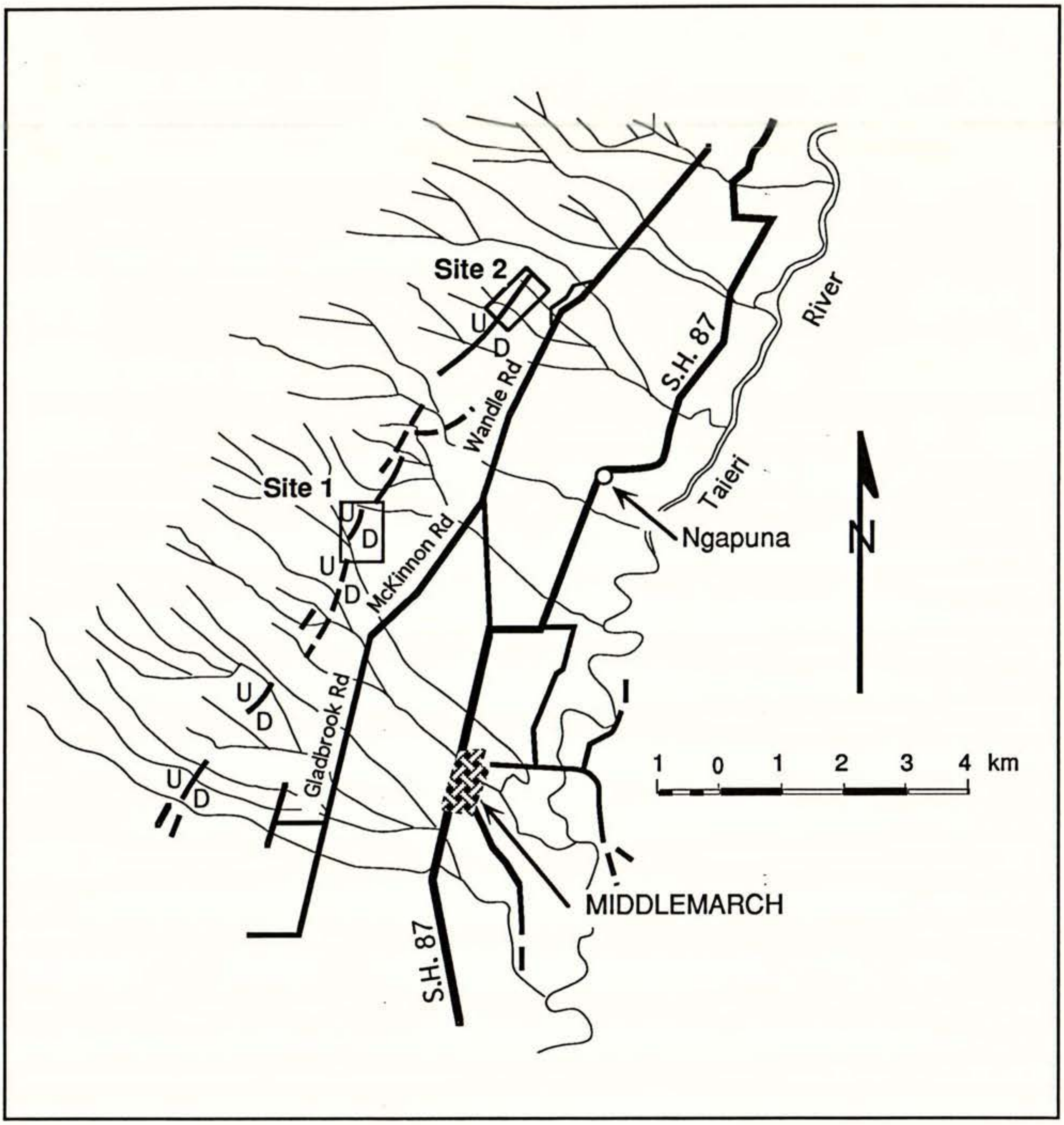

Fig. 3.2: Location of possible fault traces identified on air photos (partly after Hull, 1982). Sites examined in detail and described in text are shown.

3.3 Evidence for Faulting

3.3.1 Hyde Diggings

The type locality of the Hyde Fault is in gold diggings just north of Hyde. A sketch of this area is shown in Figure 3-3. Here it is indisputably a reverse fault thrusting schist over Tertiary sediments and Quaternary fan gravels.

The fault at this locality has only a few millimetres of poorly developed gouge with a few striations plunging directly down dip. Assuming the fault dips 50° to depth as it does at the surface, and the peneplain surface lay just above the present land surface on the upthrown block, then a minimum of only 12 metres of slip on the fault is needed.

Fig. 3.3: Photo panorama and geological sketch of field relationships at Hyde Diggings (partly after Whetter, unpub. report, 1990)

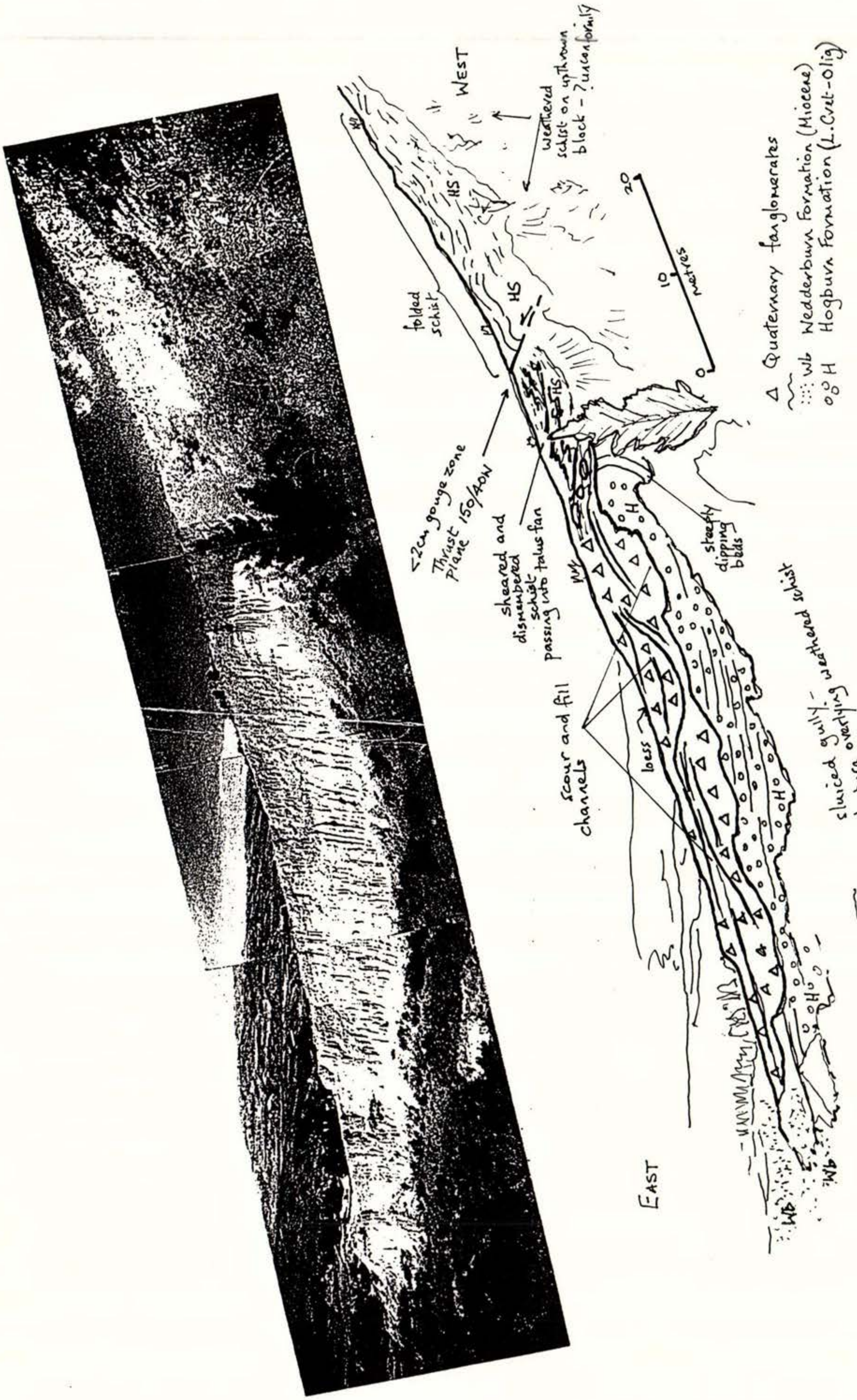

3.3.2 Detailed Investigation of Recent Scarps

Detailed investigation of the range front has uncovered evidence for faulting beneath the central part of the range, from just west of Middlemarch to Lug Creek. Figure 3-2 shows the location of the features identified by Hull (1982) on aerial photographs. Further field checking of these features was carried out to determine whether they are fault scarps or debris flows. On the ground, several of these features seem to be fence lines while others represent alluvial fan - schist contacts with no evidence of faulting. At two sites, some evidence of faulting was found, with the most convincing evidence at site 1 (Fig. 3-2).

Site 1 was surveyed and mapped at a scale of 1:1000 with 2 metre contours (Fig. 3.4) in order to provide greater detail than shown on the 1:25,000 map. The site consists of three small ridges separated by gullies about 20 m deep. The slope breaks in the ridges were identified as scarps by Hull (1982). In the southern part of this site the slope break seems to cut the fan surface producing a 12 metre scarp (Fig. 3-4). Steeply dipping schist on the upthrown side is exposed as weathered surfaces in bare patches on the hillside. The orientation of the schistosity is consistent across the hillside suggesting that it is in place. It is overlain unconformably by bouldery debris flows covered with loess. The fan surface on the southern two ridges is fairly smooth, but the northernmost one has a distinctly hummocky surface. A series of small scarps occur along the line of the break in slope in the southernmost gully (Fig. 3.4) although digging in this area failed to uncover either any gouge or a convincing fault plane. On the other hand, outcrops of grey-green clay-rich schist gouge on the north side of the gully, along strike with the mapped scarps to the south, appear to separate schist from fan gravels. East of the line of the fault, fan gravels appear to extend to the bottom of the gully and no schist is seen. Springs occur in this gully along the fault line.

The slope break is most distinct in the southernmost ridge, and becomes less abrupt to the north, as can be seen clearly on topographic profiles (Fig.3-5). The fault as delineated by these slope breaks appears to be a low angle structure dipping northwest and wrapping around topography, which could account for the confusion over its being a scarp or the toe of a debris flow.

There is little evidence to determine the magnitude of motion on the fault, especially as intact schist is not evident in the downthrown block. This absence of schist outcrop necessitates at least 20 metres (depth of the drainage) of total throw on the fault, if the downthrown block is entirely a gravel fan. To the north of this area, the trace of what would be the fault runs directly into a hillside and disappears.

Fig. 3.4: Detailed map of topography and geological features at Site 1. Mapping carried out with plane table plus telescopic alidade. Contour interval: 2m

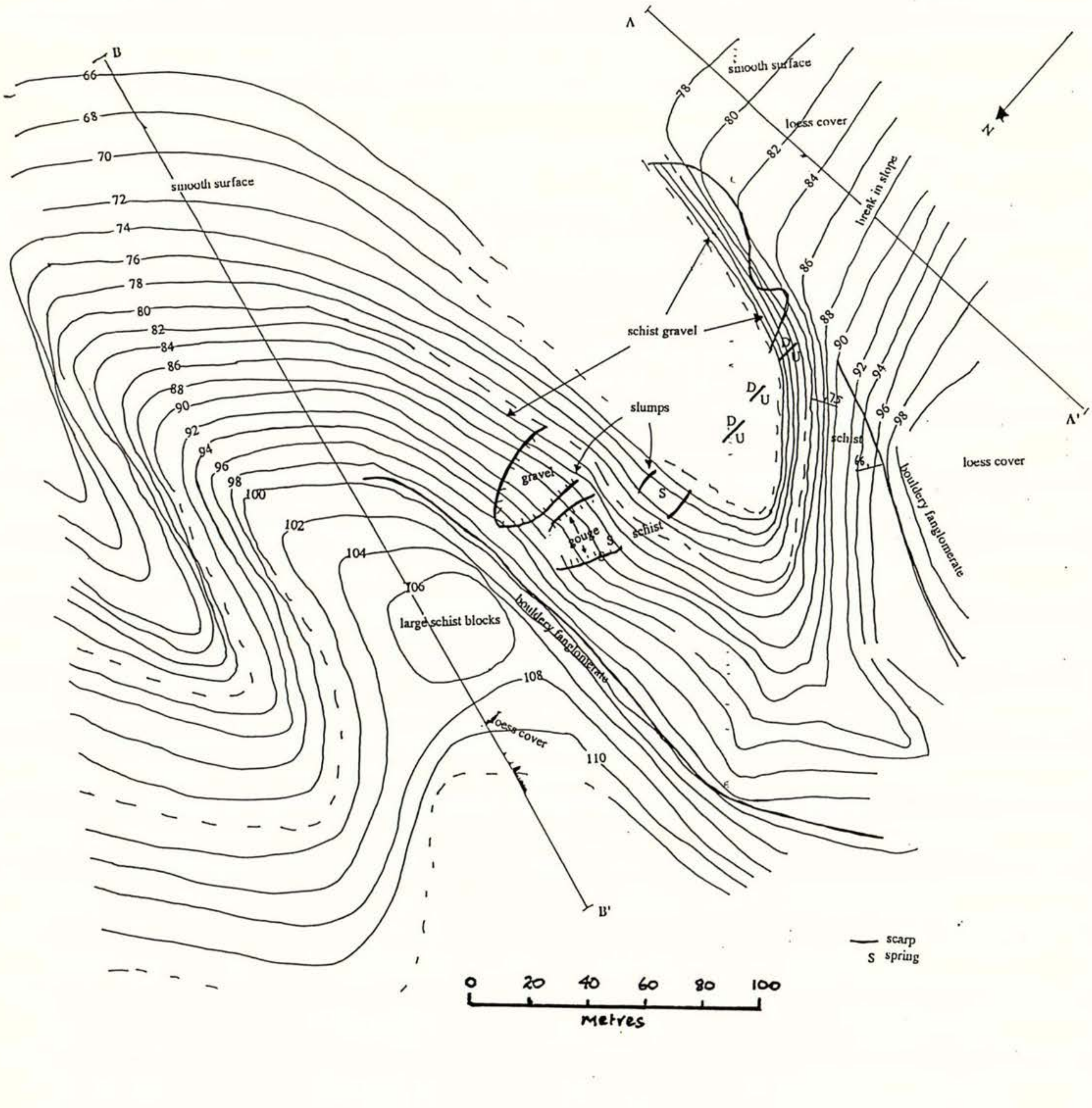

Fig. 3.5: Topographic profiles drawn along lines shown in Fig. 3.4.

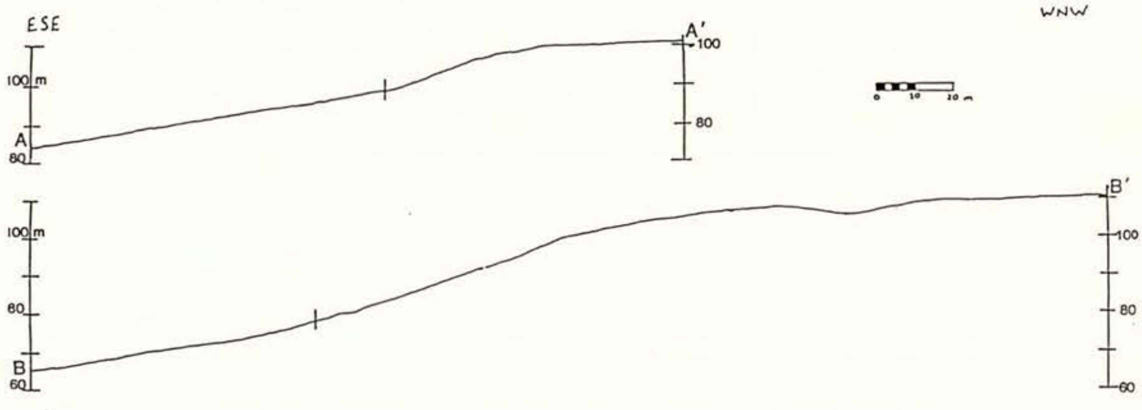

3.3.3 Gouge at Site 2 (Lug Creek)

At site 2 (Fig. 3.2), several springs and gouge zones are present. These are not sufficient to delineate a fault plane, but the gouge seems more developed than at site 1. A gouge sample from about 15cm below ground was taken.

The fault gouge collected at Lug Creek is a matrix-supported, greenish-grey, plastic clay gouge with fragments 1-10 mm in diameter. A thin section made from this gouge shows that it is clearly formed from schist. The micas are the same and the bulk composition of the matrix is similar to that of intact schist. Clasts derived from quartzose layers of schist, which are 90% - 100% quartz (some contain relatively intact chlorite), are supported in a micaceous matrix consisting of chlorite, white micas, clays, some opaques, and some smaller quartz grains. The clasts are often mantled by a 1 to 2 crystal thickness layer of mica which is much finer grained than the micas found in intact schist. This mantling gives the rock the appearance of a ductilely deformed rock in which flow has occurred in the matrix. However, in hand sample it is not lithified, but rather a soft plastic clay gouge. It appears that the more micaceous layers of schist have become disaggregated and the micas broken up into smaller flakes, providing a matrix for more quartz-rich fragments. The micas wrap around these schist clasts

3.4 Quaternary sedimentation along the range front

Quaternary sediments in the Strath Taieri depression are dominated by schist-derived gravels deposited by the Taieri River and alluvial fan sediments extending out from the range front to the river (Fig. 3.6). Loess is also widely developed. The coarser sediments are nowhere very thick, as schist basement may commonly be observed beneath them where a creek has eroded throught the sedimentary veneer. Their characteristics provide indirect evidence that the Rock and Pillar range front is dominated by folding rather than by faulting.

3.4.1 Volume of Sediments

Calculations based on the assumption of a 20 metre thickness of sediment everywhere in the basin (which provides a maximum estimate as this is the largest thickness observed even in the large fans at the highest part of the range) provide an estimate of roughly 10^5 m^3 of sediment in the Strath Taieri basin for every metre of range front.

Had the range simply been thrust up on a reverse fault dipping about 60°, roughly 2×10^6 m^3 of material would have had to have been eroded off every metre of range front to produce the current topography. Therefore the current basin is holding at most only one twentieth of the sediment that must have been shed off the range front had it been produced entirely by reverse faulting. This leaves about 6×10^{10} cubic metres of material along the 40 km long range front unaccounted for in the mass balance. On the other hand, erosion required to produce the present topography from a predominantly folded range front would provide much less sediment, in the order of 3×10^5 m^3 per metre of range front. This is much closer in magnitude to the quantity actually found. The major uncertainty in the argument is the amount of material transported out of the basin by the Taieri River With major climatic changes during the Quaternary, this factor is unknown at present.

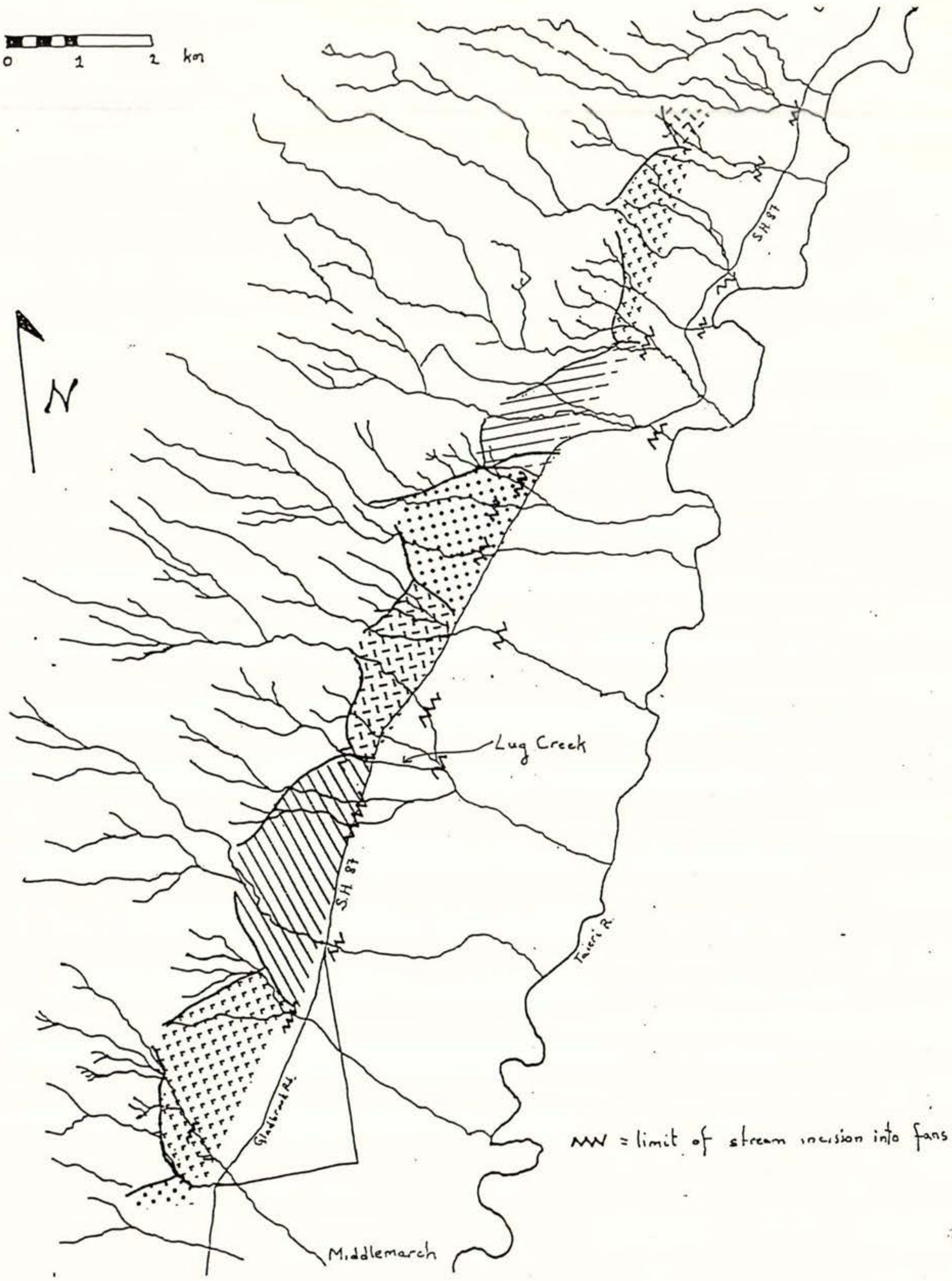

Figure 3·6 Stream incision into fans. Different patterns are to distinguish fans only. Stream incision ends at jagged line; beyond this streams are broad and braided to the Taieri River.

3.4.2 Composition of Fans

At Hyde, the fan gravels are composed of schist in a matrix of reworked Tertiary sediments (Whetter, 1990). Hesson (1981) indicates that the Quaternary gravels are composed of schist with quartz pebbles from the Hogburn Formation (the basal Tertiary unit), and volcanic boulders. This would indicate that the thin veneer of Tertiary sediments has eroded off, followed by only a small amount of schist.The composition of the alluvial fan gravels is therefore also inconsistent with large amounts of erosion of an upthrown block. Had this erosion occurred, the alluvium would be expected to consist almost entirely of schist fragments.

3.4.3 Gold Distribution

Evidence that the range front still lies relatively close to the peneplain surface, indicating little throw on the Hyde Fault and little erosion on the front of the range, comes from the presence of particulate gold in crevices in the schist all over the front of the range (J. Youngson, pers. comm.). This gold is elsewhere found at the peneplain surface -- at the Tertiary unconformity at the base of the Hogburn Formation at Hyde (Hesson, 1981), and also in Hamilton Diggings (Simpson, 1991). If the range front represents deep rock brought up along a steep reverse fault, gold would only be expected on the top of the range where the peneplain is preserved, because on the flank it would have been eroded away. Its presence all over the range front suggests that this surface is still relatively close to the peneplain surface.

3.4.4 Basalt Syncline

North of Hyde, the Tertiary sediments are preserved under a basalt flow which forms an originally flat datum. This surface has been warped along with the schist, Tertiary unconformity, and Tertiary sediments, into a syncline with the west limb dipping off the range front. This warping parallel to the range front is exactly the deformation that would be expected if the range were indeed a large fold.

3.5 Summary

The field evidence accumulated in this study indicates that the Hyde Fault is not a large, through-going structure with 1000 m of throw. Rather, at least at the surface, it is a relatively minor structure in controlling the uplift of the Rock and Pillar Range. The only exposure of a fault is in the Hyde Diggings, where only a relatively small amount of slip is required. At sites 1 and 2, evidence suggests that Quaternary fault displacement has occurred locally along the range front, although in most places, other origins of the topographic break in slope, such as flow fronts of debris flows, are equally likely. The structure of the schistosity and of the peneplain surface also indicates a dominantly folded structure for the range front. Finally, the composition and volume of Quaternary sediments within the Strath Taieri depression is more consistent with a fold than with a fault block structure.

The possibility of strike-slip displacement on the fault has not been addressed specifically. Streams flowing off the Rock and Pillars have no systematic displacement across the range front, although a small component of strike-slip may be insufficient to cause any longterm offsets of channels.

SECTION 4: COMPUTER MODELLING — A FINITE DIFFERENCE SIMULATION OF FOLD GROWTH

4.1 Introduction

Computer modelling was undertaken to evaluate the effect of different initial perturbations on the growth of the range. Modelling was done by FLAC (Fast Lagrangian Analysis of Continua, version 3.0; Itasca, 1991), a finite difference code. This programme was developed for application to geological engineering problems (e.g. mine shafts, tunnels, slope stabilisation). However it is general enough to be useful in modelling larger scale problems in geomechanics.

Modelling in FLAC involves several steps: (1) material properties are defined; (2) a grid of the proper shape is set up; (3) appropriate boundary and initial conditions such as a gravity load are applied; (4) a differential load is applied over a number of time steps. The progressive deformation, stress, strain, particle velocities, yield state, and other parameters of interest are recorded and may be viewed graphically.

FLAC proved to be most useful for modelling growth rather than initiation of structures, because it cannot model instability very well. It does come to numerical instability in some cases. For simple situations, such as a velocity load imposed on the end of a pin-jointed elastic column, numerical instability will occur at the same finite stress as a mechanical instability (i.e. at the Euler buckling stress). In general, however, there is no 1:1 correspondence between mechanical and numerical instability in FLAC. Therefore, the modelling done in this study represents growth of fold structures resulting from either motion on a fault at depth or an initial imperfection in the material.

4.2 Models

4.2.1 Material Parameters

FLAC has several built-in material models representing materials with time-independent stress-strain relations. They are: elastic, transversely anisotropic elastic, Mohr-Coulomb plastic, strain softening or hardening plastic, and ubiquitous joint. Of these, elastic and ubiquitous joint were used. Each requires input of slightly different material parameters as follows:

1) *Elastic*. Required parameters are bulk modulus, K, shear modulus, μ, and density, ρ, where E=Young's Modulus and v=Poisson's Ratio.

2) *Ubiquitous "joint"*. This models the material as a Mohr-Coulomb solid with pervasive planes of weakness oriented in a given direction. (These are called "joints" by FLAC, but are actually planes of weakness or fracture surfaces, rather than strictly tensional features). Required parameters are as for the elastic model, plus internal friction angle, cohesion, dilation angle, and tensile strength for the rock mass. In addition, the properties of the "joints" required are: "joint" cohesion, "joint" friction angle, "joint" tensile strength, and "joint" angle (measured ccw from the x-axis). Deformation proceeds by either shear and/or tensional failure along the "joints" or failure of the material.

The values used in all models, with exceptions as noted, are those reported in the studies for the Kawarau and Clyde Power Projects, where similar schist basement is involved, and are as follows: density =2700 kg/m^3; bulk modulus = 37 GPa; shear modulus = 20 GPa; friction angle = 30° (corresponding to μ=0.6); cohesion =

2 MPa; tensile strength = 1 MPa; "joint" friction angle - 11° (corresponding to μ=0.2); "joint" tensile strength = 0; "joint" cohesion = 0. "Joint" angle varies as discussed below.

The dilation angle for the schist was not reported, but is the same as the internal friction angle. This identity defines associated plasticity. In this study, however, plastic deformation of the material apart from simple, non-dilatant shear on the schistosity planes is expected to be minimal. Therefore dilatant behaviour does not occur, and the value chosen is of little significance.

The material which appears to best represent the schist is the ubiquitous "joint" model, with the mica-rich layers being treated as the "joints" (i.e. pervasive planes of weakness). A Mohr-Coulomb material does not transmit stresses well across long distances. This problem was addressed in two different ways. (1) In the fault analyses, an elastic layer at depth was included to transmit stresses, overlain by a ubiquitous "joint" material. (2) In some models representing schistosity misalignment, the failure envelope for Mohr-Coulomb failure was artificially high and the material stiffened (the elastic moduli increased) to transmit stresses.

4.2.2 Grids

Each grid is 20 elements long by 10 elements deep, each element representing 1 km^2. Two basic grid configurations were developed, one representing a fault at depth, the other an initial misalignment of the schistosity planes. Several variations and combinations of these were used.

Faults are constructed individually by the interface option of FLAC. This function of the programme allows the formation of an interface between two bodies of rock, and requires properties for it such as that of a fault or joint (friction angle, cohesion, shear and normal stiffness, and tensile strength). Interfaces may also be "glued", allowing no slip or separation. Two versions of a fault at depth were constructed: (1) a reverse fault dipping 58° (Fig. 4.1a), and (2) a thrust fault dipping 32° (Fig. 4.1b). The depth below the "surface" to which faulting propogated varied from 3 to 5 km.

The grid representing misalignment of schistosity is constructed by changing the "joint" angle in the ubiquitous "joint" material model. A three element wide zone of "joints" dipping at 15° is set up in the middle of the grid (Fig. 4.1c). This represents the actual initial dip of schistosity in the southern parts of the Rock and Pillars.

Finally, a combination of these initial configurations was used. This was constructed as misaligned schistosity planes overlying a faulted elastic layer (Fig. 4.1 d, e).

4.2.3 Boundary and Initial Conditions

Once the grid is set up and the material parameters specified, an initial gravity load is applied to simulate a lithostatic stress state. The edges of the grid were prevented from motion in the x-direction, the bottom prevented from motion in the y-direction, and gravity was set at 9.81 m/s^2. The programme then solves for stresses based on the density of the material. ρ_{xx} and ρ_{yy} vary linearly from 0 at the surface to 270 MPa at 10 km depth.

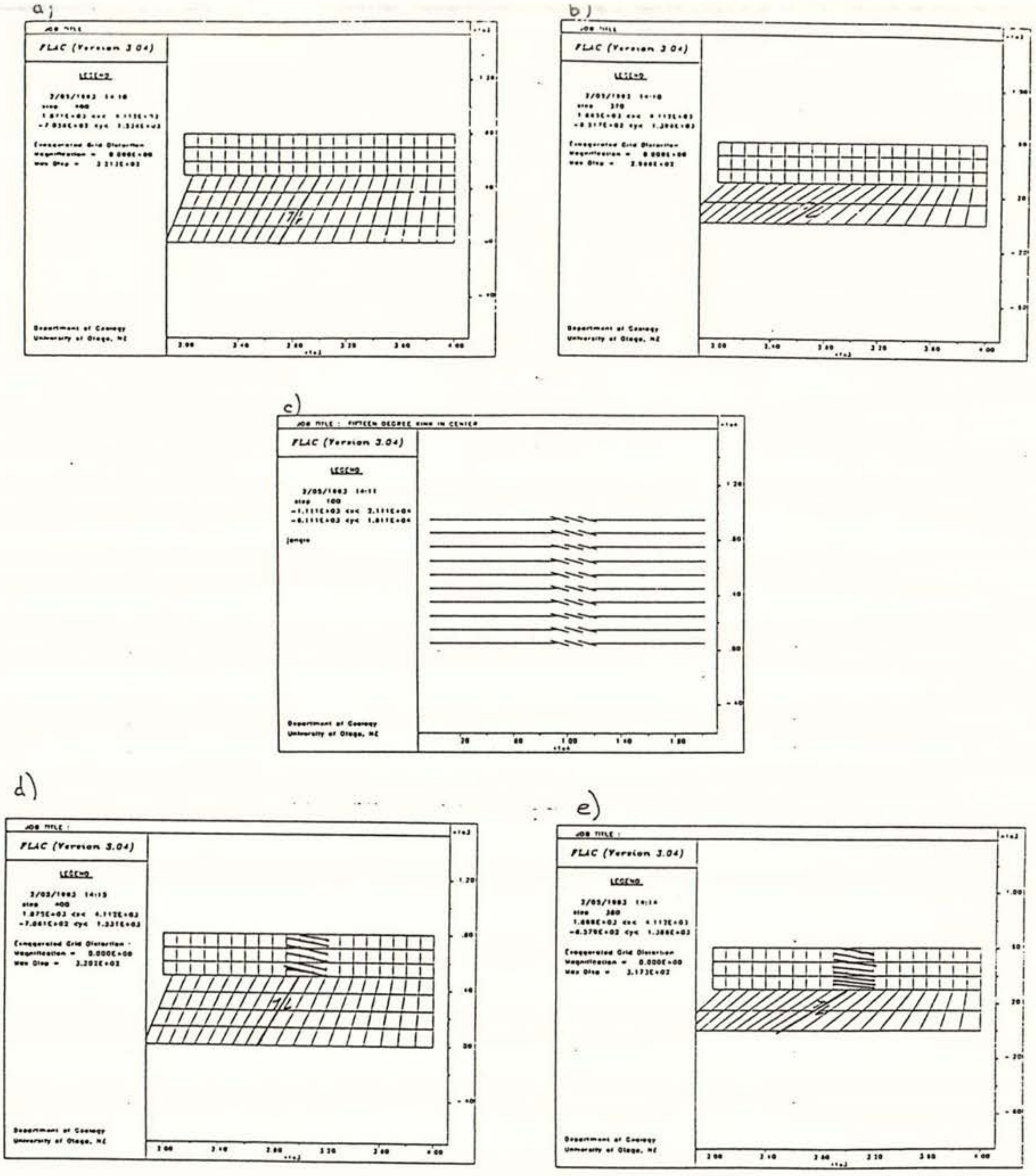

Figure 4-1: Initial grid configurations. a) 3 km. thick layer of ubiquitous "joint" material overlying elastic layer with a 58° dipping reverse fault. b) 3 km. thick layer of ubiquitous "joint" material overlying elastic layer with a 32° dipping thrust fault. c) 10 km thick layer of ubiquitous "joint" material with zone of misaligned "joints" in center. d and e) Combination grids of 3 km thick layer of ubiquitous "joint" material overlying faulted elastic layer. d) Misaligned joints over reverse fault (58° dip). e) Misaligned "joints" over thrust fault (32° dip).

4.2.4 Loading

Compressive loading was accomplished by means of a velocity load on the ends of the grid. The fault models were loaded on the left edge, and fixed at the right edge. The kinked models were loaded from both ends to more effectively transmit stresses. A compression rate of 1 metre per time-step was used for 200 to 600 time steps. At this rate of deformation, each time-step represents about 10^3a for the observed total deformation to occur in 1-2 Ma.

4.3 Results

Many variations in grid, material models and loading were run. The combinations of parameters which produced the most successful results are discussed below. A successful run is judged by how comparable the deformation of the model is to observed features of the range. Factors considered include: (1) asymmetry of the deformed shape; (2) magnitude of uplift; (3) lateral (east-west) growth of the range; (4) whether slip occurred on the schistosity planes; (5) amount of Mohr-Coulomb failure in the material; (6) whether tensile failure occurred at the range crest to produce joints. Each model predicted some of these features better than others.

4.3.1 Reverse Fault

Good results were achieved with 3 km of ubiquitous “joint” material overlying a 3 km thick elastic layer with a 58° reverse fault in it. Asymmetric uplift occurred above the fault (Fig. 4.2a). The magnitude of uplift is about 300 m for 400 time steps. If each time step represents 10^3a, this rate of uplift would produce a 1 km high range in 1.3 Ma. The zone of uplift is about 10 km wide. This is narrower than the range today, but the width of the deformation zone grows as the amplitude increases. The “joints” rotated from flat lying to nearly vertical on the steeper limb of the fold (Fig. 4.2b). This rotation mimics the schistosity seen on the front of the range, which is steeper than the topography.

Plastic failure along the schistosity planes occurred almost everywhere in the upper layer (Fig. 4.2c). Mohr-Coulomb yield occurred only in a few elements close to the edges of the model, which may be attributable to edge effects. If the fault were to propagate into the upper layer, more widespread yielding in the upper layer above the fault would be expected. Some tensile yielding, which would produce joint surfaces in real shocks, occurred in the surface elements in the region of greatest uplift.

Increasing depth of faulting to 5 km results in less uplift on the surface and a more symmetric shape of the uplifted zone.

4.3.2 Thrust Fault

For a 32° dipping thrust fault at 3 km depth, results similar to those for a reverse fault were obtained. The surface uplift is less symmetric, smaller in magnitude (about 200 m for 370 time steps), and occurs over a slightly wider zone than for the reverse fault (Fig. 4.3a). This model produces a fold shape more like the schistosity fold than that produced by a reverse fault model in agreement with the analysis of the folds as fault-propagation features, which predicts a low angle fault at depth.

Again the fold defined by the "joints" has a steeper forelimb than the topographic fold (Fig. 4.3b).

The failure modes of the model are similar to those in the reverse fault model (Fig. 4.3c). Slip on the schistosity planes occurred in most of the elements, with tension failure occurring in elements near the crest of the uplifted region.

Increasing the depth of faulting to 5 km resulted in smaller uplift magnitude and greater symmetry. More tensile failure occurred in the uplifted zone.

4.3.3 Kinked Grids

The main shortcoming of the kinked grids was the inability of the ubiquitous "joint" material to transmit stresses, as discussed above. This problem was circumvented by stiffening the Mohr-Coulomb material. This precludes valid study of failure modes, because failure is constrained to occur on the "joints". Uplift occurred by slip on the schistosity planes to a magnitude of 918 metres at 500 time steps. The width of the uplift zone grows over time to 9-10 km wide by rotation of the "joints" (Fig. 4.4a-c). This deformation is faster and restricted to a narrower zone than that observed in the faulted models.

Asymmetry developed on the west side of the grid rather than the east (Fig. 4.4c). A possible interpretation is that the schistosity misalignment is responsible for the steep back of the range in the south and fault-propagation folding is responsible for the steep front. This possibility can be investigated by use of a combination grid.

4.4.4 Combination Grid

Two combination grids were investigated, one with a reverse fault and the other with a thrust fault, overlain by 3 km of ubiquitous "joint" material with a zone of misaligned joints above the fault. Both resulted in deformed configurations resembling superposition of the deformed fault and kink grids (Fig. 4.5a, b). An 11 km wide zone of uplift with steep sides and a flat top was produced. The magnitude of uplift was about 200 m for 400 time steps. Both slip on the "joints" and tensile failure of material near the top of the uplifted zone occurred.

4.5 Summary

FLAC is not ideal for modelling large deformations, because it crashes for large element distortions. However, up to that point, it represents well the deformation observed in the field. The results achieved with this modelling imply that deformation in the Rock and Pillar Range is primarily driven by faulting at depth. In the north, this produces a strongly asymmetric fold. In the south, the fold shape is also controlled by the initial dip of the schistosity planes, producing a range with steep sides and a flatter top. These models also show that deformation takes place primarily by slip on the schistosity planes, and that Mohr-Coulomb failure at orientations cross-cutting schistosity is a minor part of the total deformation.

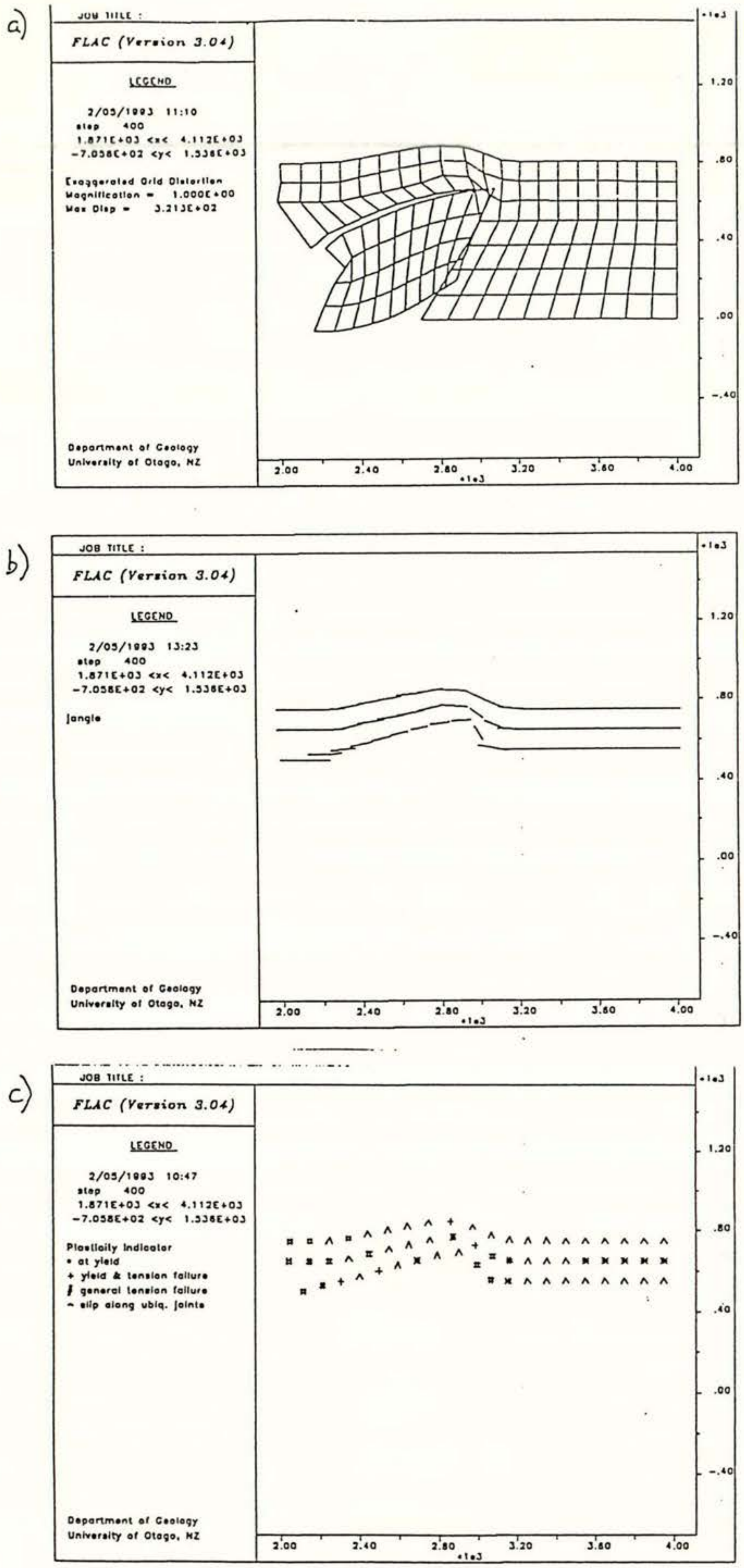

Figure 4-2 : Deformation features of grid with reverse fault (Fig 4-1a). a) Grid deformation. b) "Joint" rotation (corresponds to schistosity rotation). c) Failure mode indicator (most elements show slip on "joints").

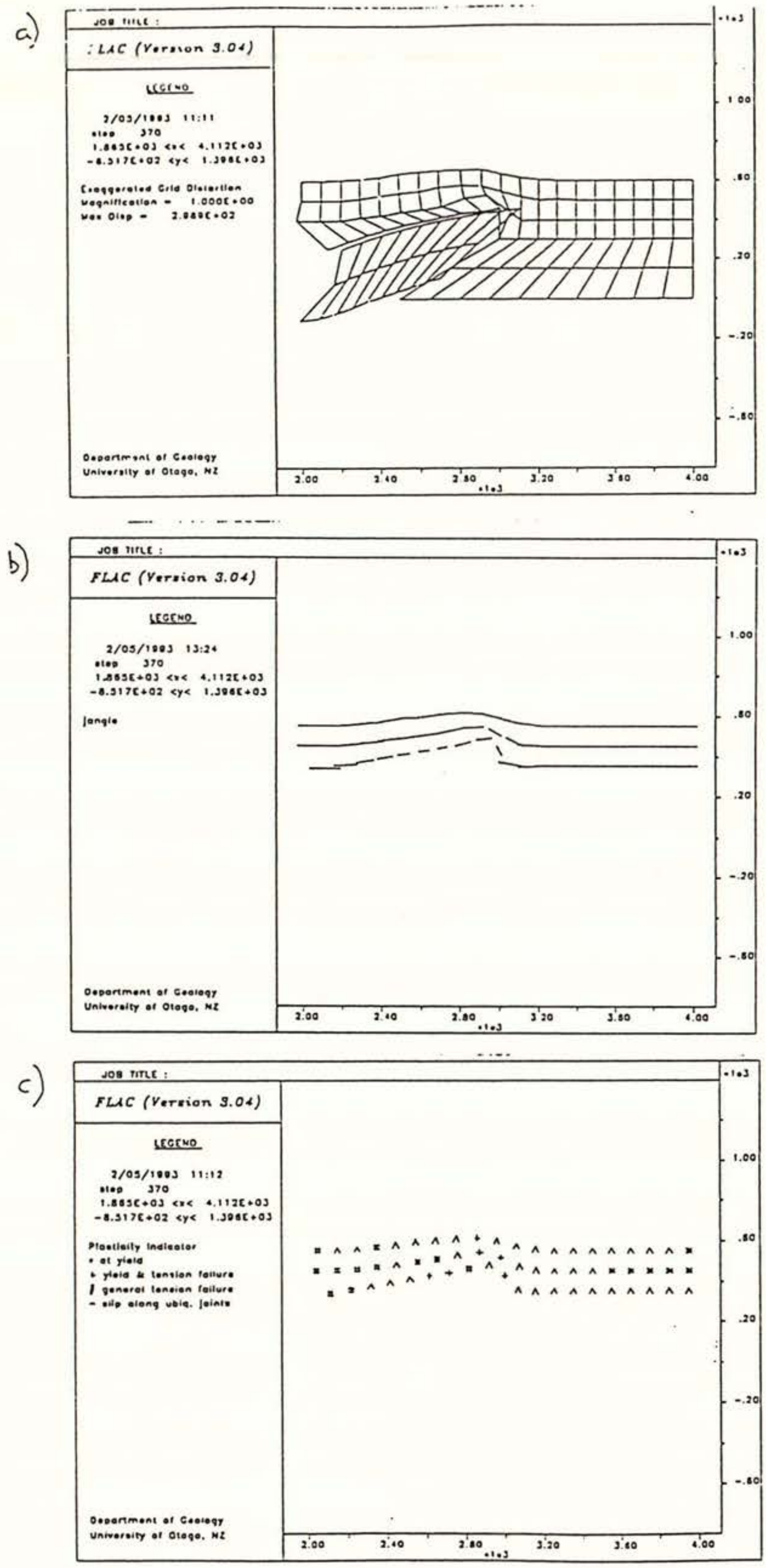

Figure 4-3 : Deformation features of grid with thrust fault (Fig. 4-1b). a) Grid deformation. b) "Joint" rotation (corresponds to schistosity rotation). c) Failure mode indicator (most elements show slip on "joints").

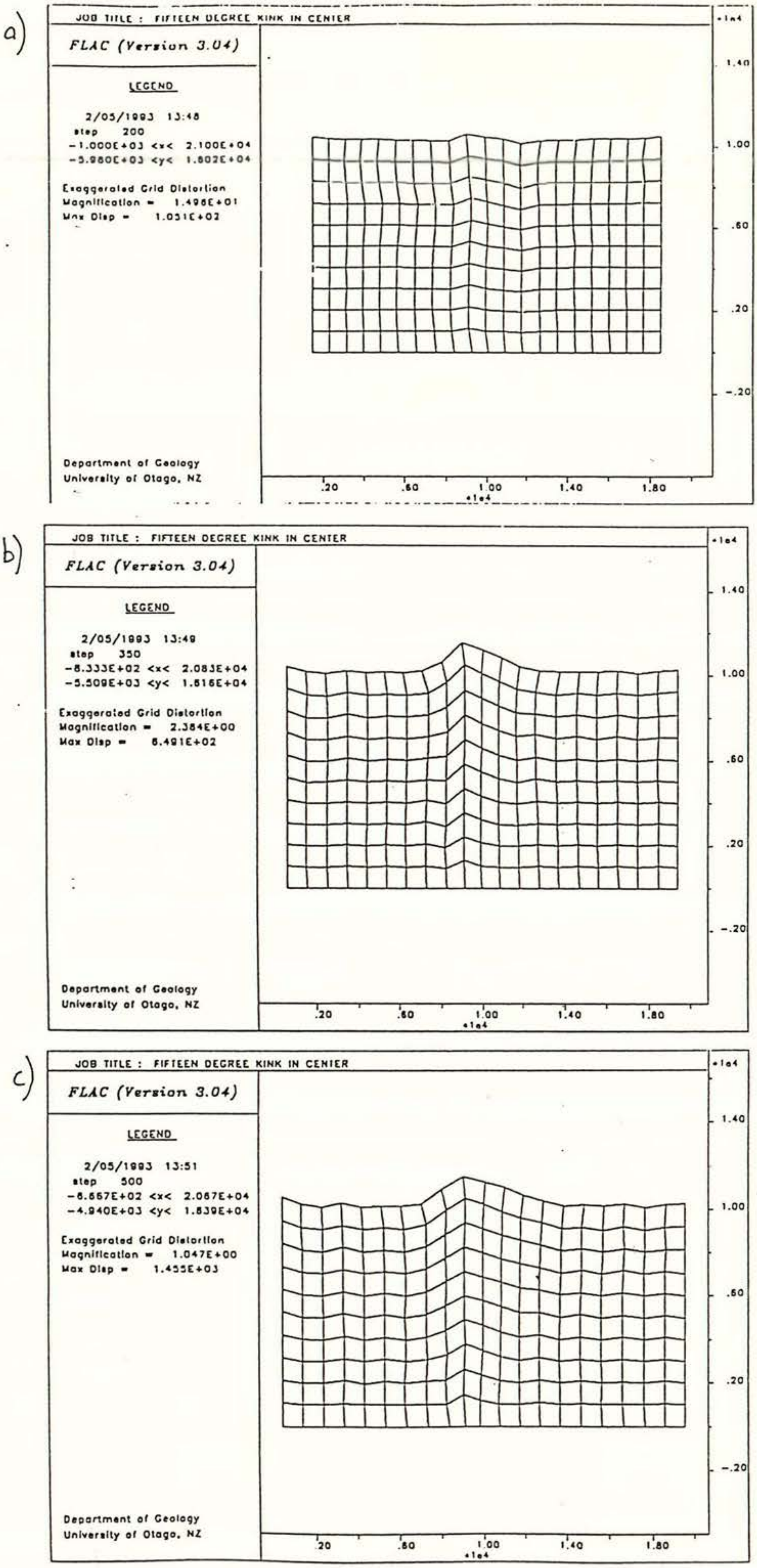

Figure 4-4 : Progressive deformation of grid with misaligned "joints" in center (Fig 4-1c). a) after 200 time steps. b) after 350 time steps. c) after 500 time-steps.

a)

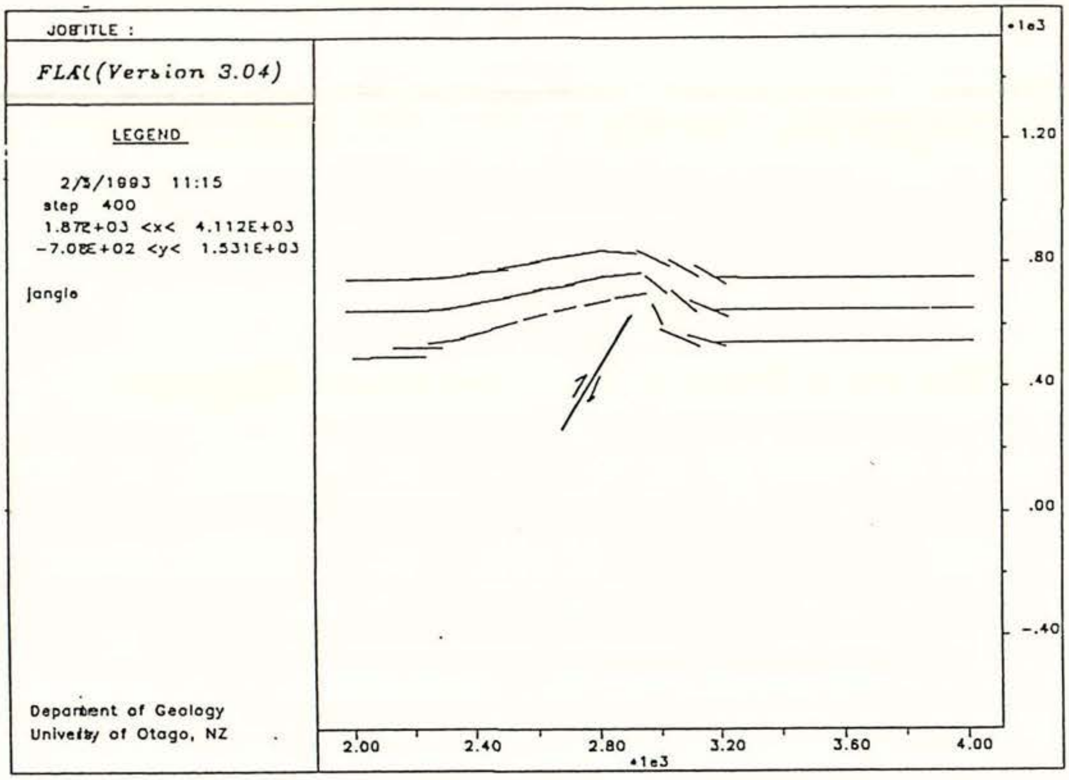

b)

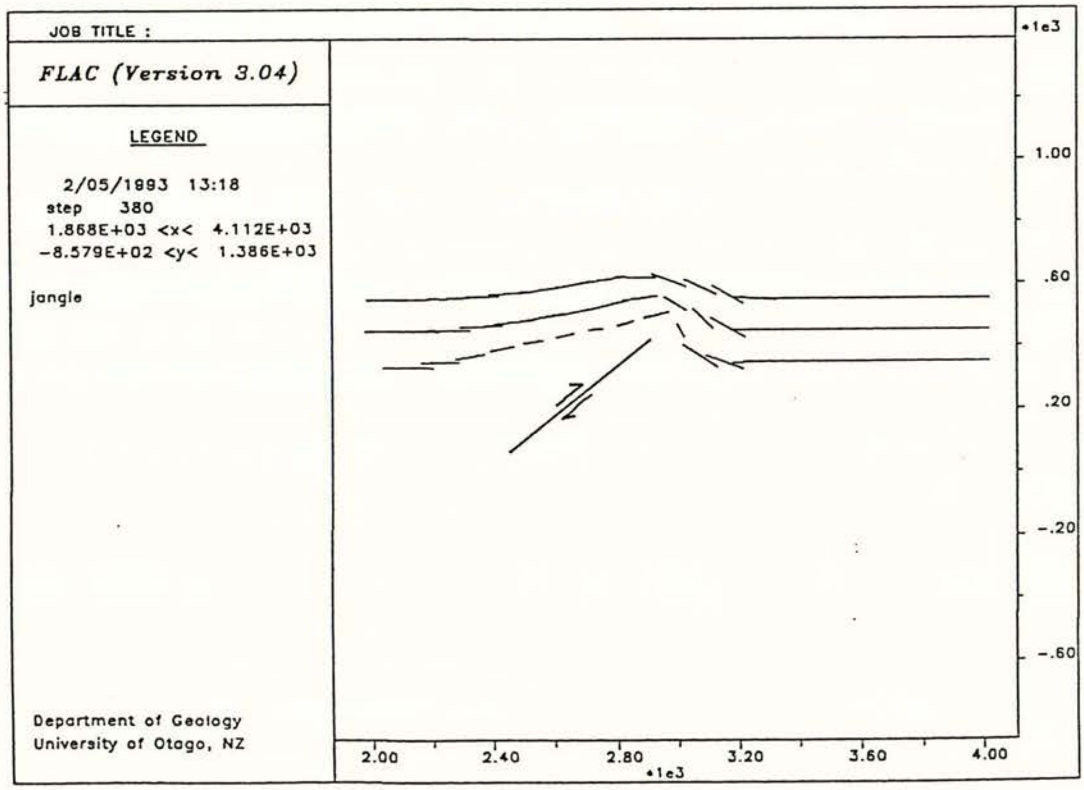

Figure 4-5 : Rotation of initially dipping "joints" in layer above fault. a) reverse fault in elastic lower layer (Fig 4-1d). b) thrust fault in elastic lower layer (Fig 4-1e).

SECTION 5: DISCUSSION AND CONCLUSIONS:

5.1 Structure of the Rock and Pillar Range

The Rock and Pillar Range is shown on the 1: 250000 geological map as being bounded to the southeast by the Hyde fault. Since there is up to 1000m of relief across the range front, a similar amount of displacement might be expected on the Hyde fault, which if spread over 2 Myr, would equate to an average slip rate of 0.5 mm/yr, or 0.5m/10^3yr. Before assessing the paleoseismic significance of fault traces or their absence along the range front, however, it is necessary to determine whether rigid block uplift along boundary faults is the most realistic mechanism for range formation.

Detailed traverses across the range show that the schistosity attitude is largely reflected by the topography, defining a slightly asymmetric fold. Dips of schistosity up to 40° are present at the range front. Where remnants of the Tertiary sedimentary cover remain, the position of the peneplain can be determined. If the peneplain location is projected over the range, it remains close to the land surface, even along the range front. We conclude from this that the range is largely a result of large scale folding of the schistosity and peneplain rather than rigid block faulting.

This conclusion is also supported by the relatively small amount of schist debris present as Quaternary fan and fluvial deposits in the Strath Taieri depression. Many of the fans also contain significant amounts of recycled Tertiary sedimentary material suggesting that the present land surface has not been eroded very far below the basal Tertiary unconformity.

5,2 Hyde Fault

Examination of the range front frevealed only two locations where possible recent fault traces were recognisable. At the first, beneath the central part of the range northwest of Middlemarch, the apparent offset of the smooth surface of a fan is approximately 10-15m. Grey-green gouge was present in the schist close to the line of the trace. The trace appears to dip at a moderate to low angle westwards, indicating a thrust fault, and to extend laterally for only about 2km.

At the second site 5 km northeast of the first, a grey-green gouge is present in the schist at the range front. A faulted contact between schist and fan deposits is possible here although it proved impractical to expose this. No fault trace on the fan surface is evident.

At the Hyde Diggings, a reverse fault outcrops separating schist in the hangingwall from Tertiary sediments and Quaternary fan deposits in the footwall. The sediments are tilted up along the range front and form the western limb of a large syncline within the Strath Taieri depression. Measurements of schistosity and the peneplain surface along the range front here indicate that the range structure is dominated by folding. The lack of any substantial gouge within the fault plane suggests a modest amount of displacement and the geometry of the unconformity may be accommodated by as little as 12m offset. The fault is largely within schist and does not cross recent fan surfaces.

Overall, the evidence strongly suggests that the Rock and Pillar Range formed mainly by a large scale flexure-fold mechanism, with limited development of faulting at the range front surface. Faulting at depth, however, is likely to be significant and may have broken through locally. Deep incision of fan surfaces close to the range front suggests continued uplift and tilting. The fault trace northwest of Middlemarch demonstrates localised late Quaternary faulting and by implication continued uplift of the range front.

5.3 Paleoseismic implications

All fan surfaces have a thick loess cover indicating a minimum age of around 14000 yr. Displacement of these surfaces in at least one and possibly two locations indicate deformation during late glacial and post glacial time. Incision of the western portions of the fans may also indicate continued warping and uplift of the range front. The lack of any dateable material within the fan deposits precludes placing any firm timing on displacement. If the mechanism of deformation of the range is dominated by folding and distributed faulting rather than by a single range front master fault, then the problem of seismic hazard is more complex.

Numerical modelling of folding of the schists on the scale of the range discussed in section 4 shows that the most realistic model, mechanically and geometrically, is a situation where displacement occurs at depth within a westerly dipping fault zone, but becomes distributed nearer the surface by flexural slip on the foliation leading to a range front fold. The depth to the fault tip is best fitted in the models at about 3km. The implication of this for paleoseismology is that surface fault traces may not reflect the total coseismic deformation, much of which will be distributed over the whole range front.

The evidence for continued uplift of the Rock and Pillar range front summarised earlier suggests the potential exists for large earthquakes on the Hyde fault at depth. In the absence of a well-developed master fault at the surface with well-dated surface traces, the best estimate of hazard is to take the longterm average uplift rate and to estimate the length of time required for a maximum 2m displacement similar to events inferred on the parallel Akatore and Dunstan faults. At a rate of 0.4-0.5 mm/yr, a return period of 4-5000 yrs is indicated, similar to that determined on other central Otago faults. Whether the structure deforms in 2m jerks is not possible to state at present.

5.4 Further Work

Dating of the loess-covered fan surfaces may be possible, at least semiquantitatively, using thermoluminescence techniques. These are presently only available overseas, and would require a substantial outlay of funds, as several samples for comparison and calibration would be required. Excavations along the range front may provide more information on surface displacement, but extensive searches for wood material in the exposed fan deposits proved fruitless. Dating of the deposits is the principal requirement of any further study.

5.5 Conclusions

1) The structure of the Rock and Pillar range is best viewed as a large asymmetric fold in schistosity deforming the peneplain surface, rather than as a rigid block uplift along a range front master fault.

2) Modelling of fold mechanics suggests that the fold may be forming above a major thrust fault at depth. The tip of the master fault is best modelled at a depth of 3-5 km below the present ground surface.

3) There is little surface expression of a continuous major fault along the range front. A recent fault trace crosses and displaces an alluvial fan surface at one locality and a similar fault trace may occur at a second locality.

4) The presence of local fault traces together with rejuvenation and deep incision of the heads of alluvial fans towards the range front suggest continued uplift of the Rock and Pillar range.

5) Without any firm dates of the surfaces, the best estimate of seismic hazard is based on longterm average uplift rates and a maximum displacement similar to those determined on parallel faults in the region. A return period for a magnitude 7 event would be of the order of 5000 yr.

PART 3

NEOTECTONICS OF THE AKATORE FAULT

by R. J. Norris, C. A. Landis and P. O. Koons
with assistance from R. Cotton and D. Smith

Report compiled by R. J. Norris, C. A. Landis and P. O. Koons

PART 3

NEOTECTONICS OF THE AKATORE FAULT

by R. J. Norris, C. A. Landis and P. O. Koons

with assistance from R. Cotton and D. Smith

CONTENTS

Contents continued:

SECTION 1: REGIONAL GEOLOGY AND DESCRIPTION OF ROCK UNITS

1.1 Summary of Regional Geology

The Akatore Fault forms a distinctive feature in the landscape of coastal South Otago, where it displaces the conspicuous Cretaceous-Tertiary erosion surface (Fig. 1.1). This nearly planar erosion surface, commonly referred to as the "Otago Peneplain", forms an excellent datum on which to recognize fault location,measure amount of fault displacement, and quantify the extent of post-faulting erosion.

Basement rock throughout the coastal region from Dunedin south to Tokomairiro Mouth comprises schist, greywacke and argillite These rocks originated as sands and muds deposited on a deep sea floor of late Paleozoic to Mesozoic age. Following sedimentation, these strata were deeply buried, hardened and metamorphosed. Uplift and erosion of the metamorphic terrane during Late Cretaceous and early Tertiary time exposed higher grade rocks (greenschist facies)in the north near Brighton and lower grade semi-schists (pumpellyite-actinolite facies) from Taieri Mouth south. This was followed by non-marine (fluvial) sedimentation forming the Taratu Formation sands, conglomerates and coal measures which rest unconformably upon the schist basement. Taratu sedimentation was terminated by a marine transgression which inundated the area now occupied by coastal Otago. Thus the Taratu is overlain by well sorted shallow marine sands of the Wangaloa Formation. There followed a long period (ca.40 million years) of offshore marine sedimentation during which several hundred meters of sediment were deposited in the coastal Otago region (e.g. the Abbotsford Mudstone), but more recent erosion has removed these rocks from the Akatore area. During later Cenozoic time (ca 11-15 million years) an episode of gradual tectonic uplift and volcanism occurred in the Dunedin region. Although only minor volcanic activity occurred in the area south of Brighton (a region peripheral to the main Dunedin volcano), gradual uplift affected the region and associated erosion began removing the Cretaceous-Tertiary sediment cover.

1.2 Map Units

Three geological units are distinguished on the regional map (Maps 1 & 2):

1. Haast Schist
2. Taratu Formation
3. Wangaloa Formation

In addition, Quaternary sediments and volcanic rocks are shown on the more detailed local maps.

Haast Schist (hs) comprises basement for the entire area. The unit consists of Mesozoic meta-greywackes and meta-argillites, with minor occurrences of meta-volcanic rocks along the coast immediately south of Taieri Mouth. The schists possess weak but penetrative cleavage, and lack quartz foliation. As such they are mapped as belonging to Textural Zone 2A of the Haast Schists. They have been metamorphosed to the pumpellyite-actinolite schist metamorphic facies. All of these rocks are strongly indurated and fracture in a brittle manner.They tend to be strongly fractured and, in the vicinity of the Akatore Fault, fracturing may

Fig. 1.1: Map showing Cenozoic faults in East Otago and detail of Akatore fault location.

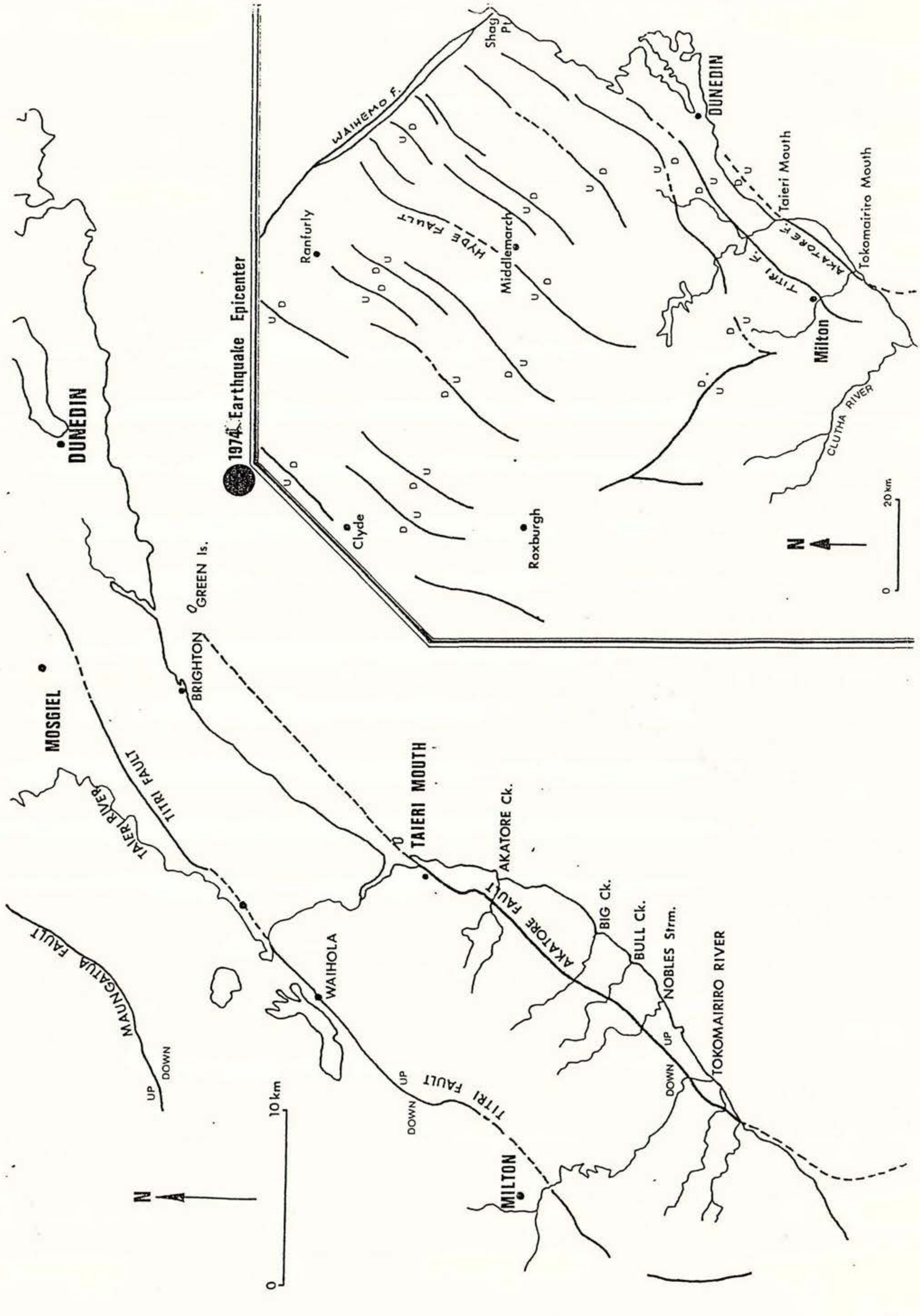

be quite intense. In these areas the otherwise resistant rocks may be quite crumbly and easily eroded.

The **Taratu** and **Wangaloa** formations rest on the Haast Schist from which they are separated by an unconformable (eroded) boundary. This unconformity comprises the Late Cretaceous-early Tertiary Otago Peneplain discussed above. The Taratu Formation consists of quartz gravels and sands with local deposits of coal and kaolinitic clays. The formation was deposited by rivers and streams flowing across the Cretaceous peneplain and in swamps and lakes adjacent to these rivers.. Taratu sediments tend to be poorly sorted and in general their induration is weak, so natural outcrops of the unit are not common. The Wangaloa Formation comprises well sorted, fine to medium sands. These rocks tend to be somewhat better indurated than the Taratu. Sedimentary structures, minerals, and rare occurrences of fossils indicate deposition under shallow marine conditions. Both of these units, along with the underlying peneplain, have been tilted gently southeast. Amount of dip varies, but angles of 6-8° are common.

An igneous dike of basaltic composition cuts the Wangaloa sediments in a roadside exposure north of Akatore Creek (see inset figure in Map 1). On the basis of similarity to volcanic rocks in the Dunedin area, the dike is regarded as Middle Miocene (12-15 million years) in age. The dike is oriented parallel to the Akatore Fault, however whether there is any genetic relationship to the fault is unknown.

Sediments of Pleistocene age occur widely in the area; they are only shown on detailed maps. During the Pleistocene (the last 1.8 m.y.), New Zealand experienced cyclic changes in climate with cold/dry conditions alternating with warmer/moister periods. The cold intervals were characterized by glaciation in mountainous regions, while cool (but ice-free) climates prevailed along the Otago coast. At least four such cycles are recognized. During glacial periods, large amounts of wind-blown dust accumulated throughout coastal Otago. These deposits, known as **loess**, mantle much of the Akatore region's landscape. In most areas we recognize only one layer of loess and therefore interpret it as having accumulated during the last glaciation, probably about 12-14000 years ago. In areas of steep slopes characterized by mass-wasting, and in regions with gentler slopes during periods of intense freeze-thaw activity, gravity-driven sediment accumulated on sloping ground and at the bases of slopes. These deposits are mapped as **colluvium**. Stream channel and flood-plain deposits are mapped as **alluvium**. If they formed since deposition of the last loess (i.e., within the past 10000 years) they are mapped as being of Holocene age. **Beach sands** occur along parts of the modern coast where they have accumulated since the last glaciation; older beach sands formed at many times in the past; these older deposits can be recognized by their occurrence beneath loess or colluvium. Since Pleistocene sea level fluctuations are known with some precision, if a beach deposit can be dated, it is possible to determine the amount of vertical tectonic displacement which has occurred in the area.

SECTION 2: THE AKATORE FAULT TRACE

2.1 Field mapping

During the course of this project, the surface trace of the Akatore fault was mapped between Taieri Beach and Tokomairiro River mouth. The results are presented on Maps 1 & 2 at a scale of 1:25,000. Mapping was based on a combination of air photo interpretation and field examination. The section of fault from Taieri Beach to Big Creek was walked out and detailed field observations made. The section south of Big Creek was field checked at critical points but the whole trace was not examined in the field. Nevertheless, we are confident that we have located the trace to within ±25m over most of its length, and in many places to within a metre or two. The older, low altitude, aerial photographs (N. Z. Aerial Mapping runs 1141-1146 flown in 1946) proved to be of greatest value because they were taken prior to the extensive afforestation programme along the coast. Forest growth on more recent aerial photos tends to obscure details of the fault zone.

The line of the fault is marked along the whole of its length by a prominent fault line scarp, the height of which reaches a maximum around the centre of the block at Big Creek. The actual trace of the fault is usually located part way up the scarp and where exposure allows, is seen to separate bedded, well-sorted, fine sands of the Wangaloa Formation from slaty greywackes and argillites of the Haast Schist. In places where the trace crosses late Pleistocene and Holocene sediments, mainly in the valleys of the major antecedent streams, a clearly defined fault scarp about 2m high is observed. In other places where Holocene sediments are not present, a similar sized scarp may nevertheless be clearly visible crossing hillsides and exposing crushed Haast Schist.

The general strike of the fault is between 035° and 040°, but in two sections, north of Akatore Creek and between Big Creek and Bull Creek, the fault trace has a more northerly or even NNW strike. The structure is described in more detail below.

2.2 Field observations

2.2.1 Taieri Beach

A prominent line of rocky reefs extends offshore from the southern end of Taieri Beach delineating the upthrown side of the Akatore Fault. The reefs are composed of Textural Zone (TZ) 2 Haast Schist and in addition to the normal synmetamorphic structures, exhibit angular chevron folds and cataclastic shear zones.

The line of the fault crosses the beach and then is seen as an approximately 4m high degraded scarp cutting a flat terrace surface to the south. In section, this terrace has a metre of soil overlying a 2m thick loess deposit which is underlain by about 2m of yellow-red indurated coarse sand (interpreted as a beach sand) resting on an erosion surface in Haast Schist. The surface on the upthrown side is around 9-10m above the highest water level of the present beach.The presence of the loess indicates that the beach sands are older than 14 ka.

Along the coast on the uplifted side of the fault, a lower raised beach is evident. This one consists of about 1.5 m of non-indurated, bedded, fine sand resting on schist and overlain locally by soil, slump deposits and carbonaceous silt with wood fragments (Fig. 2.1). A carbon date on a piece of wood from this overlying material gave 1010 yr BP. The top of the sand is about 2m above the present beach level.The significance of the offset terrace and raised beaches is discussed further in section 4.

2.2.2 Taieri Beach to Akatore Creek

The line of the fault follows the fault-line scarp to Akatore Creek. The trace crosses the coast road close to the entrance to the Forestry Headquarters and continues south as a prominent change in slope about half-way up the hillside. Exposures of Cretaceous sediments west of the trace and Haast Schist imediately east of it confirm the topographically determined location of the fault. GR924527, the trace appears to split and a well-defined scarp appears about 30m to the west. The topography here appears to be displaced, possibly with a small right-lateral component.

South of the minor, westward-heading road, the trace is clearly expressed as an approximately 2m high scarp intermittently exposing Haast Schist part way up the hillside. Exposures of sedimentary rocks to the west confirm this as the main fault line. The strike of the trace is 039°.

At GR917537, a continuous section up a gorse-filled gully exposes flat-lying interbedded gravel and sand, with channel bedding of gravel. The pebbles in the gravels are up to 1 cm diameter and are mainly composed of well-rounded quartz. The interlayering of sand and gravel becomes more pronounced upwards, with continuous beds of finer, well-sorted sand becoming prominent. The top 4m or so of the 25m thick sequence is composed entirely of horizontally bedded, well-sorted, fine sands of the Wangaloa Formation. The lower material is identified as Taratu Formation, with what appears to be a gradational contact between them.

At the top of the gully, the sands of the Wangaloa Formation are abruptedly truncated by a steep face in cataclastically deformed Haast Schist. A grey-green coloured clay gouge up to 30 cm thick is locally exposed at the contact. The fault contact strikes 350° and dips approximately 45°E. This represents a swing in strike of almost 50°, although the fault appears to be a continuous feature through here. The fault line continues with this strike to where it recrosses the coast road at GR918528. Immediately south of this point, the strike swings back to about 040°. The NNW striking portion of the fault is just over 1km long.

At GR918528, the coast road describes a hairpin bend and the fault plane is well exposed in roadcuts on either side of the bend (Plate 1b). The detailed geology of the site is shown in the inset map on Map 1 and a view looking northeastwards along the the fault across Akatore Creek towards the NNW striking portion is shown in Plate 1a. Horizontally-bedded fine yellow sands of the Wangaloa Formation are found on the western side and these are intruded by a basalt dyke, presumably belonging to the Dunedin Volcanics.

The fault zone itself consists of about 4cm of grey plastic clay gouge overlain by about 30cm of cataclastically deformed schist with numerous thin gouge zones and shears (Plate 1b, Fig. 2.2). The fault plane strikes on average 015° and dips at 60°E. Slickenside striations within the basal gouge trend 090° and plunge about 58° E. Above this, the schist is folded into angular kink-style folds verging westwards with further isolated thin gouge zones. The whole zone of intense deformation is about 1m thick, although deformation within the basement rocks

A6

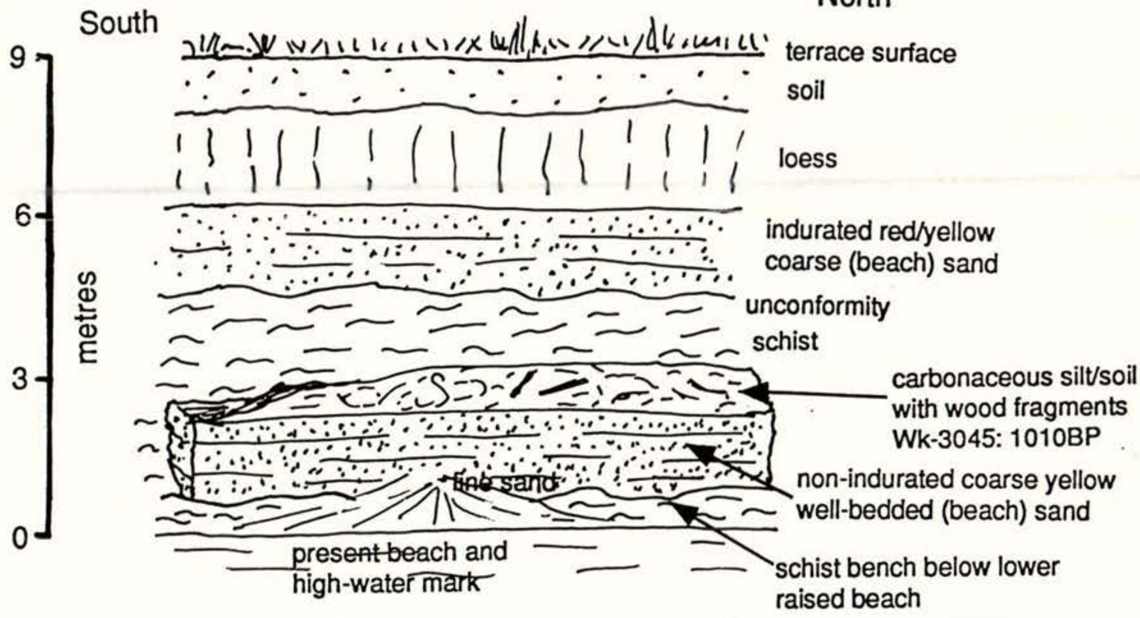

Fig. 2.1: Field sketch of section exposed on coast south of Taieri Beach (GR 934537). Lower raised beach is plastered against cliff face in schist.

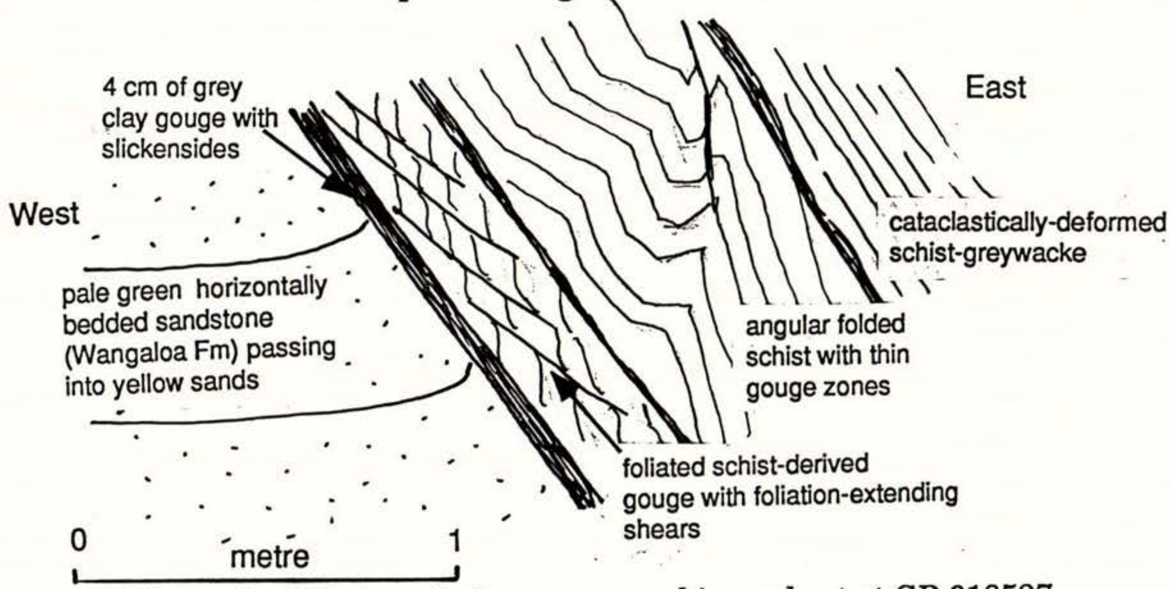

Fig. 2.2: Field sketch of Akatore fault zone exposed in road cut at GR 918527. See Plate 1b. Structures in gouge indicate reverse slip.

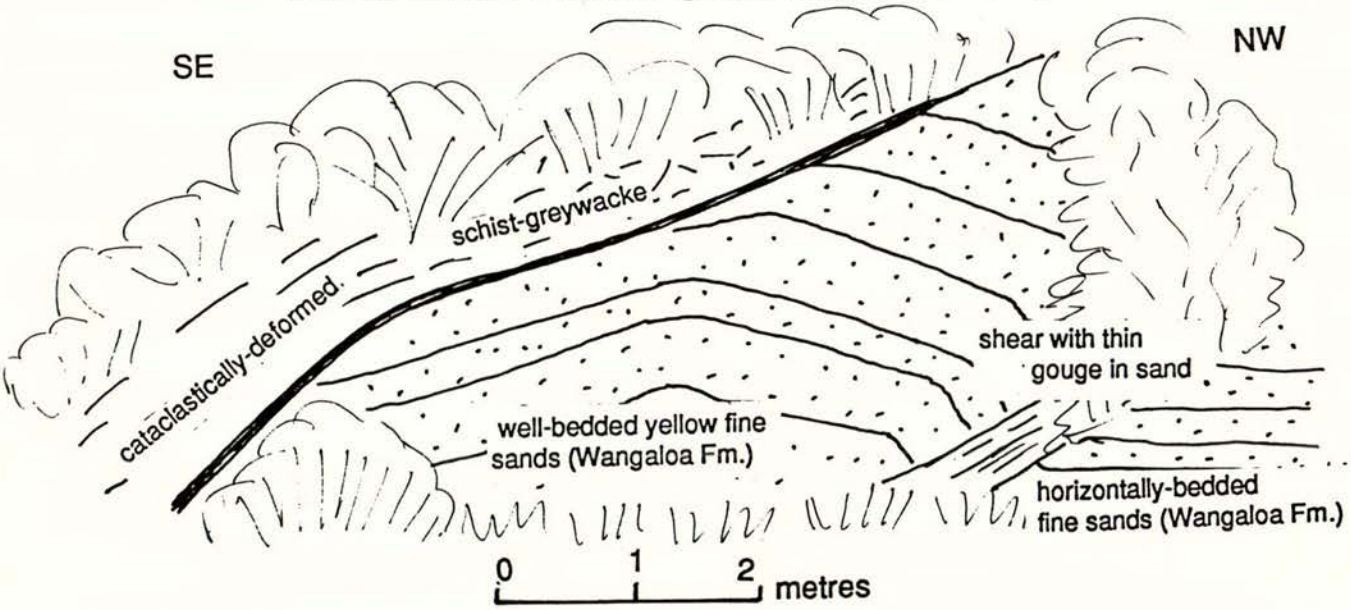

Fig. 2.3: Field sketch of Akatore Fault zone exposed in quarry south of Big Creek (GR 871471).

continues beyond this. One of the problems here is that it is difficult beyond this point to isolate deformation related to the fault and earlier deformation within the schist. Several minor gouge-filled fault zones, commonly exhibiting normal displacement, occur within the schist but the indurated nature of the gouge suggests earlier structures than the present Akatore Fault. However, at GR919528, about 150m up the road from the main fault outcrop, a fault zone striking 016° and dipping 58°E contains a 30cm gouge zone including soft clay gouge. Secondary structures within the gouge indicate reverse displacement. We are fairly confident that this represents a minor fault related to the main Akatore structure.

The change in fault strike from 350° to 040° takes place through the road section and the attitude of the fault in outcrop is intermediate between the two sections, again indicating that the fault is a continuous structure through the swing in strike. For the two sections to be part of a continous fault surface, the slip direction should be constant around the bend. If the slickenside striations represent the slip direction on both sections of the fault, we would expect a component of right-lateral displacement on the 040° sections whereas the northerly striking sections would be almost pure reverse slip. The change in dip of the different sections required to accommodate this is minimal (6°).

2.2.3 Akatore Creek to Big Creek

The fault trace disappears beneath the recent alluvium of Akatore Creek. The creek has cut an antecedent gorge through the uplifted fault block. Haast Schist basement is exposed on both sides of the gorge virtually up to the line of the fault. On the south side of the gorge, a rough bench appears to be cut into Haast Schist approximately 2m above the high tide river level and extends upstream as far as the fault line.

South of Akatore Creek, the line of the fault is obscured to some extent by pine plantations, but it is easily discernible on the 1946 aerial photographs. Exposures created along logging roads within the forest also allow detailed mapping of the fault. At two places, the fault gouge zone is exposed (GR893497 and GR891495) and the attitude may be measured: strikes and dips of 030°/50°E and 035°/55°E were recorded.

South of GR888490, there appear to be two clear lineaments on the aerial photographs. The western lineament is in places sharply defined and at GR887488, has a clear scarp on topography. Exposures in the neighbourhood show that this lineament is the contact between the Cretaceous sediments to the west and the Haast Schist to the east, and therefore represents the main Akatore Fault plane. The lineament to the southeast is also well defined in places and at GR881480, road cuts expose Haast Schist faulted against Quaternary gravel. This may represent a secondary parallel fault within schist as also recorded in roadcuts north of Akatore Creek (section 2.2.2 above).

Along this section of the fault, some creeks appear to have slight right-lateral kinks in their valleys coincident with the line of the fault. While not definitive evidence, particularly as other creeks show no deviations, this is consistent with a component of right-lateral slip on the northeast trending sections of the fault as suggested by the slickenside striations (section 2.2.2 above).

2.2.4 Big Creek to Bull Creek

At Big Creek (Map 1, GR872472) the fault trace is clearly seen as a 2m high west-facing scarp across the Holocene alluvium (Plate 1c). This has had the effect of damming the creek and creating a swamp on the upstream side of the scarp. Haast Schist is exposed in the creek upstream from the scarp and is overlain on the sides of the valley by Wangaloa Formation. On the downstream (upthrown) side of the fault, schist extends up to the exhumed peneplain surface on top of the fault block at over 220m above sealevel, making the total throw on the fault here approximately 130m. Detailed mapping and investigations were carried out at this locality and are reported in Section 4.

Immediately south of Big Creek valley, a small quarry on the fault exposes a clay gouge zone separating cataclastically deformed schist from Wangaloa Formation sands. Close to the fault, the underlying sands are folded into an angular fold which is in turn thrust along a lower gouge horizon over horizontally bedded sands (Fig. 2.3). This is the only locality where deformation extending into the sands below the fault is seen. Combined with the observations of the trace across the river, a strike of 039° and a dip of 60°E were measured.

The trace south of Big Creek is not well defined, in part due to slumping, but picks up again north of Bull Creek where a second trace just to the east of the main fault is again discernible. This section of the fault strikes about 015°, considerably more northerly than the "normal" 040° strike. It appears to be a similar bend in the fault as the bend north of Akatore Creek.

A well-defined west-facing scarp delineates the fault trace across the Holocene alluvium of Bull Creek, very similar in appearence to the scarp at Big Creek.

2.2.5 Bull Creek to Tokomairiro River

South of Bull Creek, the fault trace is clearly demarcated in many places by a degraded scarp around 2m high about halfway up the slope of the fault escarpment. At Nobles Stream (GR846433), a west-facing scarp across the Holocene alluvium of the valley has dammed the creek as at Big Creek, creating a swampy area upstream of the scarp. This has been drained by the owner by the construction of a drainage channnel through the scarp into the antecedent gorge (Plate 1d). Dating of samples from this excavation are reported in Section 4. The height of the uplifted peneplain and the total throw on the fault here are both substantially lower than at Big Creek, the throw being about 75m.

The trace of the fault continues southwards as a degraded scarp with a strike of about 040° (Plate 1d) until the neighbourhood of GR835420 where it becomes less clear and the escarpment falls in altitude towards the Tokomairiro River. Beach deposits below a terrace surface approximately three metres above river level on the upthrown side of the fault are cut and truncated by the fault. Shell material within these uplifted beach sediments (collected by McKellar in 1963) has been dated as 1865±50 yr BP (before correction for the marine reservoir and calibration to a calendric timescale). This date is further discussed in Section 4.

On the coast north of the mouth of Nobles Stream, a prominent raised rocky bench with beach sands but no loess cover may correlate with the dated sequence at Tokomairiro River.

2.3 Discussion

The fault is everywhere a moderate to steeply eastward dipping structure with dominantly reverse slip. In two sections of between 1 and 1.5 km long, the strike swings more northerly to 015° in the case of the Bull Creek–Big Creek section and to 350° in the section north of Akatore Creek. In both these sections, the fault appears to be a single continuous structure with the more northeasterly striking sections.

The only kinematic information on the fault plane comes from the freshly exposed gouge in road cuts north of Akatore Creek where slickenside striations trend east-west. This direction is quite compatible with a single fault plane and would indicate dominantly reverse motion on the more north-south striking sections, with a more significant right-lateral component on the longer northeast striking portions. For instance, for an event with a 2m throw on these sections, a strike-slip component of 0.85m would be predicted. Such a small amount would be difficult to detect in offset of natural features, although small right-lateral kinks in some stream channels along the line of the fault may represent the cumulative effect of strike-slip displacements. If the total maximum throw of about 130m, in the vicinity of Big Creek, took place with a constant slip direction, a cumulative total of about 55m of right-lateral strike-slip would be expected. The fact, however, that the total offset on the fault is a maximum in the centre and reduces both to the northeast and southwest (see next section) means that change in orientation of the net slip vector along the fault is required as there must be a net rotational component to the slip.

The youthful appearance of the escarpment suggests a young age for the fault displacement, as discussed in the next section. In particular, Holocene fault scarps across river valleys and degraded but still distinct scarps along the slope of the fault escarpment in many places indicate a geologically recent age for the last ground displacement. These scarps are generally between 1 and 2 metres high. Their age and significance is discussed more fully in Section 4.

PLATE 1

(a) View of Akatore fault-line scarp looking northeast across Akatore Creek. The creek flows to the right and cuts through the antecedent gorge on the centre right of the photo. the smooth peneplain surface on top of the Akatore block is clearly visible. The actual fault trace is about half-way up the scarp.

(b) Exposure of fault plane of Akatore Fault in roadcut at GR 918528. East is to the right. The fault plane dips to the east and emplaces fractured basement greywacke over horizontally-bedded sands of the Wangaloa Formation. The light-toned material along and above the fault is gouge. See Fig. 2.2 for a detailed sketch of the fault plane structure.

(c) View to southwest of fault scarp at Big Creek. The downthrow side of the fault is swampy due to damming of the creek by the scarp. The quarry figured in Fig. 2.3 is on the hillside in the top right corner.

(d) Aerial view of the fault scarp across Nobles Stream. The view is to the southeast - the fault trace runs from left to right across the centre of the photo. The creek flows towards the top of the photo through the antecedent gorge. A recent scarp can be seen crossing the creek and extending across the hillslope through the bend in the road.



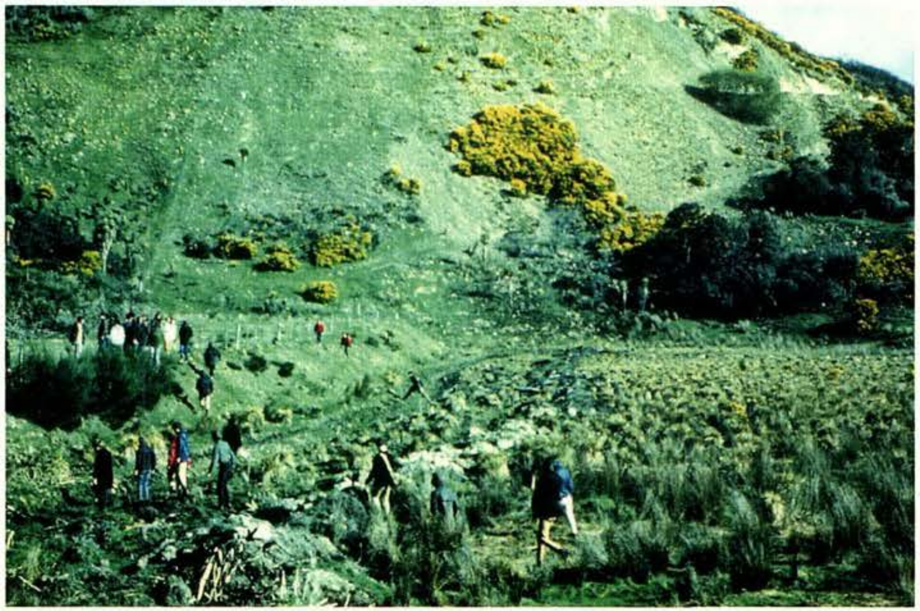


SECTION 3: GEOMORPHOLOGY OF THE TITRI AND AKATORE FAULT BLOCKS

3.1 Introduction

Two major Quaternary faults occur between the Taieri Plains and the coast: the Titri Fault which bounds the plains to the east and the Akatore fault which extends parallel to the coast between the Taieri and Tokomairiro Rivers. Both are dominantly reverse faults dipping to the east. The uplifted block above and southeast of the hangingwall of the Titri Fault, is here referred to as the Titri block, whereas the block above the hangingwall of the Akatore fault, between the fault and the coast, is referred to as the Akatore block.

3.2 Shape of the deformed peneplain

Uplift on the Titri and Akatore faults has deformed the late Cretaceous unconformity which approximates a peneplain surface in this area. By smoothing and contouring the height of this surface in the area of interest, the shape of the deformed surface can be displayed (Fig. 3.1). The uplifted Titri block clearly has the shape of a half dome with its centre approximately halfway between the Taieri and Tokomairiro rivers. The uplifted Akatore block shows a similar shape with the highest point of the dome around Big Creek, more or less in line with the Titri block domical uplift. The seaward bulge of the coastline here reflects the dome shape of the uplifted peneplain surface.

The Akatore "halfdome" may be interpreted as a due to a planar fault of constant slip offsetting an already existing dome structure (the Titri "dome"). Alternatively the Akatore halfdome may reflect differential uplift along the length of the fault with maximum uplift in the central part (vicinity of Big Creek) and displacement decreasing to the north and south from the vicinity of Big Creek.

Offset of the peneplain surface across the Akatore Fault is graphed in longitudinal profile in Figure 3.2. Data points indicate a broad curve with maximum vertical offset (120-130m) in the Akatore Creek-Big Creek area decreasing to northeast and southwest. At Taieri Mouth where the fault crosses the coast line, displacement is reduced to 50m. The fact that the zone of maximum displacement extends from Big Creek as far as Akatore Creek, where the deformed peneplain surface is more than 100m lower than at Big Creek, indicates that the fault has displaced the already-formed southeast plunging Titri block anticline. On the other hand, the significant differences in amount of vertical displacement along the length of the Akatore Fault suggest that the fault propagated outward from a central break near Big Creek. Thus both hypotheses suggested in the previous paragraph appear to be valid.

Holocene displacement is evident at Taieri Mouth where the fault crosses the coast passing northeast out to sea. Here a Holocene beach has been raised 2m by the fault, a displacement similar to Holocene movement in the center of the halfdome. This suggests that as the fault propagated outward, individual surface ruptures became longer and seismic events became more intense. Offshore from Taieri Mouth, the trace of the fault can be recognized in seafloor scarps as well as in sub-bottom seismic profiles (see Section 5). Approximately 30m displacement of the peneplain is recognized off Dickson Road, approximately 8 km north of Taieri Mouth. The fault clearly continues north from here, but whether it comes back on shore remains unknown.

Fig 3.1: Smoothed contour map of the Cretaceous peneplain/unconformity surface on the Titri and Akatore Blocks. The dissected scarp area west of the watershed on the Titri Block is left blank as the peneplain surface is not preserved here.

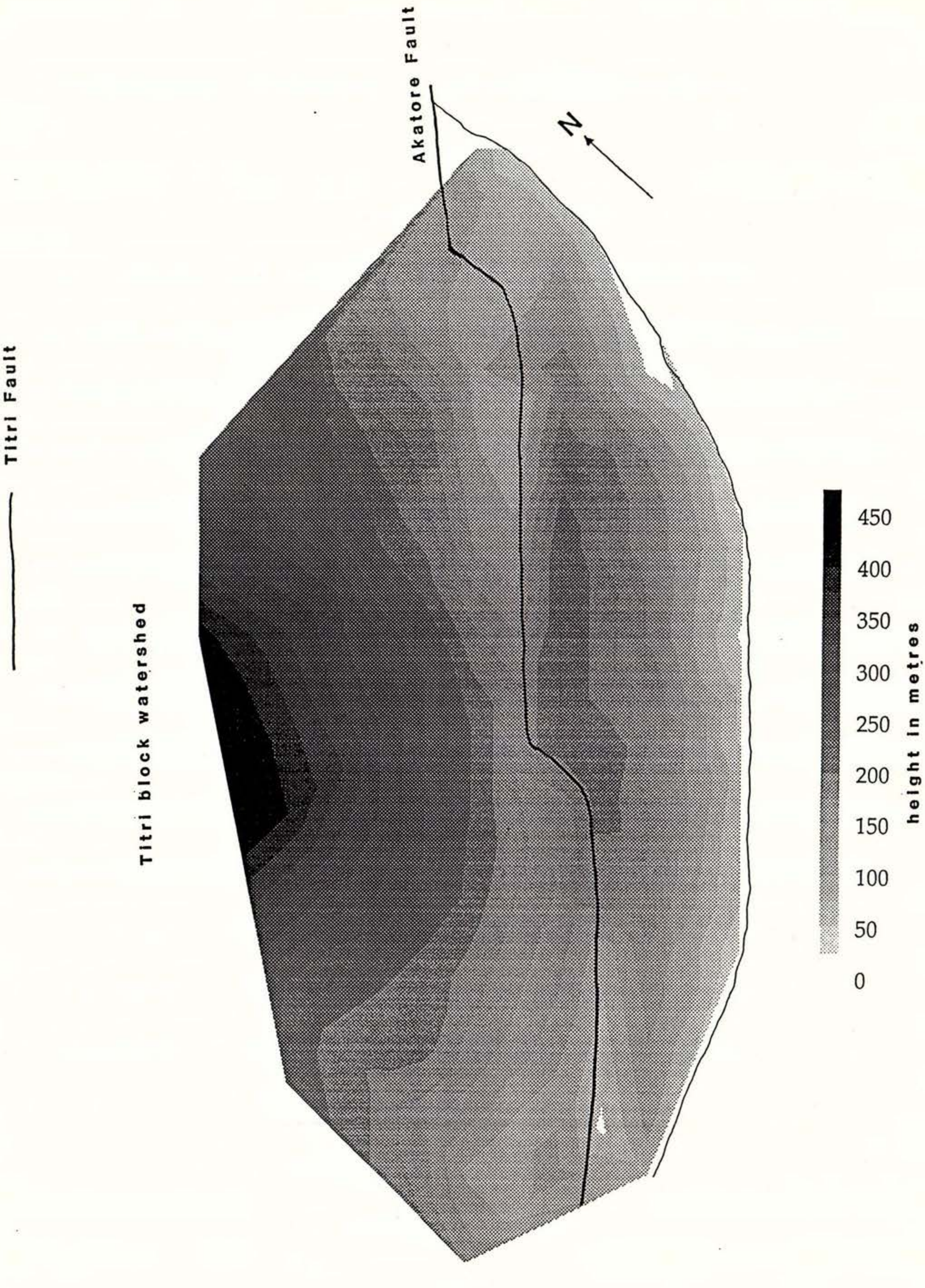

Fig. 3.2: Chart showing height of the peneplain surface on either side of the Akatore fault. The circles are heights on the west side (footwall) projected where necessary to the base of the fault scarp; crosses are heights on the east side (hangingwall) of the Akatore Fault. The difference between the two lines represents the net vertical offset (throw) of the peneplain across the fault. This quantity is graphed in the second chart below.

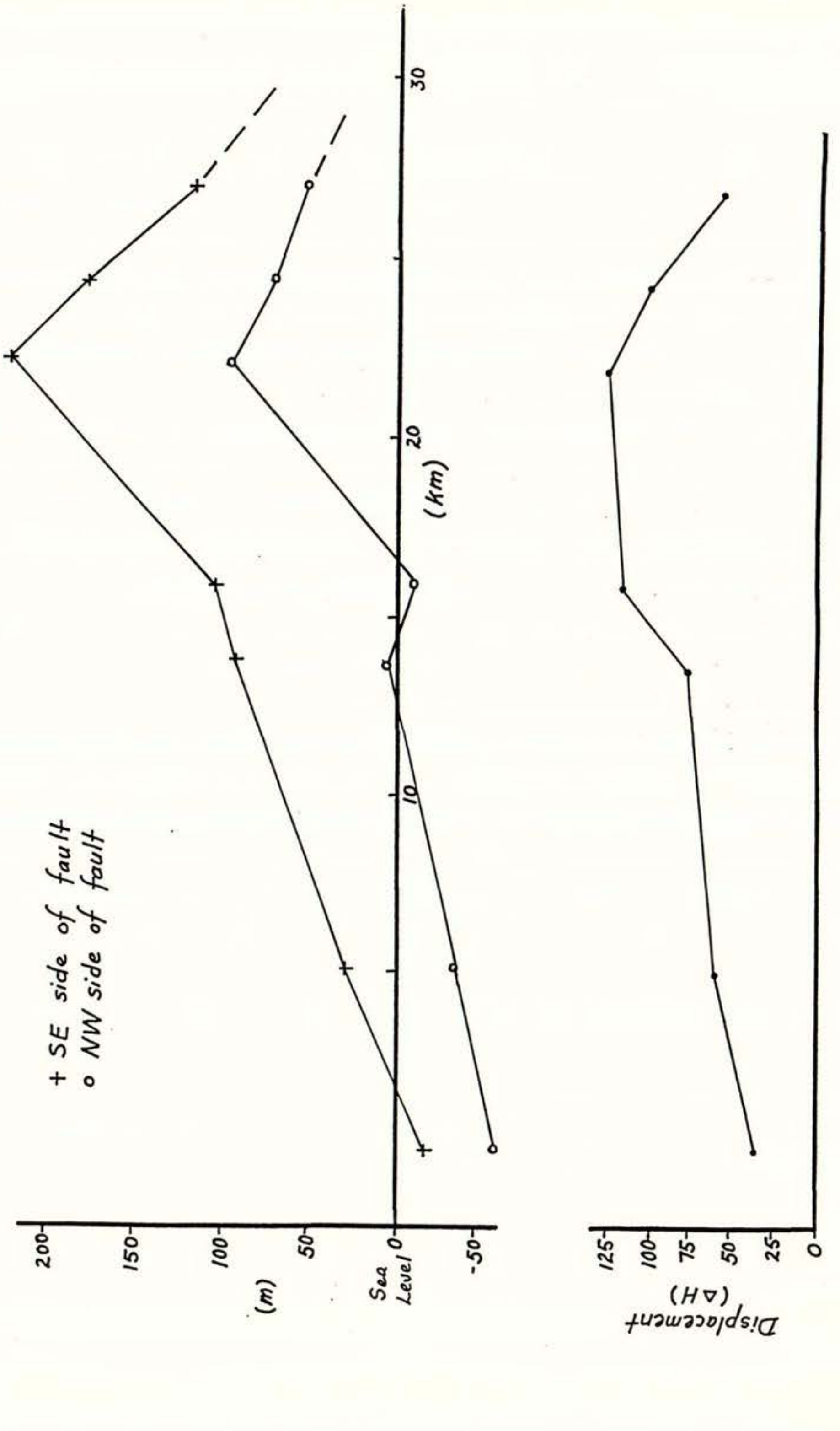

3.3 Drainage patterns

The Titri block is both larger and more dissected than the Akatore block. The drainage divide is up to 6km from the fault and the escarpment along the fault is cut and eroded by many creeks. The escarpment of the Akatore Fault, in contrast, is extremely steep and well-preserved, with the drainage divide no more than two or three hundred metres from the fault trace (Fig. 3.3). The scarp is eroded by steep, shallow gullies, but no west flowing creeks have cut their headwaters back through the scarp. These observations are strong evidence that the Akatore Fault is a much younger structure than the Titri fault.

Only two rivers cut through the Titri Fault in antecedent gorges. These are the Taieri and Tokomairiro Rivers, and the gorges are at the northern and southern ends of the halfdome defined by the deformed peneplain. Between these gorges, the drainage on the Titri block is dominated by major consequent streams flowing southeastwards down the dip of the peneplain to the sea. Since remnants of the late Cretaceous sedimentary cover of the peneplain are found everywhere along the footwall of the Akatore Fault, it is assumed that these consequent streams formed initially on the dip slopes of the sedimentary rocks and have subsequently eroded through into the Haast Schist.

Four major stream catchments, those of Akatore, Big and Bull Creeks and Nobles Stream, cover the Titri block between the Taieri and Tokomairiro Rivers and drain eastwards down the dip of the block. The Akatore fault escarpment cuts across these catchments and in each, the main channel cuts through the Akatore block in an antecedent gorge (Fig. 3.3). Thus it appears that the consequent drainage on the dip slope of the Titri block was well enough established prior to the Akatore fault inception that the major creeks could continue to cut down sufficiently quickly to keep pace with the uplifting Akatore block.

The antecedent gorges of Nobles Stream and Bull Creek, south of the summit of the Akatore "halfdome", are both at the southern extremity of their respective catchments, whereas the Akatore Creek gorge is at the northern margin of its catchment. The Big Creek gorge, along the axis of the "halfdome", is central to its catchment. Presumably the creeks were deflected away from the growing dome as the fault propogated north and south of Big Creek. The catchments are coloured in Fig. 3.3; the areas of the Big Creek, Bull Creek and Nobles Stream catchments are similar in size, whereas that of Akatore Creek is approximately twice the size. Several prominent channels exist in the Akatore block between Akatore and Big Creeks, and the top of the fault escarpment exhibits two very prominent air gaps (abandoned channels). It is likely that originally, a fifth catchment (and possibly a sixth) existed between Akatore and Big Creeks, but was then captured by the more rapidly downcutting Akatore Creek before it was able to establish a deep antecedent gorge. A similar capture has occurred southwest of Nobles Stream, where a prominent air gap exists in the fault scarp and the stream on the downthrown side turns and flows along the scarp to join the Tokomairiro River.

It is also possible that Akatore Creek itself occupies the site of a Late Cretaceous valley cut into the peneplain surface as evidenced by inflections in profiles of both upper and lower surfaces (Fig 3.2).

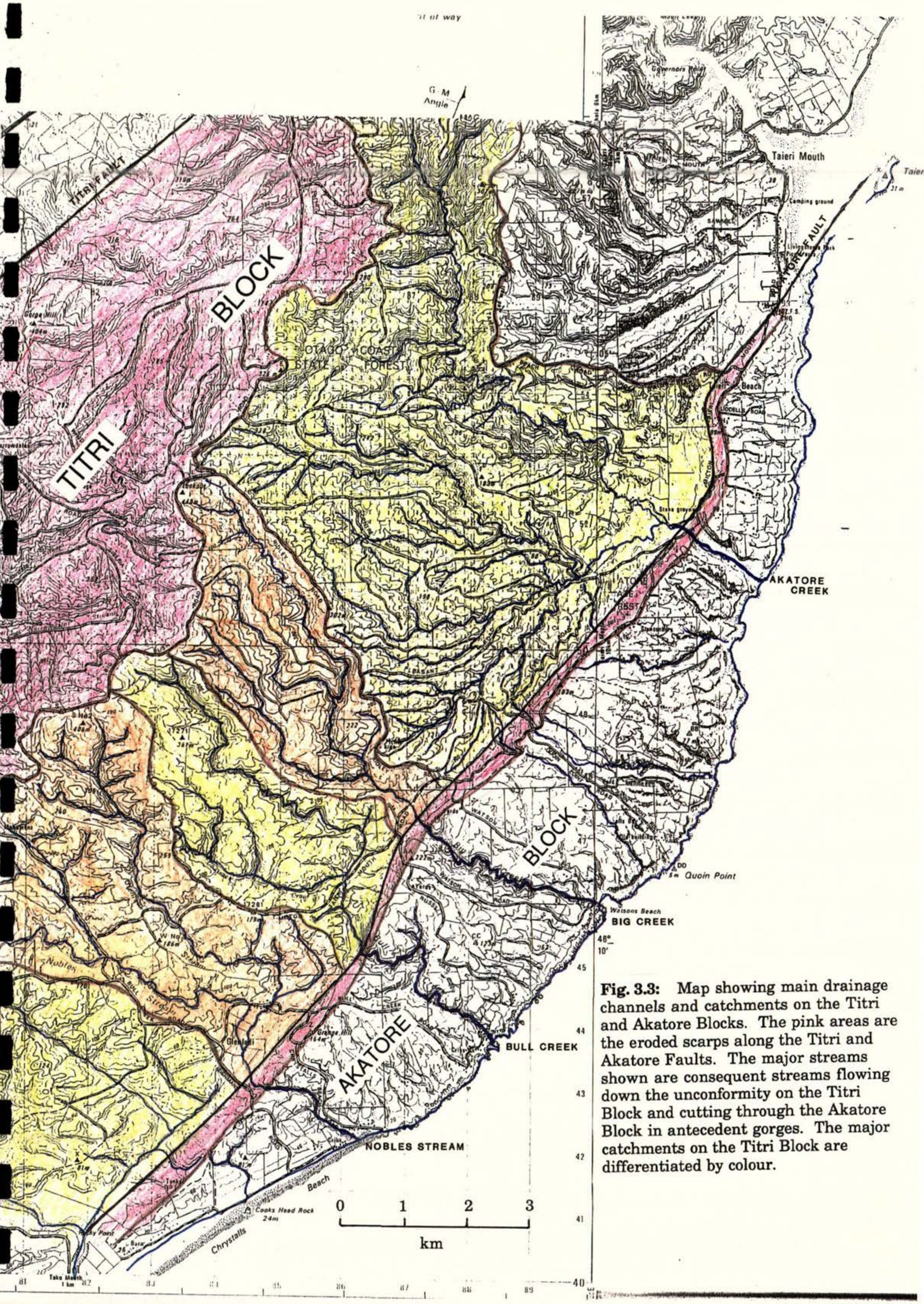

Fig. 3.3: Map showing main drainage channels and catchments on the Titri and Akatore Blocks. The pink areas are the eroded scarps along the Titri and Akatore Faults. The major streams shown are consequent streams flowing down the unconformity on the Titri Block and cutting through the Akatore Block in antecedent gorges. The major catchments on the Titri Block are differentiated by colour.

SECTION 4: FIELD DATA FOR HOLOCENE DISPLACEMENT ON THE AKATORE FAULT

4.1 Introduction

As described in Section 2, the Akatore Fault exhibits scarps at a number of places where it crosses latest Pleistocene and Holocene deposits. In addition, slightly degraded scarps occur locally on hillsides and post-glacial marine benches and raised beaches are found on the Akatore block. During the course of this study, some of these sites were examined in more detail, and the data combined with existing unpublished data held by the authors. In this section of the report, these data are presented and their significance for Holocene fault activity discussed.

4.2 Taieri Beach

A 4-5 m scarp is observed displacing a loess-covered marine surface at Taieri Beach (Map 1). A section through this raised beach is given in Fig. 2.1 and described in Section 2. The surface of the terrace on the uplifted side of the fault is some 9m above high water mark while the top of the underlying beach sands are 6m above high water level. The age of the underlying erosion surface is not known. It has commonly been viewed as dating back to the last interglacial (c. 120,000 yr BP) although there are no specific data to support this. Several things suggest that this view is incorrect.

Firstly, given the total offset of the peneplain across the fault at this locality (see Section 3), and the very youthful character of the fault escarpment along its length, a total of only 4 or 5 m displacement on the fault since the last interglacial seems unlikely. The amount of displacement of the surface is similar to postglacial displacement at other sites further south (see below), which is expected since the scarp on the terrace cuts the youngest loess deposit. This would suggest no further displacement for over 100,000 yr. if the beach sands were of last interglacial origin, again unlikely given the young appearance of the fault morphology.

Secondly, if the beach sands dated back to the last interglacial, three loess deposits would be expected to overlie them. In fact, only one loess deposit is discernible above the sands (R. Cotton, P. McIntyre, pers. comm.), again suggesting a younger age for the surface.

A lower raised beach was also described in Section 2 (Fig. 2.1) about 2m above high water level. Twigs in soil and debris above these beach sands was radiocarbon dated as 1010 ± 45 yr BP (Table 4.1, sample Wk-3045), which converts to a calendric age range of 1065–975 yr BP. This deposit must post-date the uplift of the beach sands. As there is no loess cover on this beach, it is presumably younger than the last glaciation (c. 14,000 yr BP). This raised beach is widely preserved south of Taieri Beach on the upthrown side of the fault and is interpreted as originating by uplift during the last major earthquake accompanying surface displacement on the Akatore Fault.

TABLE 4.1

Details of Radiocarbon dates obtained from material in the vicinity of the Akatore Fault. Material from Big Creek, Bull Creek & Nobles Stream is from drill cores or excavations.

Material from Taieri Beach was collected by R. J. Norris & P. O. Koons, from Big Creek by C. A. Landis & K. Makgill, from Bull Creek and Nobles Stream by K. Makgill, and from Tokomairiro River by I. C. McKellar.

Locality	Laboratory Sample no.	Fossil record no.	Sample material	Conventional age (yr BP)	Calendric age (yr BP)*
Taieri Beach	Wk-3045	I45/f	twigs above raised beach	1010 ± 45	1065—975
Big Creek	Wk-314	H45/f040	woodchips in peat horizon	1570 ± 70	1530—1345
Big Creek	Wk-3046	H45/f	twig in peat horizon	1300±45	1275—1170
Bull Creek	Wk-317	H45/f041	peat	900 ± 70	920—700
Nobles Stream	Wk-313	H45/f037	heartwood from 1m diam. tree	2090 ± 50 (less 600 rings)	2120—1950 1520—1350#
Nobles Stream	Wk-315	H45/f039	twigs & peat	1480 ±60	1390—1295
Nobles Stream	Wk-316	H45/f038	twigs from peat horizon	1440 ± 50	1345—1285
Tokomairiro River mouth	GS-9211	S180/f551	shells from raised beach	1865 ± 50	1410—1310†

* Calendric age ranges calculated from Stuiver & Pearson (1986) after applying S. hemisphere correction

estimated age of death of tree after subtracting 600 years from calendric age

† Calendric age calculated from marine calibration curves of Stuiver et al. (1986)

4.3 Taieri Beach to Akatore Creek

Along parts of this section of the fault, a fairly sharply defined scarp about 2m high occurs at the break in slope that more commonly marks the surface location of the fault. The scarp locally exposes schist basement while elsewhere it is mantled by a thin veneer of soil and debris. The scarp has the appearance of a slightly degraded, and therefore geologically recent, fault scarp, and we interpret it as forming during the last major ground-displacing earthquake on the Akatore Fault.

4.4 Akatore Creek

No fault trace is discernible across the alluvial deposits of Akatore Creek. On the true right (south) bank of the river, however, a poorly developed erosional bench in basement schist occurs at a height of approximately 2m above present river level on the downstream (upthrown) side of the fault. We correlate this with the lower raised beach on the coast south of Taieri Beach, and interpret it as being uplifted during the last major displacement on the Akatore Fault.

4.5 Big Creek

4.5.1 Introduction

At Big Creek, a prominent scarp about 2m high is clearly visible along the line of the fault where it crosses the present alluvial fill of the creek (Plate 1c). This site was chosen for detailed investigation, including detailed plane-table mapping, coring using a percussion corer, and shallow seismic refraction using a "Bison" seismic hammer.

4.5.2 Description of site and seismic hammer investigations

The geology of the area is shown in Fig. 4.1. The basement consists of weakly foliated TZ 2 greywacke, which is overlain unconformably west of the fault trace by sands of the Wangaloa Formation. Taratu Formation appears to be missing in this area. On the eastern, upthrown side of the fault, the unconformity is at an elevation of over 200m, the net displacement being in excess of 120m. Pleistocene and Holocene units include fluvial gravel, loess, silts and peat horizons. These are discussed more fully in section 4.5.3.

A “Bison” seismic hammer was used to try and locate the depth of the basement unconformity on the downthrow side of the fault. The system employs a sledgehammer wired to an oscillator recording unit. The hammer is used to strike a metal plate on the ground creating a seismic signal. This is received by a geophone that also feeds into the recording unit, allowing the travel time of the P-wave to be measured. By changing the hammer-geophone distance, a time-distance plot of first arrivals can be constructed. The change from the direct to the refracted wave as first arrival allows the depth to an interface and the velociies of the two layers to be determined. In order to correct for a dipping interface, each line was also shot in the reverse direction.

Fig. 4.1 Detailed map of the Big Creek site showing geology, drill core locations, seismic lines, and the fault trace. Map prepared by plane table survey.

Fig. 4.2
Graphic logs of percussion cores collected from the Big Creek site
Locations of cores are shown on Fig. 4.1

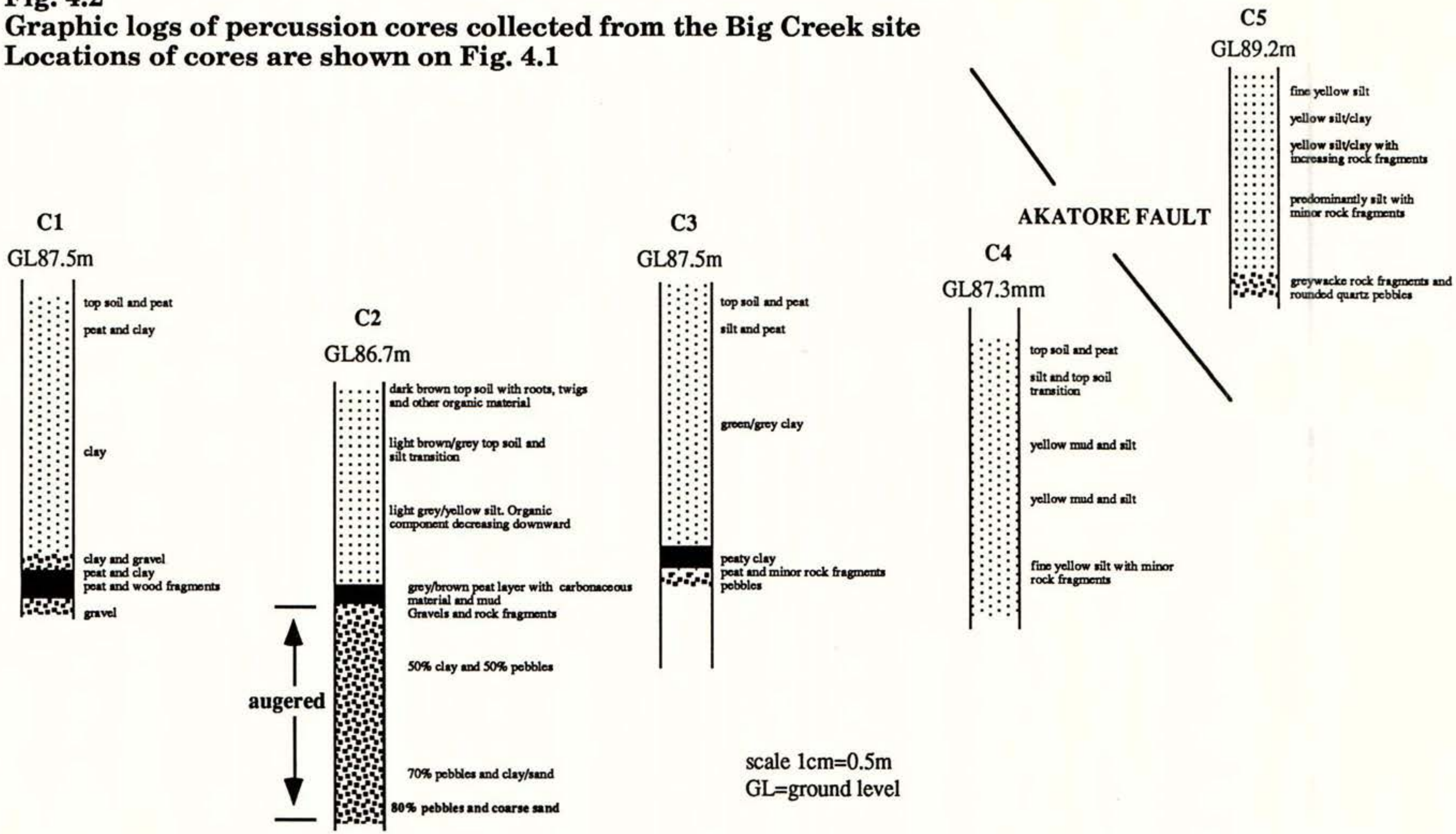

Several seismic lines were measured; the locations of these are shown in Fig. 4.1, together with the depth to the first major interface. Examples of the dataplots are given in Appendix 1. In general, the interface gets deeper towards the fault trace, increasing from 1.4 to nearly 4m depth.

4.5.3 Core data and interpretation

Five cores were collected from the vicinity of the Akatore Fault in the valley of Big Creek (Figures 4.1, 4.2). Three of these contain a Carbon-dated peat horizon which can be interpreted in terms of paleoseismic history.

The top 1-2 meters of cores C1-C4 comprise modern top soil underlain by a sticky silt/clay layer. This layer contains occasional roots and twigs and is generally unstratified. The deposit is similar to the Pleistocene loess (wind blown dust deposited during periods of Pleistocene glaciation) which mantles hills in the Big Creek valley, however it is less well compacted and structured. Similar sediment forms the suspension load of Big Creek at times of high discharge when the loessic sub-soil in the headwaters is being eroded. This upper layer in the cores is thus interpreted as reworked loess deposited in a ponded flood-basin, immediately upstream from the Akatore Fault at the point where Big Creek enters the deeply incised gorge leading to the sea. In contrast, core C5, taken beneath the terrace surface on the upthrown southeastern side of the fault comprises 1.5m of weathered silt and clay resting on older channel gravels and sands This silt/clay deposit is more strongly compacted than the muds underlying the floodplain directly upstream from the fault at this locality (e.g.cores 1-4). In addition, it is lacking in carbonaceous material and is characterised by a distinct yellow brown colour quite unlike the more greyish sediment underlying the adjoining floodplain. This sediment underlying the uplifted terrace surface downstream from the fault is interpreted as loess dating from the closing stages of the last glaciation (ca. 12-14,000 years ago). The gravel underlying the loess on the upthrown block is interpreted as a channel deposit formed by the Pleistocene ancestor of the present Big Creek.

A distinctive carbonaceous horizon underlies the floodbasin clays in cores C1-C3. Locally this bed becomes sufficiently rich in plant debris to be regarded as peat.

Although none of the cores reached pre-Pleistocene basement rock, schist is exposed in the bed of Big Creek, just downstream from the road bridge (Fig. 4.1). Very gentle dips of the Paleogene cover strata exposed in the valley walls adjacent to the floodplain indicate that the contact with basement at this locality is also sub-horizontal to very gently dipping. Using the unconformable upper surface of schist exposed at Big Creek and the exhumed Cretaceous-Paleogene erosion surface exposed at the top of the ridge along either side of Big Creek gorge, total displacement along the Akatore Fault at this locality is estimated to be 130 m.

Fault displacement responsible for creating the 2m high scarp at Big Creek and for damming the creek to form the ponded mud deposits in cores 1 to 4 indicates a minimum of 4.5 m since deposition of the loess.

The presence of swamp and slackwater deposits abutting the fault on the downthrown northwestern side suggests damming of the creek by seismic uplift of the southeastern side. However absence of loess at the base of this sequence requires removal of any older Quaternary sediment from basement prior to deposition of the slackwater deposits. Although this interpreted erosion interval (i.e. between 1500 and 14000 years ago). may have been triggered by a seismic event, it is equally likely that it was caused by climatic factors. In view of the straight nature of the scarp of loess exposed on the terrace face, it is likely that the loess is resting on an erosion-resistant greywacke basement at approximately the level of the adjoining floodplain (ca, 87.5 m).

Based on the above discussion and interpretation, the most likely scenario for earthquake faulting at Big Creek calls for two major events, each of approximately 2m displacement, in the last 14000 years. Other interpretations could postulate one 2m offset (post-1500) and multiple smaller displacements.

4.6 Bull Creek

Little detailed investigation was undertaken at Bull Creek although a scarp across the alluvial deposits is present similar to that at Big Creek. Auger samples from the downthrown side of the scarp showed similar deposits to Big Creek. A sample of peat from about 1m depth, immediately overlying silts, was dated as 900±70 yr BP (Table 4.1, sample Wk-317). A layer of organic material also occurs at about 2m depth although this was not able to be sampled adequately with the auger. This deeper layer may correspond to the dated horizon at Big Creek. Clearly coring and/or trenching would allow a clearer picture to be gained.

4.7 Nobles Stream

At Nobles Stream, a clearly defined scarp cuts across the alluvial deposits and has dammed the creek, causing a swamp to form on the upstream side (Plate 1d). In 1980, the landowner cut a drainage channel through the swamp and into the gorge on the downstream side, allowing the swamp to drain and pasture to be developed. An MSc student at that time, Ms Kathy Makgill, was able to document the excavation while it was fresh, and to collect material for radiocarbon dating.

A prominent buried forest horizon was recorded between 1 and 2 m depth, containing twigs and peat, and also tree stumps in growth position. These were buried in silt, and shells of *Hyridella sp.* freshwater mussels were found. The deposit was interpreted as being formed by drowning of a forest by damming of the stream, probably during displacement on the Akatore Fault and raising of the scarp. Dates from the peat and forest deposit are listed in Table 4.1 (samples Wk313, 315, 316) and these would predate the displacement event.

Sample Wk-313 was heartwood from a c. 1m diameter section of tree trunk. Approximately 600 rings were counted suggesting that the age of death of the tree was some 600 years after the dated heartwood (there is some uncertainty as it is not certain that all rings, and years, were discernible). The heartwood date of 2090±50 yr BP converts to a calendric age range of 2120-1950 BP, and after subtraction of 600 years, results in an estimate of the time of the tree's death of 1520-1350 yr BP. Dates on twigs from the same horizon give calendric age ranges of 1390-1295 and 1345-1285 yr BP (Table 4.1, samples Wk-315, 316). All these dates should predate, or coincide with, the creek damming event. They overlap with dates from Big Creek (see discussion above) although the youngest date there is very slightly younger (by 50-100 years) than these dates. Nevertheless, we feel that the evidence is very strong for a single event along the fault sometime between about 1350 and 1200 BP which raised scarps at Big Creek, Bull Creek and Nobles Stream, damming the respective creeks.

Downstream of the scarp at Nobles Stream, a set of abandoned meanders are clearly visible on the uplifted terrace, now well above the present height of the stream channel. These, however are themselves incised somewhat into the terrace surface. The implication from this is that there have been at least two events that have raised the terrace downstream of the scarp to its present elevation.

South of Nobles Stream, a prominent, somewhat degraded scarp is seen crossing the hillside (Plate 1d), similar in appearance to that described north of Akatore Creek. Again, it is interpreted as forming during the last earthquake-accompanying displacement on the fault, and coinciding with the scarp at nearby Nobles Stream.

4.8 Tokomairiro River

A Holocene terrace, the top surface of which is about 3m above present high water, occurs at the mouth of the Tokomairiro River and is terminated upstream by the trace of the Akatore Fault. Shell material from beach sands a little over 1.5m below the top of the terrace was collected in 1963 by Ian McKellar (of DSIR) and radiocarbon dated at 1865±50 yr BP (Table 4.1, sample GS9211). Correcting this date for the marine carbon reservoir (Stuiver et al., 1986) and converting to a calendric age gives an age range of 1410-1310 yr BP., very similar to the dated material from Big Creek and Nobles Stream. We interpret this date as preceding the same earthquake event as we have inferred for the rest of the fault, the beach sands being uplifted during the accompanying fault displacement.

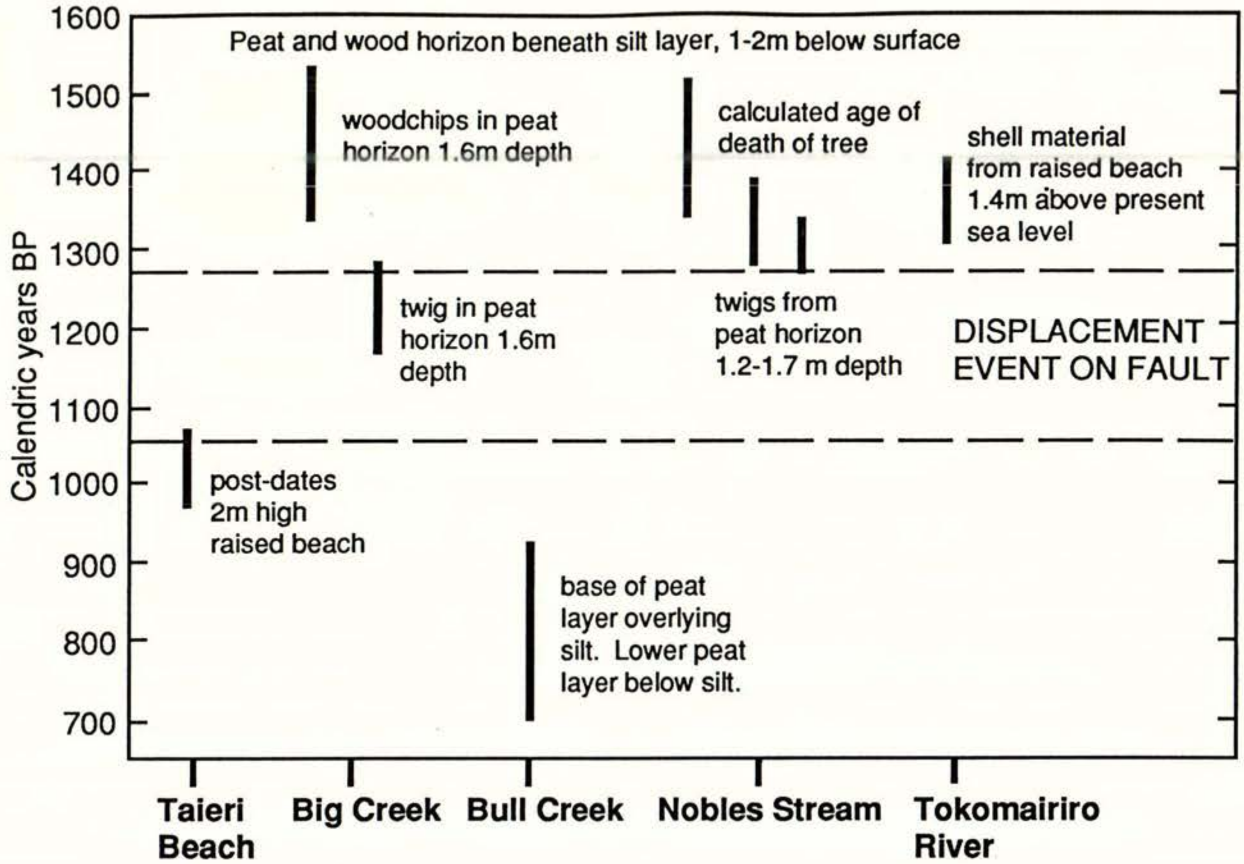

Fig. 4.3: Chart summarising age constraints on last fault displacement. Details of dates and conversion to calendric ages is given in Table 4.1.

4.9 Summary

The data on Holocene displacements on the Akatore Fault (summarised in Fig. 4.3) point strongly to a major ground-displacing earthquake sometime between 1275 and 975 yr BP (based on the youngest date on the buried organic horizon at Big Creek and Nobles Stream, and the date on the material overlying the raised beach at Taieri Beach). Given the concentration of ages between 1500 and 1200 yr BP, and possible uncertainties in the dates other than the quoted analytical precision, we are fairly confident of this conclusion. The amount of vertical displacement appears to be approximately 2m. The minimum length of fault rupture is the whole of the mapped onland trace, some 20 km. Using the graphs of Bonilla et al. (1984), as modified by Soils and Foundation Ltd (1993) (Fig. 5.1), both the length of the fault trace and the displacement give estimates of the magnitude of the event between 6.9 and 7.3.

The offset of the last loess horizon, both at Taieri Beach and Big Creek, is approximately twice that of the displacement in the last event. This suggests the possibility of two similar events since about 14,000 yr BP. We cannot distinguish between this conclusion and one with several smaller events preceding the last one. Nevertheless, two events, each of about magnitude 7 with approximately 2m of vertical displacement, in the last 14000 years, would give a minimum return period of 6500 yr and a maximum of 12500 yr. Return periods based on two events are not likely to be very reliable, but this is the best we can estimate at this time.

SECTION 5 OFFSHORE INVESTIGATIONS

5.1 Introduction

The Akatore Fault extends offshore at both ends of its onshore trace, significant net displacement on the fault at these points indicating that the potentially active fault line is present beneath the sea as well as onland. Other parallel faults may also be present further to the east. An MSc thesis study to investigate the offshore area was carried out by Tanya Johnstone at Otago University, using the University boat, R. V. *Munida* equipped with sub-bottom seismic profiling unit and side-scan sonar (Johnstone 1990). In this section we summarize the major findings of the thesis relevant to this study.

5.2 Akatore Fault system offshore

Structural geology within the first 12km offshore of southeast Otago from Blackhead to Nugget Point, situated to the northwest of the Great South Basin, has been investigated using high resolution sub-bottom profiles and side-scan sonar images (Fig. 5.1). The structures evident in the sub-bottom profiles and side-scan images can be related to those onshore and further offshore in multi-channel seismic profiles collected by Hunt International Petroleum Company (HIPCO). The sediments can be correlated with known onshore stratigraphy and offshore well data.

5.2.1 Regional offshore geology

Onshore basement consists of Haast Schist in the north and Murihiku Supergroup in the south. Cretaceous and Tertiary sediments unconformably overlie the basement. Taratu Formation extends throughout the area studied from just offshore from Brighton to the Clutha River. The Wangaloa Formation together with Tertiary sediments are present overlying the Taratu Formation further offshore and south of the Clutha River. In general, the unconformity and overlying sediments dep at a few degrees to the east and southeast. Cretaceous and Tertiary sediments are unconformably overlain by post-glacial modern sand and relict gravels which are derived mainly from the Clutha River.

Basement, Cretaceous, Tertiary and in some places the modern sediment are folded and faulted. The major structures trend at 040° to 055° between Blackhead and Mitchells Point where the major trend changes to 180°, although the Akatore Fault still trends northeast. From south of the Clutha River the trend of folding and faulting changes to 135° parallel to the offshore extension of the Castle Hill Fault Zone which coincides with the northern limb of the Southland Syncline. Most faults within the study area are reverse, some with associated asymmetric synclines and anticlines.

5.2.2 Fault structures offshore

Northeast striking structures within 20km offshore are southeast dipping, reverse faults The Korora Dome and associated reverse faulting (part of the Waipounamou Fault System, a major set of northeast trending faults), situated 40km southeast of Nugget Point, is thought to be the southeastern continuation of the Central and Eastern Otago fault system.

The northwest trending structures are contractional features whose locations are partly controlled by reactivation along pre-existing structures.
Both the Akatore Fault and Fault B (Fig. 5.1), trending parallel to and situated 2-3km to the east of the Akatore Fault, show evidence in the profiles (Figs. 5.2, 5.3, 5.4) for Holocene displacement. The Akatore Fault can be traced from its termination at the Castle Hill Fault Zone northeastwards, trending at 040° to 055°, and continuing onshore south of the Tokomairiro River mouth, and then offshore south of Taieri Mouth and extending north on the landward side of Taieri Island and Green Island before its projected on-land continuation at Waldronville (Fig. 5.1). There is, however, no evidence of any net offset on the line of the fault across the coast at this point and the fault may well have died out before reaching the shore. Fault B lies on the seaward side of Green Island and Taieri Island and has only been traced offshore in the Taieri area. Fault B's anticipated onshore extension in the south is at Akatore Creek and to the north is on the northern side of Blackhead.

Fig. 5.1: Map with location of the accompanying high-resolution seismic profiles and the positions of the Akatore fault and newly discovered fault traces. Transect 7 lies to the northeast of the mapped area (figure 2), transect 5 is in the middle (figure 3) and transect 14 lies to the south (figure 4).

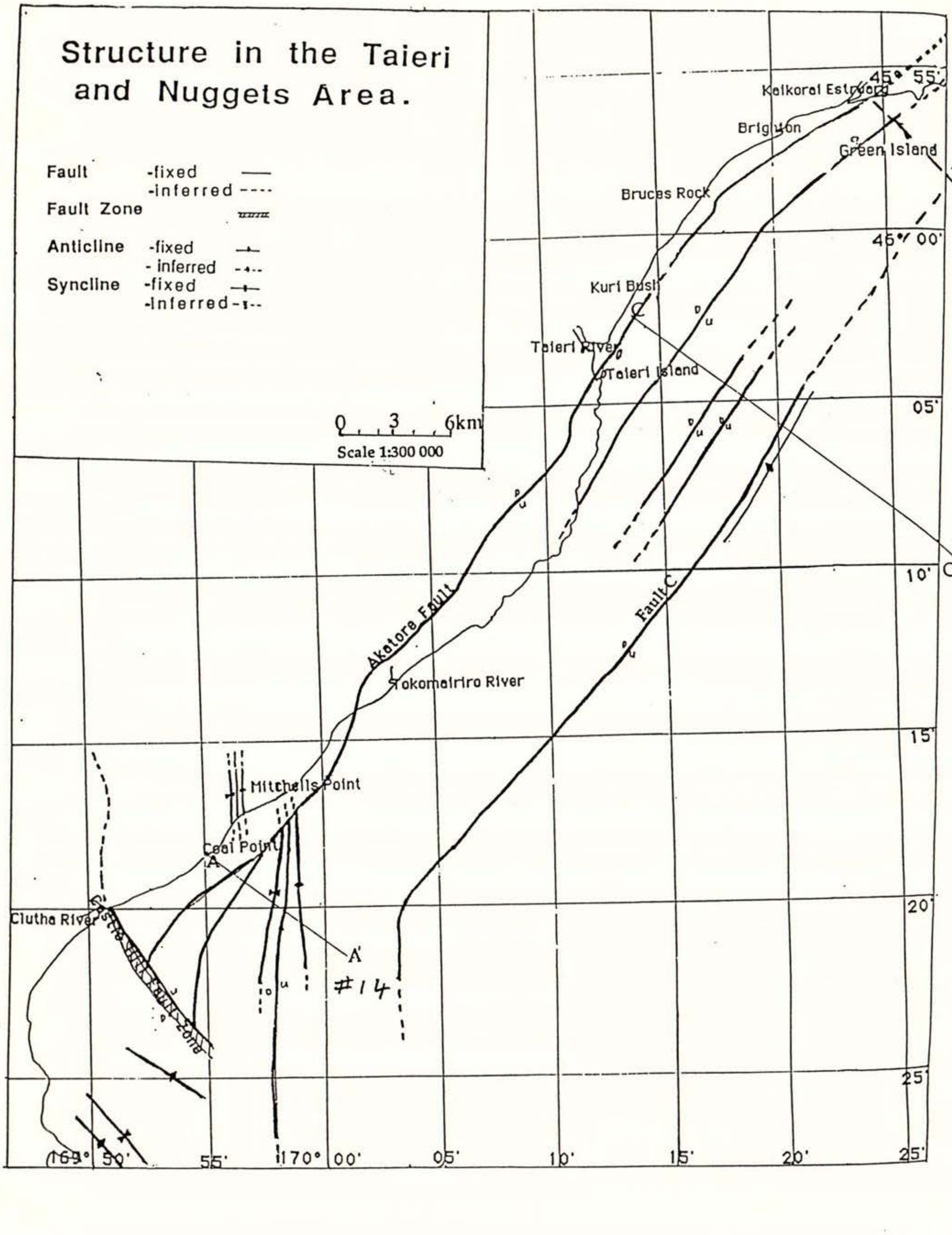

2 Transect 7- Sub-bottom profile from fix 113 to fix 117

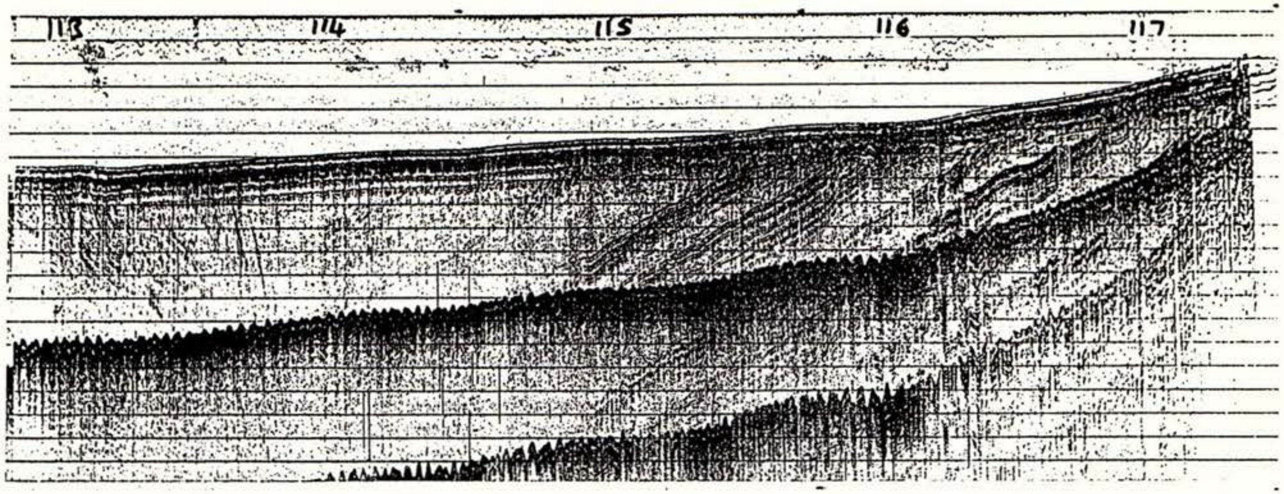

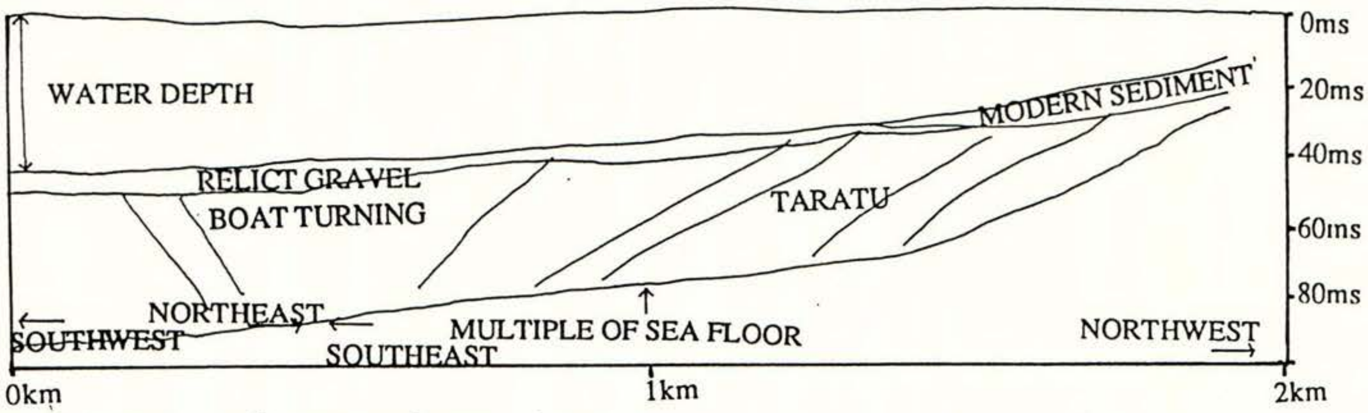

Strike of the Taratu and the Tertiary sediment is northeast-southwest.
Angle between the direction of strike and the direction of the transect is 70°.

	Fix 113	Fix 114	Fix 115	Fix 116	Fix 117
Apparent Dip		5.6°	6.7°	10.0°	3.7°
Real Dip		6.0°SE	7.1°SE	10.6°SE	3.9°SE

Fig. 5.2: Seismic profile and interpretation across fault zone to the northeast of Green Island.

3 Transect 5- Sub-bottom profile from fix 79 to fix 86

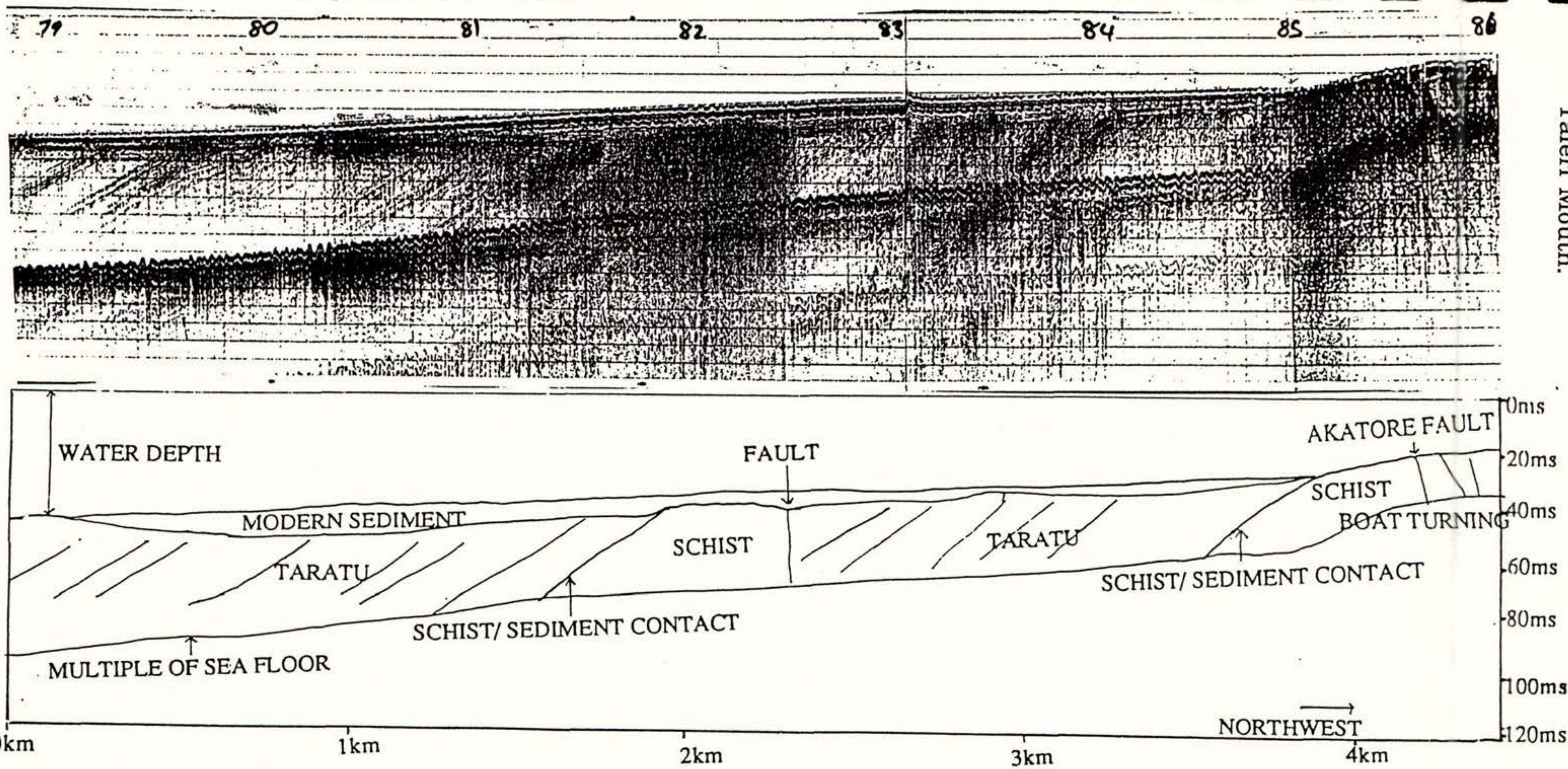

Strike of the Taratu and the Tertiary sediment is northeast-southwest.
Angle between the direction of strike and the direction of the transect is 90°.

	Fix 79	Fix 80	Fix 81	Fix 82	Fix 83	Fix 84	Fix 85
Apparent Dip	2.8°	2.8°	5.2°	5.6°	6.9°	6.4°	4.5°
Real Dip	2.8°SE	2.8°SE	5.2°SE	5.6SE	6.9°SE	6.4°SE	4.5°SE

Fig. 5.3: Seismic profile and interpretation across fault zone to the northeast of Taieri Mouth.

4 : Transect 14- Sub-bottom profile from fix 273 to fix 278.

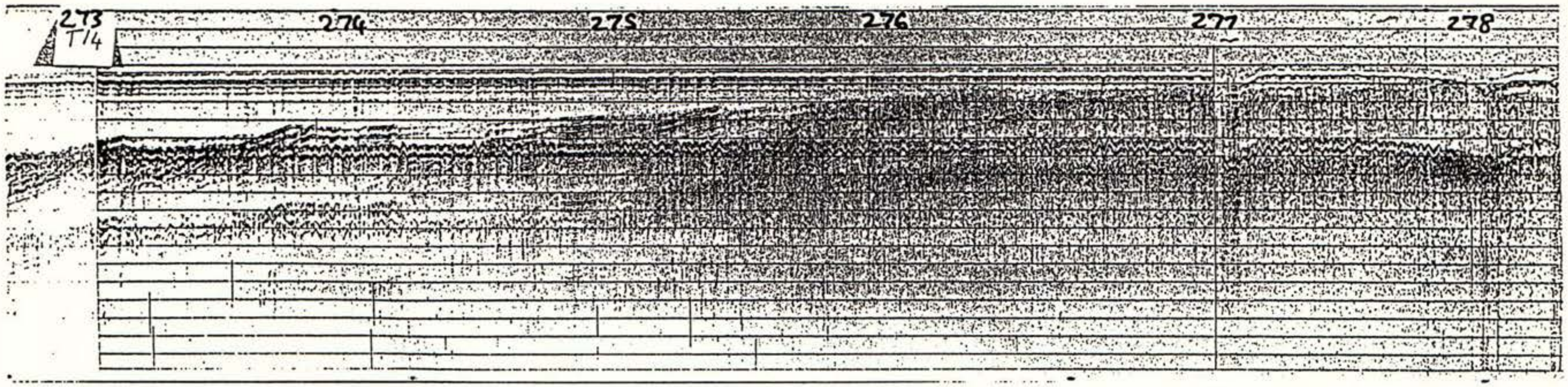

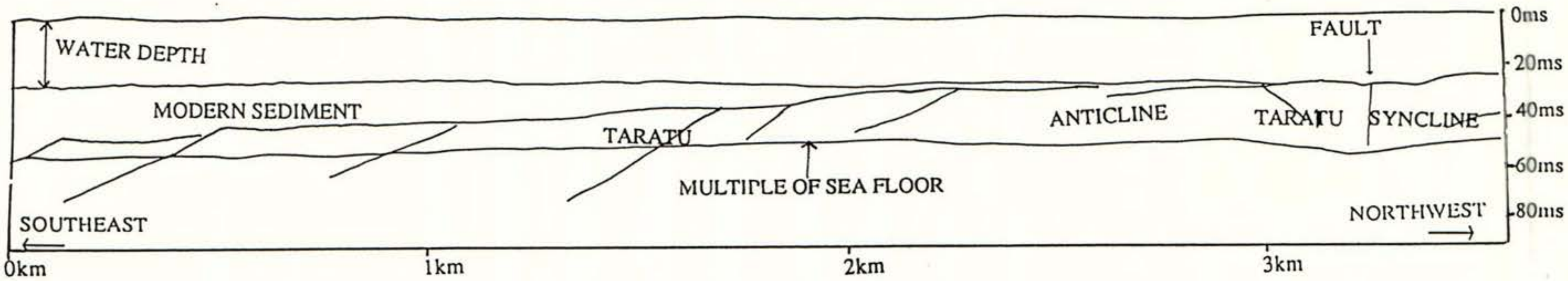

The strike of the Taratu is north-south.
The angle between strike and the direction of the transect is 30°.

	Fix 273	Fix 274	Fix 275	Fix 276	Fix 277
Apparent Dip	3.1°	3.3°	2.2°	2.9°	2.5°
Real Dip	6.2°E	6.6°E	4.4°E	5.8°E	5.0°E

Fig. 5.4: Seismic profile and interpretation across fault zone to the southeast of Mitchell Point.

SECTION 6 RECENT SEISMICITY

6.1 Frequency of felt earthquakes along Akatore System

In addition to the 1974, M=5 event generated on the Akatore system of faults, numerous smaller earthquakes have been recorded since 1982 by the three component seismograph housed at the University of Otago. The largest of these earthquakes was the M=4 event of 1989 located offshore near Taieri Mouth. The remainder of the recorded and felt earthquakes with M<3.5 are poorly located and occur at one- to two-year intervals.

6.2 Location of felt earthquakes along Akatore System

Uncertainty about location of all felt earthquakes in east Otago prior to 1990 arose from the sparse distribution of seismic recorders and the poor velocity models available. Since 1982, epicentral distance of earthquakes with M<4 within a 100 km radius of Dunedin were recorded on the University of Otago seismograph, but location was not possible without felt intensity reports. The seismograph traces together with the felt reports constrain many of the smaller events to lie within the Akatore Fault System, but more precise assignment to an individual trace or segment has not been possible.

Adams and Kean (1974) located the 1974, M=5 event approximately 7km southeast of St Clair at a focal depth of 20km. They note however that the precision of location is severely limited by the lack of any stations close to the epicentre. Given the lack of precision, it is impossible to assign the event to any individual structure within the Akatore System.

Adams and Kean (1974) also noted the clear first motion pattern of the event which yields a focal mechanism of either dextral strike-slip along a steep northeast striking plane or sinistral strike-slip on a north-northwest striking plane.

SECTION 7: DISCUSSION AND CONCLUSIONS

Summary of fault data

Observations arising from field investigations, isotopic dating, and air photograph interpretation of the Akatore and Titri Blocks may be summarised as follows:

(1) An approximately 2m high scarp exists along the base of the northwestern slope of the entire Akatore Block. This scarp, which strikes northeast at ~035° along most of its 20km length and dips to the southeast at ~60°, separates upthrown Haast Schist from Tertiary or recent sediments on the downthrown side.

(2) In two sections, north of Akatore Creek and between Big and Bull Creeks, the fault trace turns to the north and slightly northwest. The scarp appears continuous through these northerly jogs.

(3) Sense of displacement determined from slickensides is oblique reverse movement along the northeast sections and nearly pure reverse across the north-striking sections.

(4) The degree of river incision and drainage development on the Akatore Block is much less than on the adjacent Titri Block reflecting the more recent uplift of the Akatore Block.

(5) Doming of the Akatore Block towards the elevation high in the centre is closely correlated with doming of the Titri Block. This doming is a regional feature and represents differential displacement on the Titri Fault which was then inherited by the Akatore Block when the Akatore Fault became active. This pattern is consistent with an easterly migration of deformation with time. The vertical displacement of the peneplain surface along the Akatore Fault is more or less constant between Big and Akatore Creeks but reduces rapidly to the southwest. and more slowly to the northeast along the offshore trace between Taieri Mouth and Green Island.

(6) Isotopic dating of various material above and below the fault constrains the latest fault movement to between 975 and 1275 calendric years BP. Good spatial coverage along the fault trace gives some confidence that a single event is being resolved by the dating techniques.

(7) Displacement of the last loess deposit suggests at least two events of similar magnitude have occurred since loess deposition, i.e. since about 14000 BP.

7.2 Seismic hazard assessment

The last identifiable event along the Akatore Fault at about 1200 calendric years BP appears to have ruptured the entire onland trace. The absence of datable submarine material on the offshore trace north of Taieri Mouth, trending towards Dunedin, precludes positive identification of the northern extent of this single rupture. If only the onshore trace is used in the rupture length-magnitude relation of Bonilla et al. (1984), an estimate of maximum credible earthquake of between M=6.8 and M=7.3 is obtained. The approximate vertical slip in the last event appears to be 2 m. Using the fault slip size–magnitude relation of Bonilla et al. (1984) also produces an estimate of the maximum credible earthquake of between 6.8 and 7.3 (Fig. 5.1).

Together, these observations suggest that a single event on the Akatore Fault is capable of large (~2m) displacements, resulting in magnitude c.7 earthquakes, at epicentral distances from Dunedin of less than 10km.

The return period of such events is more difficult to estimate. The probability of two such events since 14000 BP would suggest a return period of between 6000 and 12000 years. At this rate, the total slip on the Akatore Fault could have been accomplished in 350,000 to 700,000 years, a time commensurate with the youthful appearance of the fault. With the limited data available, however, there is no reason to suppose that displacement has occurred at a constant rate, or that the return period suggested is a valid measure. Nevertheless, the return period is similar to that suggested for other NE-striking faults in Otago (Officers of the Geological Survey, 1983) which suggests that the Akatore fault is not abnormally active, but is relatively young.The existence of other parallel active faults offshore, however, suggests that the seismic hazard is greater than that calculated for the Akatore Fault alone.

The northward extension of the Akatore Fault offshore brings it quite close to Dunedin City. The evidence suggests that the fault is propogating northeast and southwest with time. A future break could extend into Dunedin's southern suburbs. Despite its relatively long return period (compared with major faults in the north of the country) and the relatively recent timing of the last event, the Akatore Fault System must be viewed as a potentially serious hazard for Dunedin City.

7.3 Conclusions

(1) The Akatore Fault is a single structure striking generally NE-SW and dipping 60° E. The slip is right-lateral reverse over most of its length except in two more northerly striking sections where it is nearly pure reverse.

(2) The total vertical offset of the Late Cretaceous peneplain reaches a maximum of 120-130 m between Big and Akatore Creeks and reduces to the NE and SW. This together with the drainage pattern suggests that the fault has propogated NE and SW with time.

(3) The fault is relatively young and postdates drainage development on the Titri block to the west.

(4) Evidence of postglacial displacements is strong. The last event has an offset of approximately 2m and occurred about 1200 years ago. This would correspond to an earthquake of magnitude 6.8-7.3.

(5) At least two such events have occurred since 14000 years ago.

(6) Parallel faults offshore also show Holocene displacements.

(7) The Akatore Fault System represents a significant potential hazard for the City of Dunedin.

Fig. 5.1: **Graphs from Bonilla et al. (1984), modified by Soils & Foundations Ltd (1993), showing relation between earthquake magnitude and (a) rupture length and (b) fault displacement.**

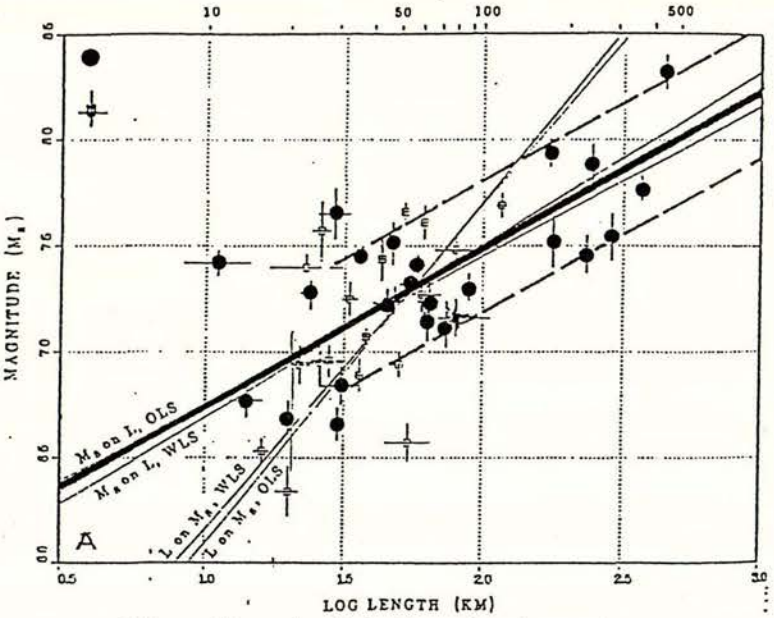

(a) **Magnitude - Rupture Length**

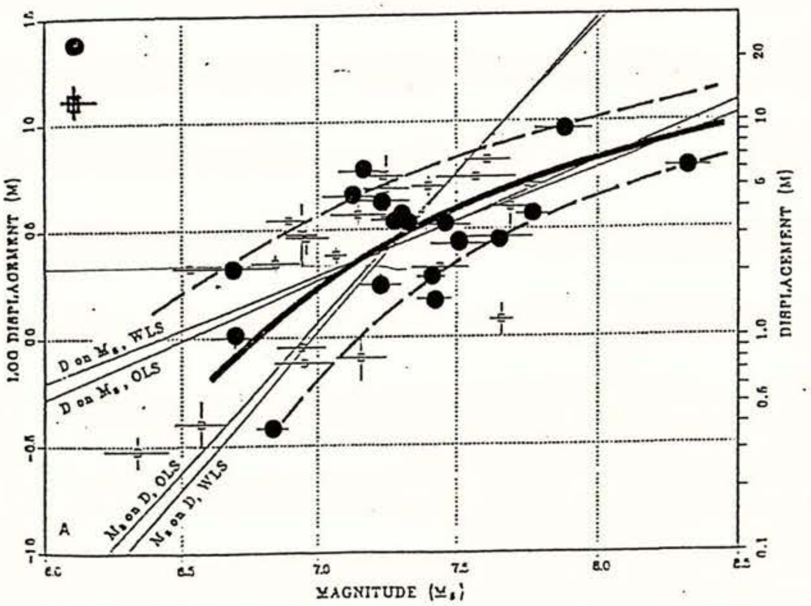

(b) **Magnitude - Fault Displacement**

Key

- Strike slip faults
- Other fault types
- Bonilla et al linear relationship
- Best fit - this study
- ±1 standard deviation

REFERENCES CITED

REFERENCES

Adams, R. D.; Kean, R. J. 1974: The Dunedin earthquake, 9 April 1974, Part 1: Seismological studies. Bulletin of the NZ National Society for Earthquake Engineering 7: 115-122.

Beanland, S.; Berryman, K. R.; Hull, A. G.; Wood, P. R. 1986: Late Quaternary deformation at the Dunstan Fault, Central Otago. Royal Society of New Zealand Bulletin 24: 293-306.

Beanland, S.; Berryman, K. R. 1989: Style and episodicity of late Quaternary activity on the Pisa-Grandview Fault Zone, Central Otago, New Zealand. New Zealand Journal of Geology & Geophysics 32: 451-461.

Benson W.N. 1968: Dunedin district 1:50,000. Map 1, N. Z. Geological Survey Miscellaneous Series, DSIR, Wellington.

Benson, W. N.; Turner, F. S. 1940: Mugearites in the Dunedin district. Royal Society of New Zealand Bulletin 70 : 188-199.

Bibby H.M. 1981: Unbiased estimate of strain from triangulation data using the method of simultaneous reduction. Tectonophysics 82: 161-174.

Bishop, D. G. 1974: The Dunedin earthquake, 9 April 1974, Part 2: Local effects. Bulletin of the NZ National Society for Earthquake Engineering 7: 123-129.

____________ 1972: Progressive metamorphism from prehnite-pumpellyite to greenschist facies in the Dansey's Pass area, Otago, New Zealand. Geological Society of America Bulletin 83: 3177-3197.

____________ 1974: Tertiary and Early Cretaceous geology of the Naseby and Kyeburn areas. New Zealand Journal of Geology & Geophysics 17: 19-39.

____________ 1971: Transposition structures associated with cleavage formation in the Otago Schists. New Zealand Journal of Geology & Geophysics 15: 360-367.

Bonilla, M. G.; Mark, R. K.; Lienkaemper, J. J. 1984: Statistical relations among earthquake magnitude, surface rupture length, and surface fault displacement. Seismological Society of America Bulletin 74: 2379-2411.

Brill R.P. 1981: Akatore Site. NZ Geological Survey EDS Report, Lower Hutt.

Brown, E. H. 1962: The Geology of the Mt Stoker area. MSc Thesis, lodged in the Library, University of Otago, Dunedin.

____________ 1963: The geology of the Mt Stoker area, Eastern Otago, Part 1--Metamorphic geology. New Zealand Journal of Geology & Geophysics 6: 847-871.

____________ 1964: The geology of the Mt Stoker area, Eastern Otage, Part 2 -- Post-metamorphic geology and volcanism. New Zealand Journal of Geology & Geophysics 7: 193-204.

Cobbold, P. R.; Watkinson, A. J. 1981: Bending anisotropy : a mechanical constraint on the orientation of fold axes in an anisotropic medium. Tectonophysics 72: T1-T10.

Cotton, C. A. 1917: Block mountains in New Zealand. American Journal of Science 44: 249-293.

Engelder, T. 1987: Joints and shear fracture in rock. in: Atkinson, B. K. Editor, Fracture Mechanics of Rock. Academic Press, London.

Hesson, S. 1981: The Geology of the Hyde area. Bsc Honours Dissertation, lodged in the Library, University of Otago, Dunedin.

Hull, A. G.; Beanland, S.; Berryman, K. R.; Bishop, D. G.; Wood, P. R.; Paterson, B. R. 1982: Reconnaissance Stranraer and Hyde Faults, Central Otago. NZ Geological Survey, Wellington, Unpublished Immediate Report.

Johnstone, T. 1990: A seismic reflection investigation of the extent and geometry of recent northeast-trending faults on the Otago shelf. Unpublished MSc Thesis, lodged in the Library, University of Otago, Dunedin.

Makgill, K. P.; Norris, R. J. 1983: Recent movements on the Akatore Fault, East Otago, and its relationship to regional tectonics (Abstract). Proceedings, Pacific Science Association 15th Congress, Dunedin

McCahon, I. F.; Yetton, M. D.; Cook, D. R. L. 1993: The earthquake hazard in Dunedin. Unpublished report to EQC, Soils & Foundations Ltd, Christchurch.

McKellar I.C. 1990: Southwest Dunedin Urban Area 1:25,000 Map (1 sheet) and Notes (64pp). Map 22, N. Z. Geological Survey Miscellaneous Series, DSIR Wellington.

McKellar, I. C. 1966: Sheet 25 - Dunedin. Geological Map of New Zealand 1:250,000., D. S. I. R., Wellington.

Means, W. D. 1966: A macroscopic recumbent fold in schist near Alexandra. New Zealand Journal of Geology & Geophysics 9: 173-194.

____________ 1963: Mesoscopic structures and multiple deformation in the Otago Schist. New Zealand Journal of Geology & Geophysics 6: 801-816.

Mutch, A. R. 1963: Sheet 23 – Oamaru. Geological Map of New Zealand 1:250,000., D. S. I. R., Wellington.

Mutch, A. R.; Wilson 1952: Reversals of movement on the Titri Fault. New Zealand Journal of Science and Technology 33B: 398-408.

Officers of the Geological Survey 1983: Seismotectonic hazard evaluation of the Clyde Dam Site. NZ Geological Survey EG Report 375.

Pollard, D. D.; Segall, P. 1987: Theoretical displacements and stresses near fractures in rock : with applications to faults, joints, veins, dikes, and solution surfaces. in: Atkinson, B. K. Editor, Fracture Mechanics of Rock. Academic Press, London, 277-350.

Simpson, G. D. H. 1991: The geology of Hamilton, Central Otago. Third year report, lodged in the Geology Department, University of Otago, Dunedin.

Stirling, M. W. 1988: Tectonic geomorphology of the Old Man range and Garvie mountains, Central Otago. MSc Thesis, lodged in the Library, University of Otago, Dunedin.

Stuiver, M.; Pearson, G. W. 1986: High-precision calibration of the radiocarbon time scale, AD 1950-500 BC. Radiocarbon 28: 805-838.

Stuiver, M.; Pearson, G. W.; Braziunas, T. 1986: Radiocarbon age calibration of marine samples. Radiocarbon 28: (2B).

Suppe, J. 1985: Principles of structural geology. Prentice-Hall, Eaglewood Cliffs, New Jersey.

Walcott R.I. 1984: The kinematics of the plate boundary zone through New Zealand: a comparison of short and long term deformation. Geophysical Journal of the Royal Astronomical Society 79: 613-633.

Walcott, R. C. 1988: The structure across an area spanning the eastern front of the Dunstan Mountains in the vicinity of Thompson's Gorge. BSc Honours Dissertation, lodged in the Library, University of Otago, Dunedin.

Waters, S. 1990: The geology of Tyroiti, Hyde. Third year report, lodged in the Geology Department, University of Otago, Dunedin.

Whetter, N. 1990: Hyde the facts: the geology of the Hyde area, Central Otago. Third year report, lodged in the Geology Department, University of Otago, Dunedin.

Williamson, J. H. 1939: The geology of the Naseby Subdivision, Central Otago. New Zealand Geological Survey Bulletin 39: 141.

Wood, B. L. 1963: Structure of the Otago Schists. New Zealand Journal of Geology & Geophysics 6: 641-680.

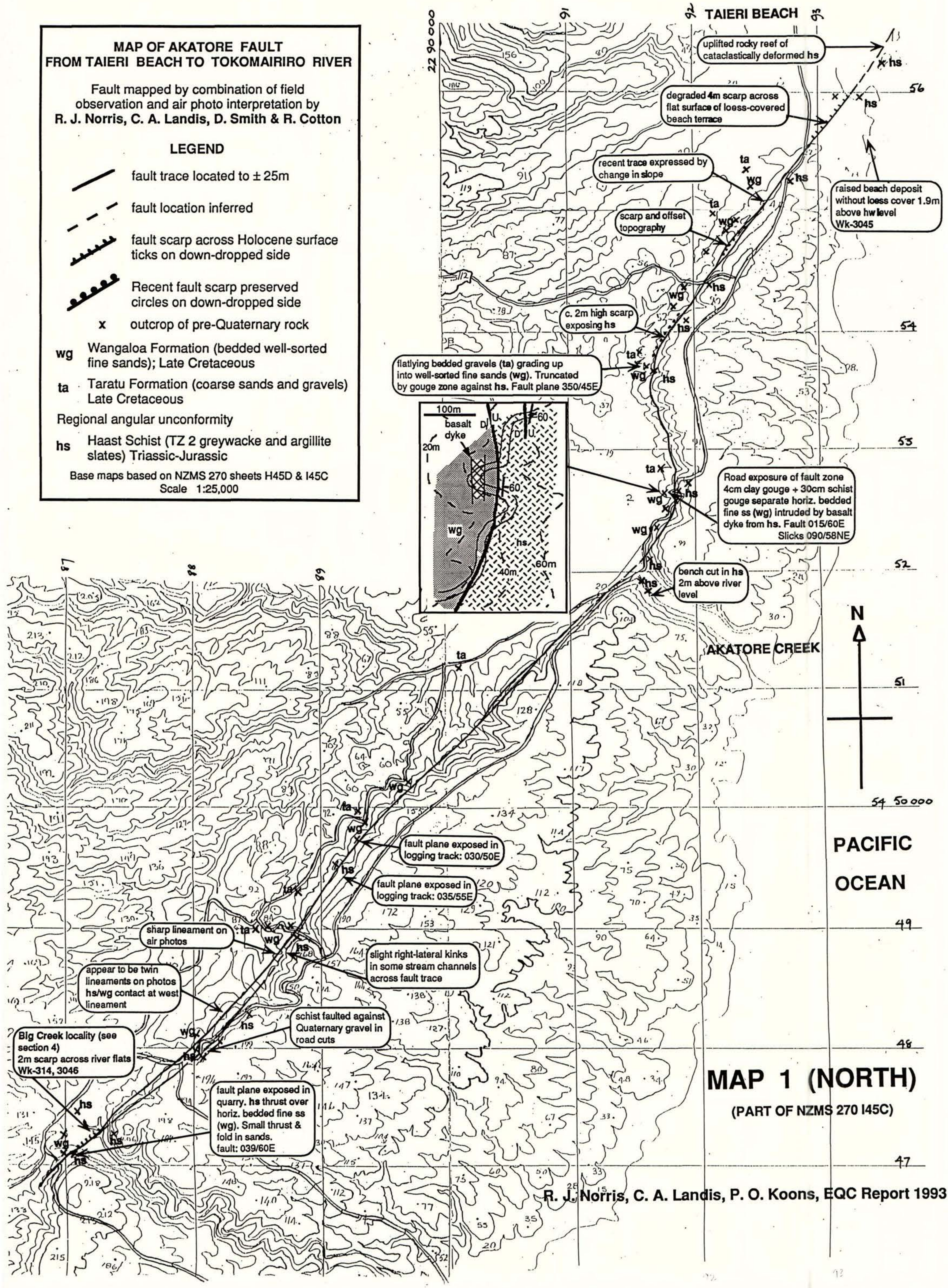
MAP OF AKATORE FAULT
FROM TAIERI BEACH TO TOKOMAIRIRO RIVER
Fault mapped by combination of field observation and air photo interpretation by
R. J. Norris, C. A. Landis, D. Smith & R. Cotton
LEGEND
fault trace located to ± 25m
fault location inferred
fault scarp across Holocene surface ticks on down-dropped side
Recent fault scarp preserved circles on down-dropped side
x outcrop of pre-Quaternary rock
wg Wangaloa Formation (bedded well-sorted fine sands); Late Cretaceous
ta Taratu Formation (coarse sands and gravels) Late Cretaceous
Regional angular unconformity
hs Haast Schist (TZ 2 greywacke and argillite slates) Triassic-Jurassic
Base maps based on NZMS 270 sheets H45D & I45C
Scale 1:25,000
TAIERI BEACH
uplifted rocky reef of cataclastically deformed hs
degraded 4m scarp across flat surface of loess-covered beach terrace
recent trace expressed by change in slope
raised beach deposit without loess cover 1.9m above hw level Wk-3045
scarp and offset topography
c. 2m high scarp exposing hs
flatlying bedded gravels (ta) grading up into well-sorted fine sands (wg). Truncated by gouge zone against hs. Fault plane 350/45E
100m
basalt dyke
Road exposure of fault zone 4cm clay gouge + 30cm schist gouge separate horiz. bedded fine ss (wg) intruded by basalt dyke from hs. Fault 015/60E Slicks 090/58NE
bench cut in hs 2m above river level
AKATORE CREEK
N
PACIFIC OCEAN
fault plane exposed in logging track: 030/50E
fault plane exposed in logging track: 035/55E
sharp lineament on air photos
slight right-lateral kinks in some stream channels across fault trace
appear to be twin lineaments on photos hs/wg contact at west lineament
schist faulted against Quaternary gravel in road cuts
Big Creek locality (see section 4) 2m scarp across river flats Wk-314, 3046
fault plane exposed in quarry. hs thrust over horiz. bedded fine ss (wg). Small thrust & fold in sands. fault: 039/60E
22 90 000
54 50 000
MAP 1 (NORTH)
(PART OF NZMS 270 I45C)
R. J. Norris, C. A. Landis, P. O. Koons, EQC Report 1993

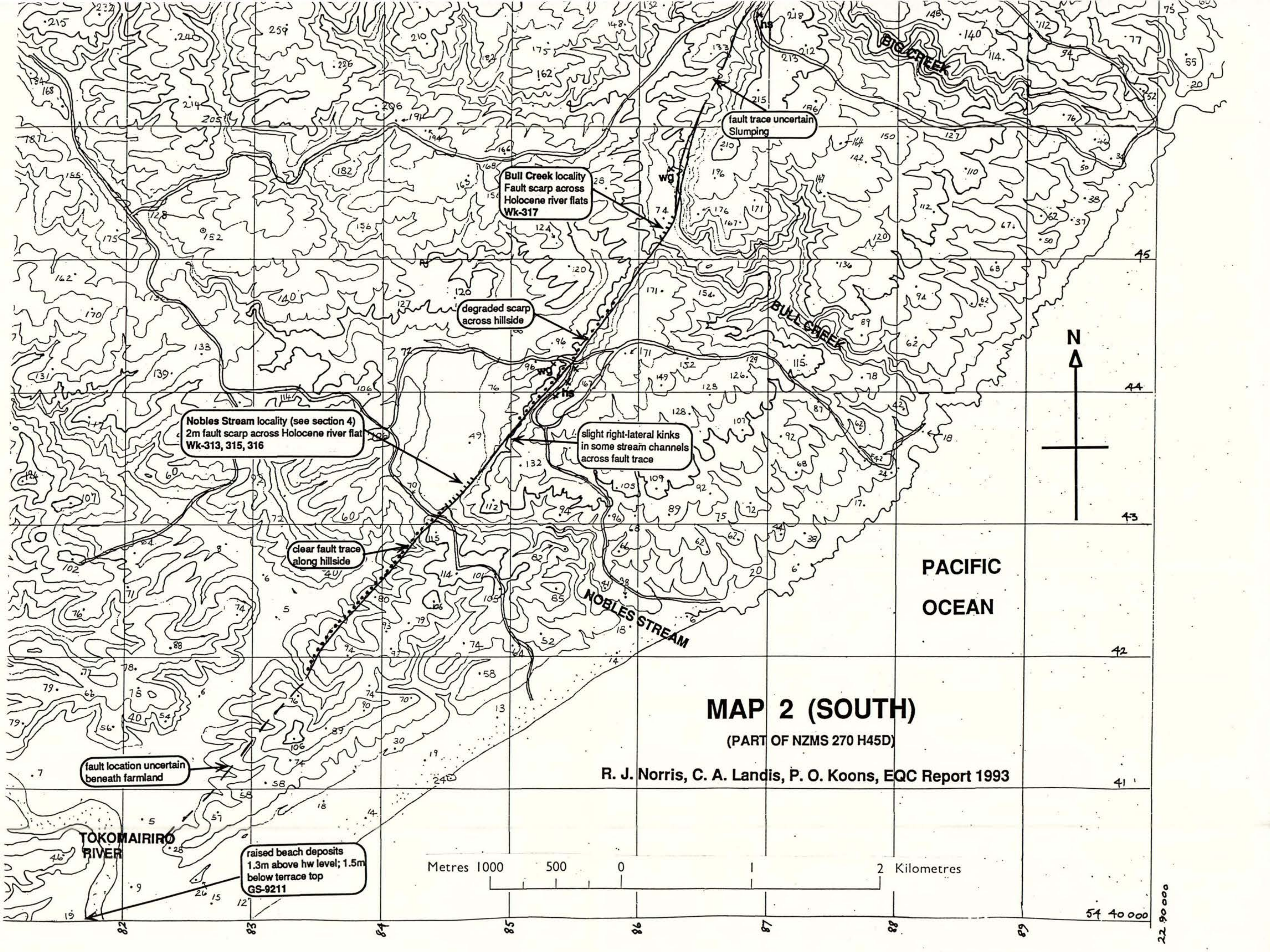

MAP 2 (SOUTH)
(PART OF NZMS 270 H45D)
R. J. Norris, C. A. Landis, P. O. Koons, EQC Report 1993
PACIFIC
OCEAN
N
BIG CREEK
BULL CREEK
NOBLES STREAM
TOKOMAIRIRO
RIVER
fault trace uncertain
Slumping
Bull Creek locality
Fault scarp across
Holocene river flats
Wk-317
degraded scarp
across hillside
Nobles Stream locality (see section 4)
2m fault scarp across Holocene river flat
Wk-313, 315, 316
slight right-lateral kinks
in some stream channels
across fault trace
clear fault trace
along hillside
fault location uncertain
beneath farmland
raised beach deposits
1.3m above hw level; 1.5m
below terrace top
GS-9211
Metres 1000 500 0 1 2 Kilometres
wg
hs
45
44
43
42
41
82
83
84
85
86
87
88
89
54 40 000
22 90 000